

Nanotransport Laboratory
nanotransport.ornl.gov

PFM of Piezoelectric Materials: Contact Mechanics, Cantilever Dynamics, and Resolution Theory

Sergei V. Kalinin

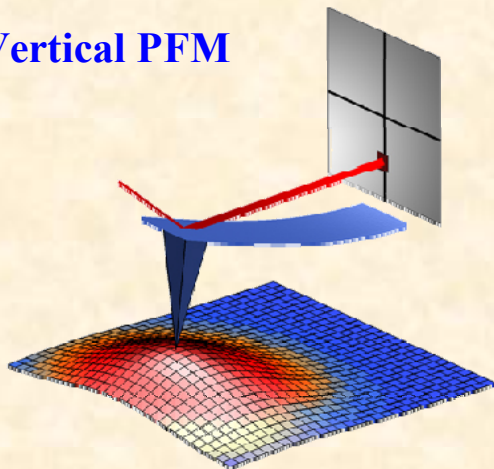
*The Center for Nanophase Materials Sciences and
Materials Sciences and Technology Division
Oak Ridge National Laboratory,*

OAK RIDGE NATIONAL LABORATORY
U. S. DEPARTMENT OF ENERGY

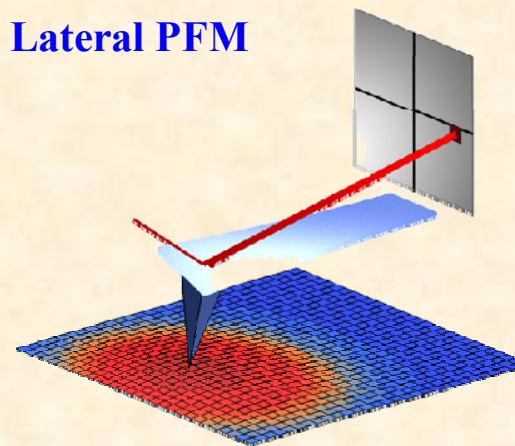

UT-BATTELLE

Probing NanoElectromechanics

Vertical PFM



Lateral PFM



Piezoresponse Force Microscopy

Application of AC bias to the tip

$$V_{tip} = V_{dc} + V_{ac} \cos(\omega t)$$

results in cantilever deflection

$$d = d_0 + A(\omega, V_{dc}) V_{ac} \cos(\omega t + \varphi)$$

due to piezoelectric effect

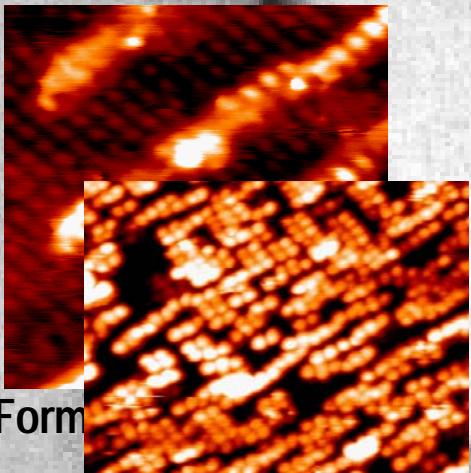
PFM = Nanoelectromechanics

OAK RIDGE NATIONAL LABORATORY
U. S. DEPARTMENT OF ENERGY

 UT-BATTELLE

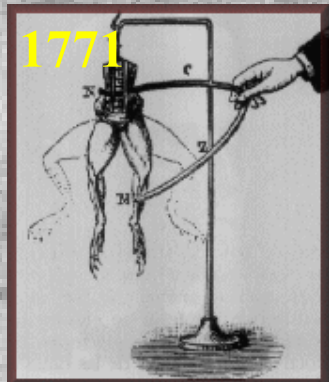
Philosophy of SPM

Current techniques

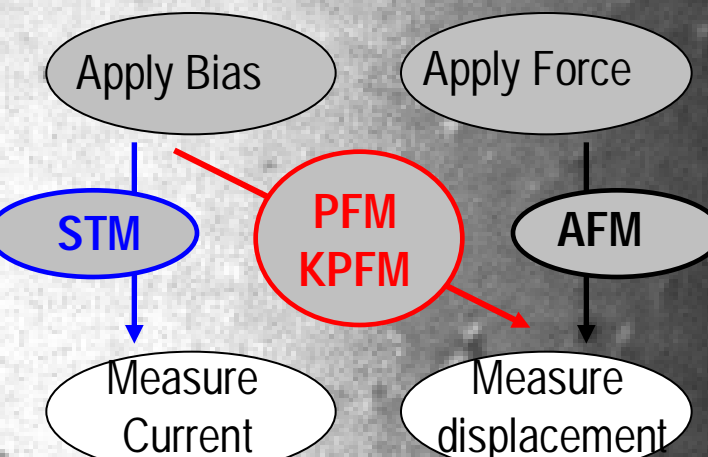
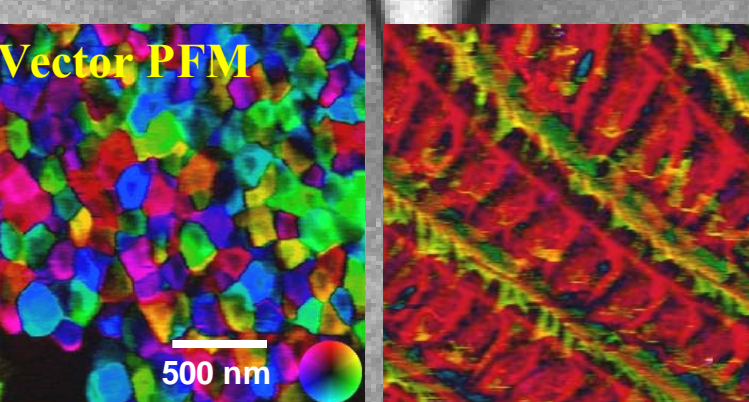
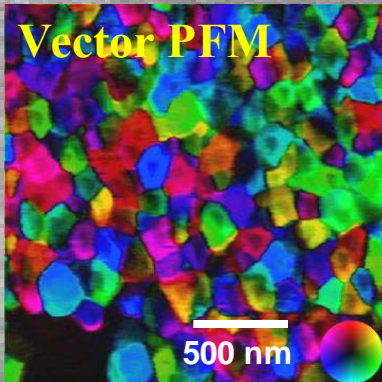


SrRuO₃ (100)

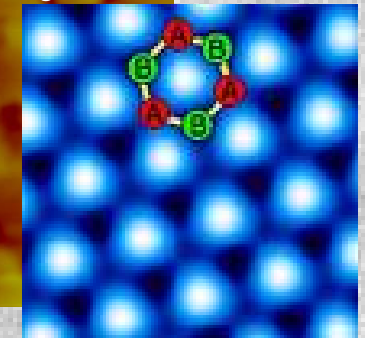
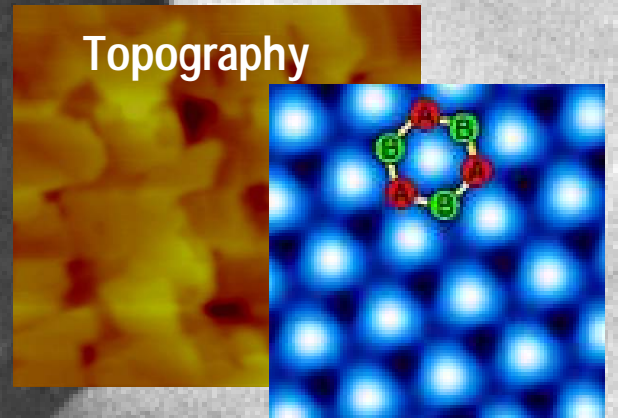
- Atomic resolution imaging
- Spin-polarized imaging
- Vibrational spectroscopy



1771



Force techniques



- Topography
- Adhesion
- Elasticity
- Magnetism

Electromechanical techniques

- Imaging polar materials
- Local bias-induced transitions
- Biomaterials
- Spectroscopy

Philosophy of SPM

Current techniques

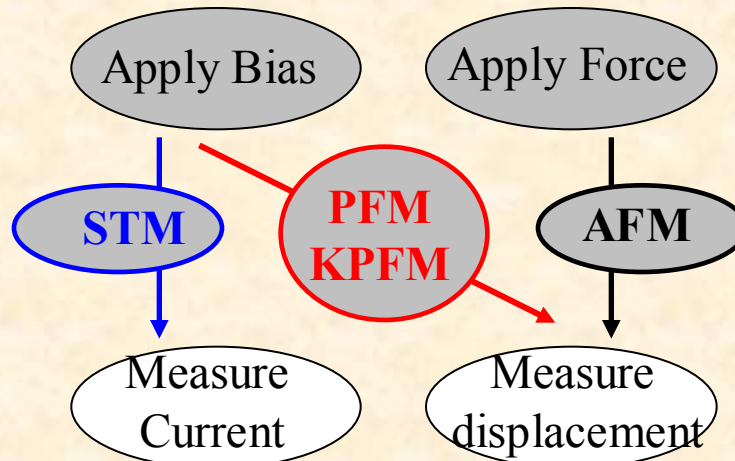
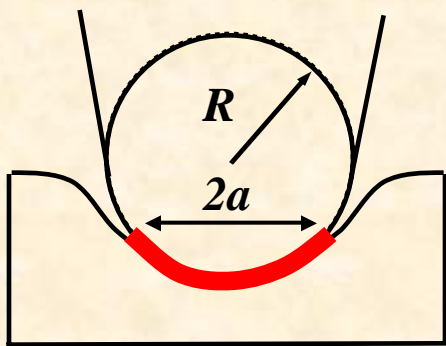
$$I = \Sigma V$$

Conductance scales as:

$\Sigma \sim a^1$ Classical

$\Sigma \sim a^2$ Sharvin

$\Sigma \sim a^0$ Tunneling



Electromechanical techniques

$$\begin{pmatrix} w_1 \\ w_2 \\ w_3 \end{pmatrix} = \begin{pmatrix} d_{34} \\ d_{35} \\ d_{33} \end{pmatrix} V$$

Responses scales as:

$d_{ij} \sim a^0$ Classical

$d_{ij} \sim ?$ Quantum limit

Force techniques

Couples to vertical

$$\begin{pmatrix} w_1 \\ w_2 \\ w_3 \end{pmatrix} = \begin{pmatrix} a_{11} & a_{12} & a_{13} \\ a_{21} & a_{22} & a_{23} \\ a_{31} & a_{32} & a_{33} \end{pmatrix} \begin{pmatrix} F_1 \\ F_2 \\ F_3 \end{pmatrix}$$

Lateral AFM Vertical AFM

Contact stiffnesses scale as:

$a_{ij} \sim a^1$ Classical

$a_{ij} \sim a^0$ Single atom/molecule

PFM is complementary to STM and AFM in terms of imaging mechanism!

Piezoresponse Force Microscopy

2.1. Elementary theory of PFM

- 2.1.1. PFM among other scanning probe microscopies
- 2.1.2. Vertical and lateral PFM
- 2.1.3. PFM signal vs. materials properties
- 2.1.4. Electromechanical and electrostatic contributions to the PFM signal

2.2. Contact mechanics of PFM

- 2.2.1. Exact solutions
- 2.2.2. Decoupled approximation
- 2.2.3. Implications for imaging

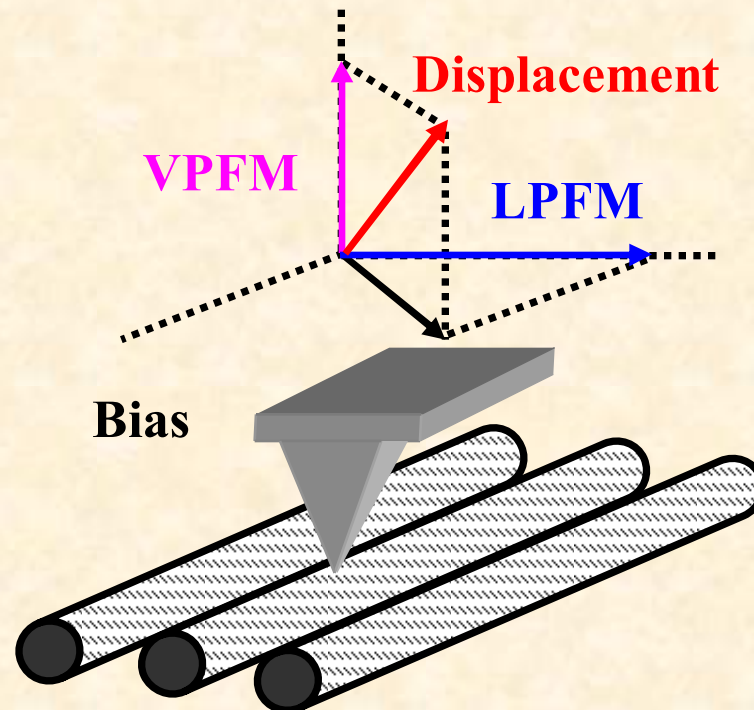
2.3. Cantilever dynamics in PFM

- 2.3.1. Generalized PFM dynamics
- 2.3.2. “PFM equation” for low frequencies
- 2.3.3. Optimal frequency and topographic cross-talks

2.4. Resolution theory in PFM

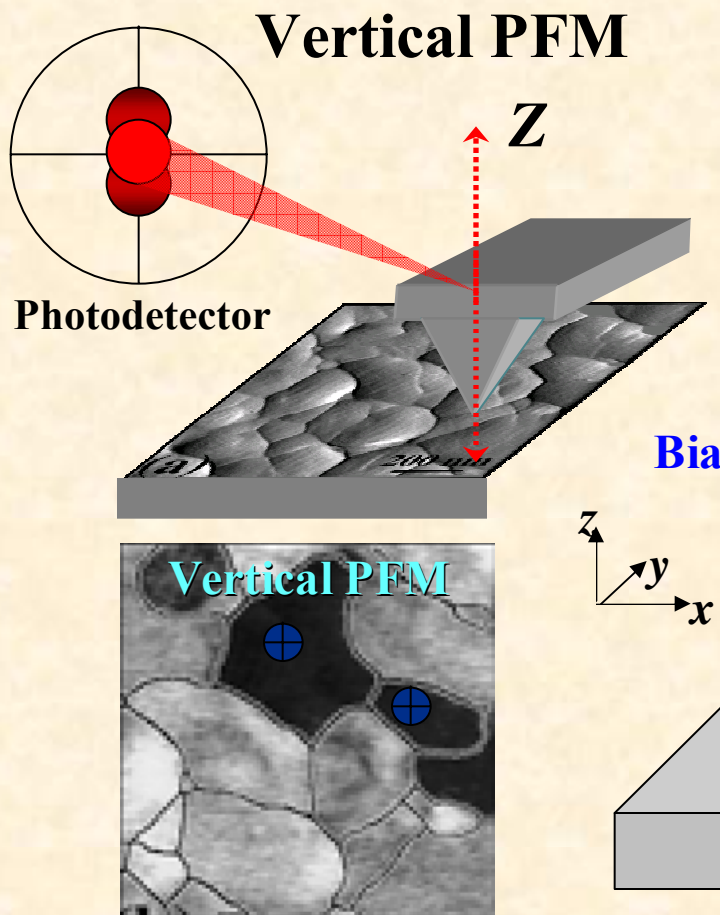
- 2.4.1. Resolution and Information limit
- 2.4.2. Tip calibration
- 2.4.3. Image reconstruction

Vertical and Lateral PFM

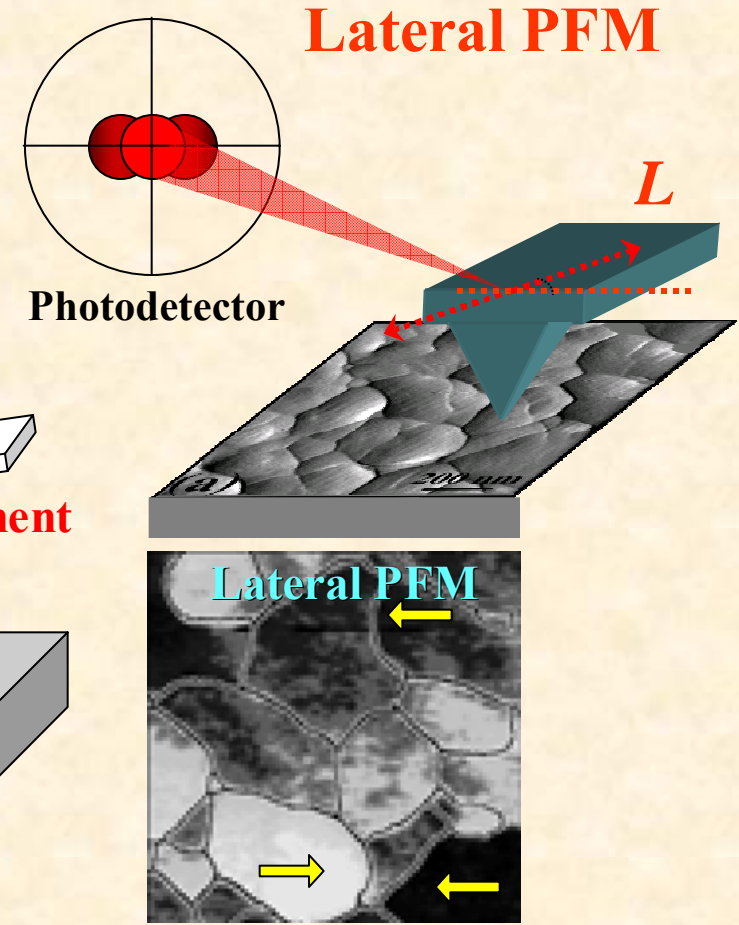


Vertical signal: vertical surface displacement
Lateral signal: in-plane surface displacement

Piezoresponse Imaging in 3 Dimensions



$$\Delta Z = \pm d_{33} V \cos(wt + \varphi)$$



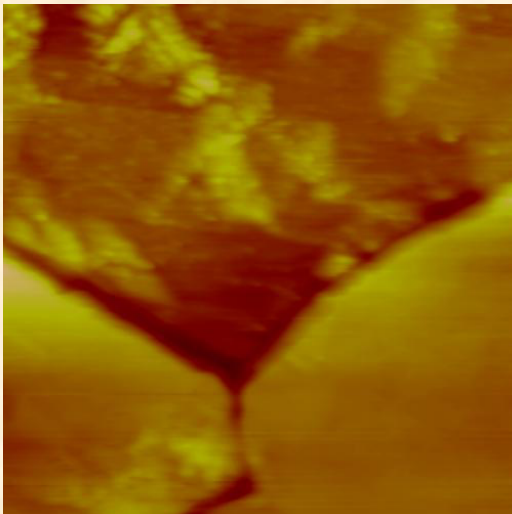
$$\Delta L = \pm d_{15} V \cos(wt + \varphi)$$

PFM allows complete 3D reconstruction of polarization vector at the nanoscale level:
Vertical + Lateral PFM (x) + Lateral PFM (y) = 3D PFM

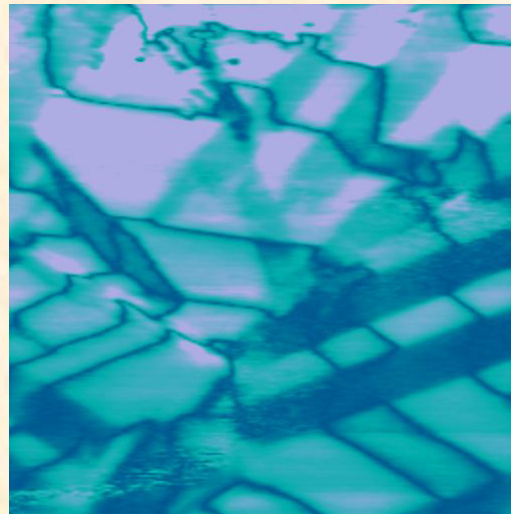
OAK RIDGE NATIONAL LABORATORY
U. S. DEPARTMENT OF ENERGY

UT-BATTTELLE

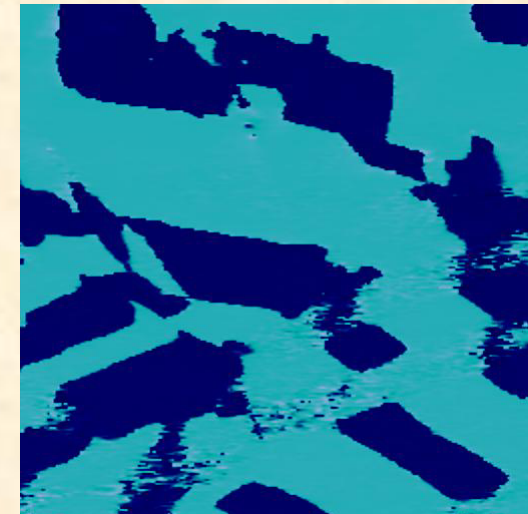
Vertical and Lateral PFM



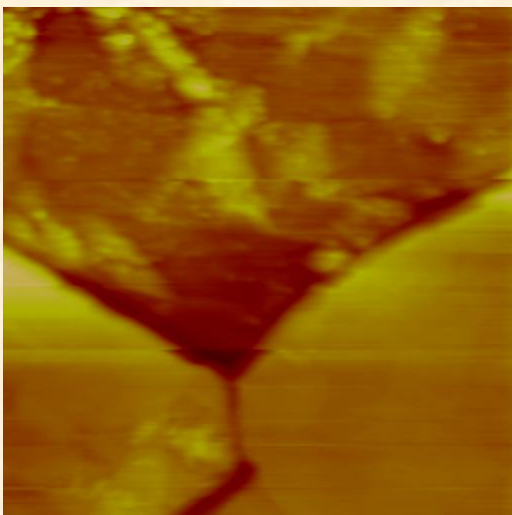
Topography, scale 100 nm



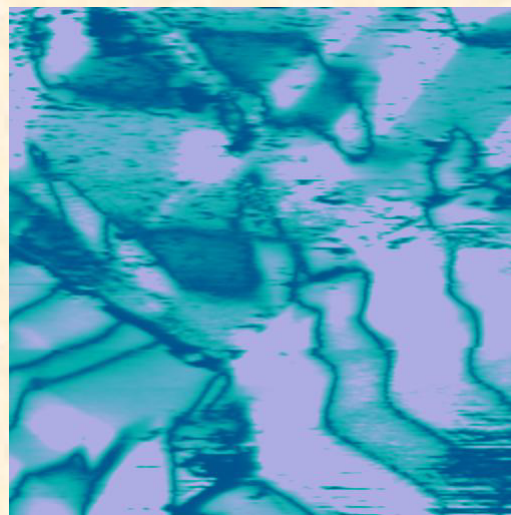
Vertical amplitude, scale 2V



Vertical phase, scale 20V



Topography, scale 100 nm



Lateral amplitude, scale 2V

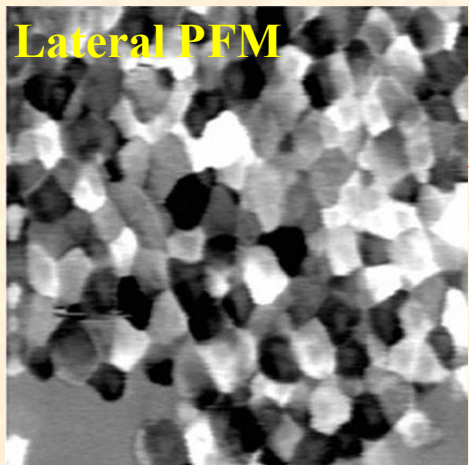
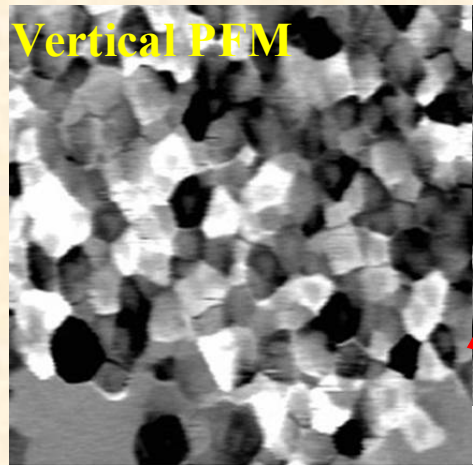


Lateral phase, scale 20V

OAK RIDGE NATIONAL LABORATORY
U. S. DEPARTMENT OF ENERGY

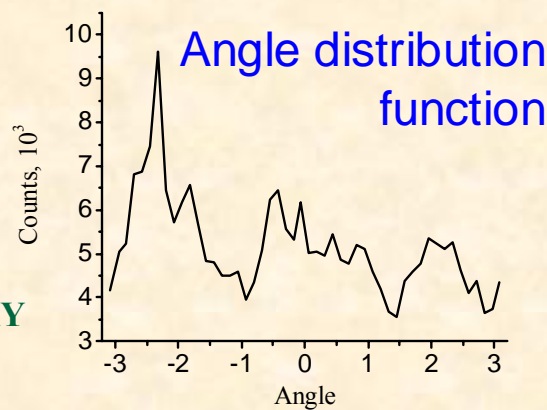
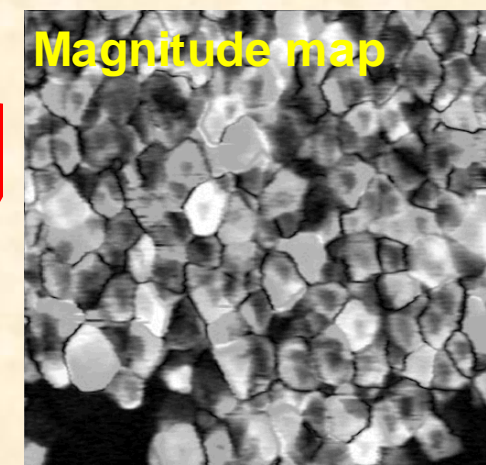
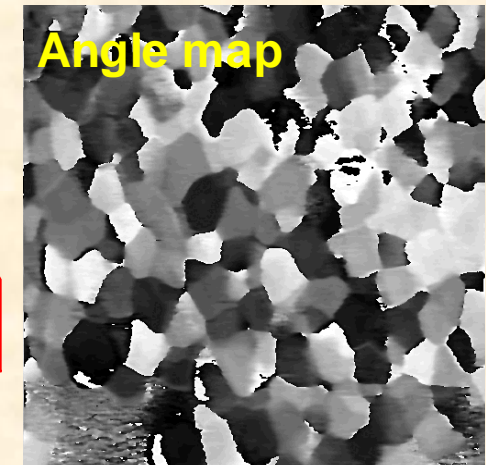
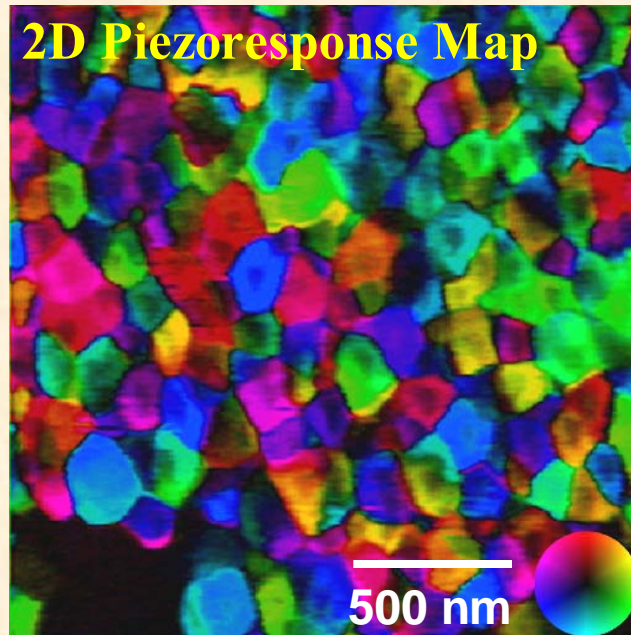


3D PFM: Materials Applications



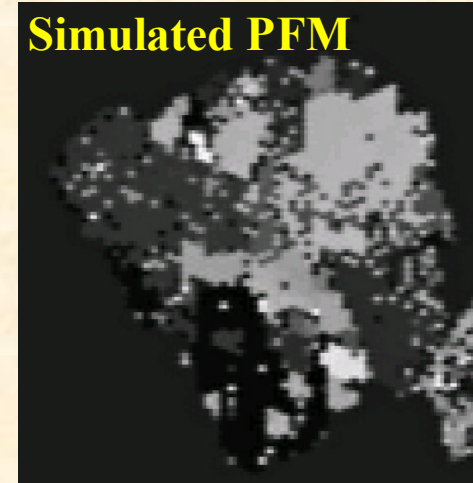
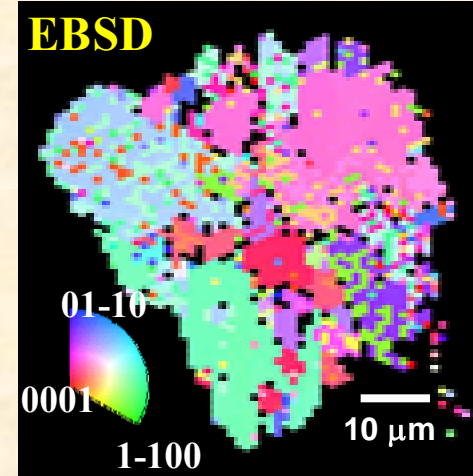
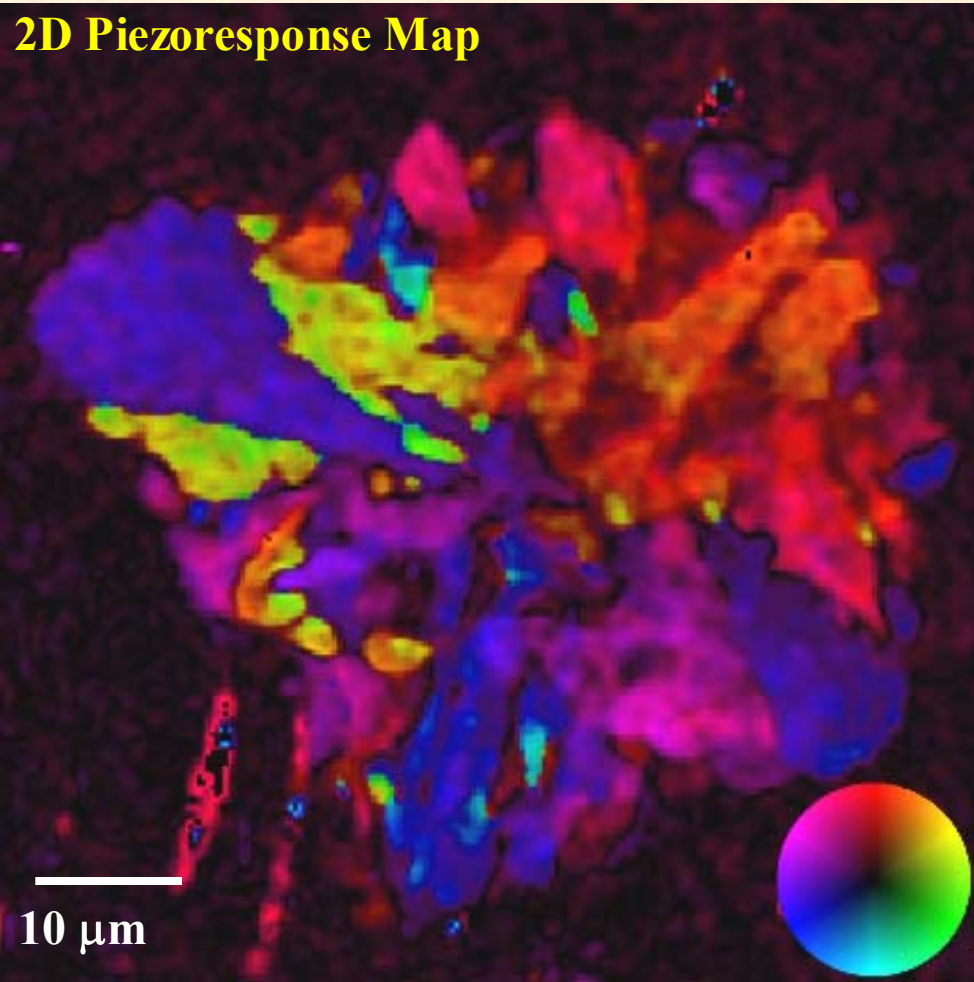
Ferroelectric PbTiO_3/Pt film:

- single domain grains
- constant orientation in the grains
- oriented film



with A. Gruverman, NCSU
OAK RIDGE NATIONAL LABORATORY
U. S. DEPARTMENT OF ENERGY

Practical Implementation of 3D PFM



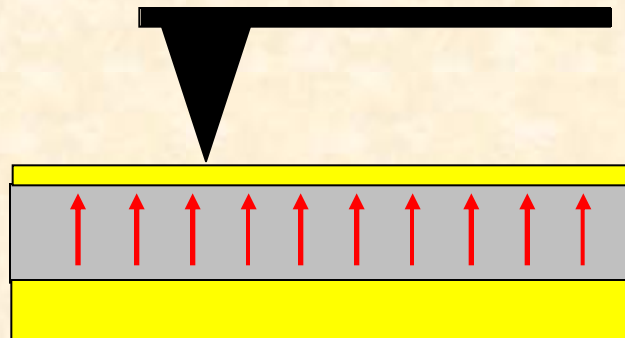
Vector PFM maps allow to visualize electromechanical response vector in 2D and 3D
Correlation to EBSD and other microscopies

OAK RIDGE NATIONAL LABORATORY
U. S. DEPARTMENT OF ENERGY



How is PFM related to Materials Properties

Global Detection:



The bias is applied between top and bottom electrode

Pro: The electric field is uniform

1. Tip quality does not matter
2. Easy to interpret

Con: 1. Resolution is low (electrode effect)

2. Writing is impossible

Signal Interpretation

Tetragonal material (4mm):

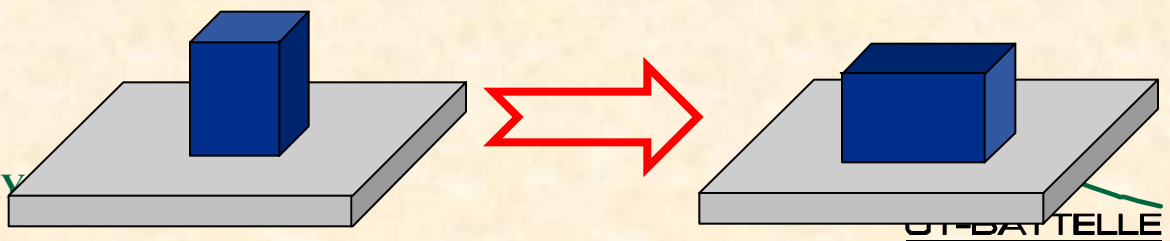
$$\begin{pmatrix} 0 & 0 & 0 & 0 & d_{15} & 0 \\ 0 & 0 & 0 & d_{15} & 0 & 0 \\ d_{31} & d_{31} & \boxed{d_{33}} & 0 & 0 & 0 \end{pmatrix}$$

↑
Vertical PFM
↑
Lateral PFM (x)
↑
Lateral PFM (y)

Rotated by 90°

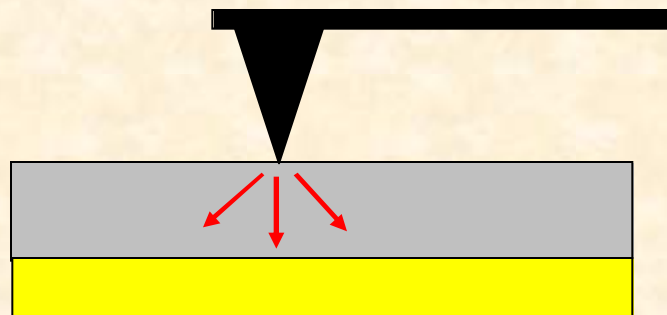
$$\begin{pmatrix} 0 & 0 & 0 & 0 & 0 & d_{15} \\ d_{31} & d_{33} & d_{31} & 0 & 0 & 0 \\ 0 & 0 & 0 & d_{15} & 0 & 0 \end{pmatrix}$$

Lateral PFM (x)



How is PFM related to Materials Properties

Local Detection:

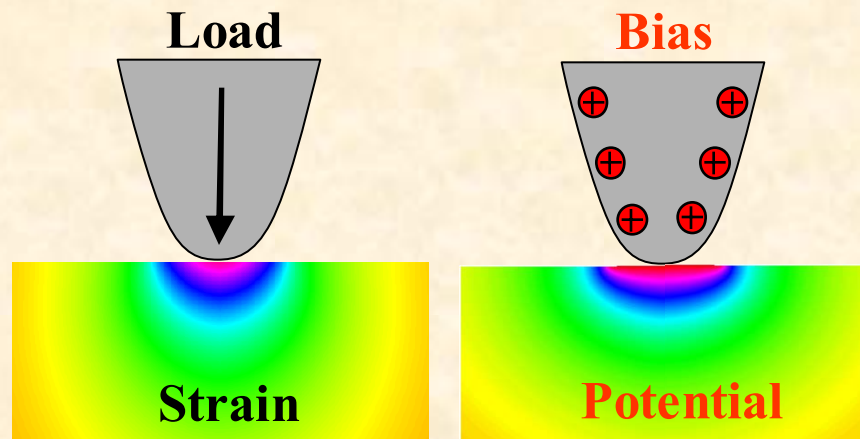


The bias is applied between tip and bottom electrode

- Pro:**
1. Resolution is higher
 2. Writing is possible

- Con:**
1. Very sensitive to tip-surface contact
 2. Difficult to interpret

Components of PFM and AFAM contrast



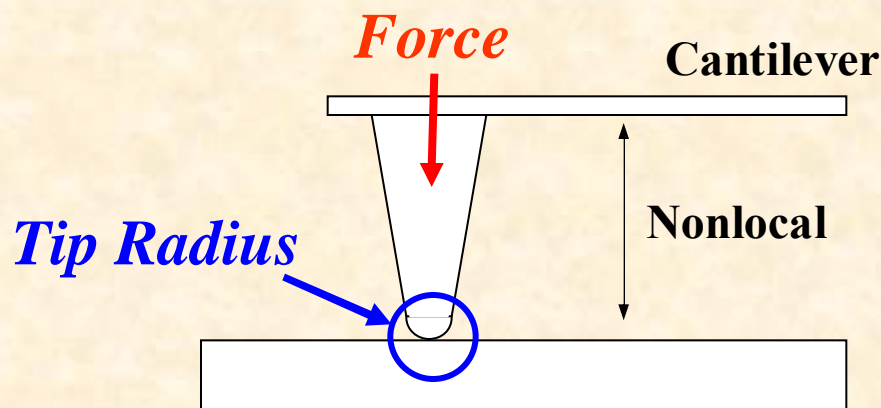
In piezoelectric materials, electrical and mechanical phenomena are coupled

1. **Tip-surface contact mechanics**
 - origins of PFM signal
2. **Cantilever dynamics**
 - Detection mechanism
3. **Field structure in material**
 - Resolution
 - hysteresis measurements
 - switching phenomena

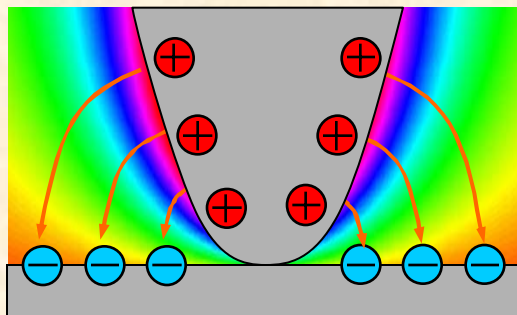
In a local detection case, exact solution is available only for transversally isotropic materials. For general case, we conjecture that $v_{\text{PFM}} = d_{33}$, $x\text{-LPFM} = d_{34}$ and $y\text{-LPFM} = d_{35}$.

PFM in a Real World

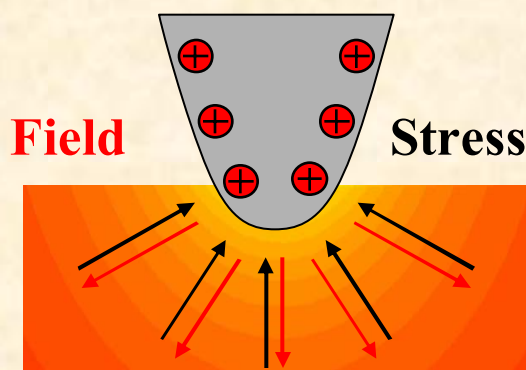
In a real world, measured signal contains additional contributions from local and distributed electrostatic forces.



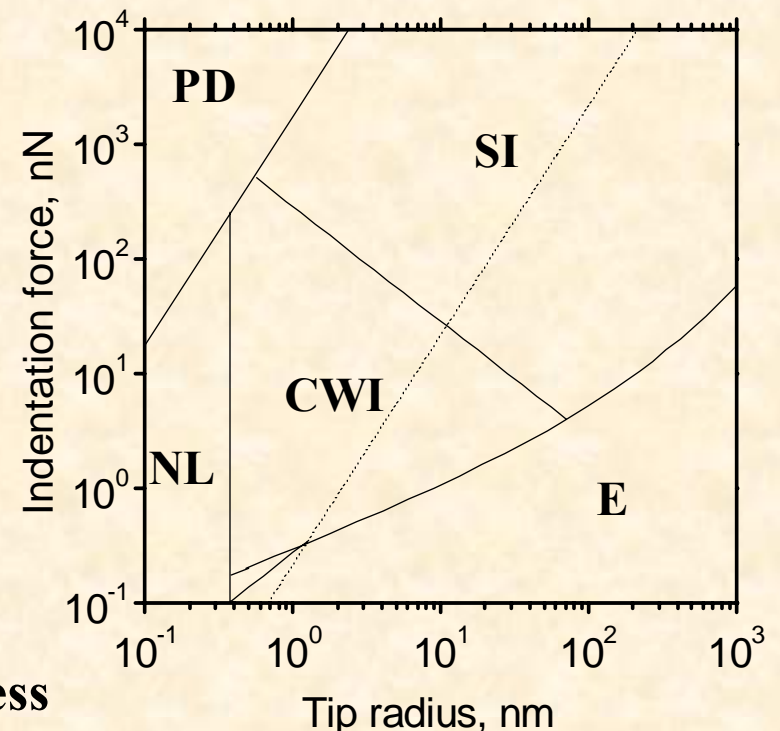
Local Piezoresponse Contrast



Electrostatic



Electromechanical



Tip radius, nm

E - Electrostatic

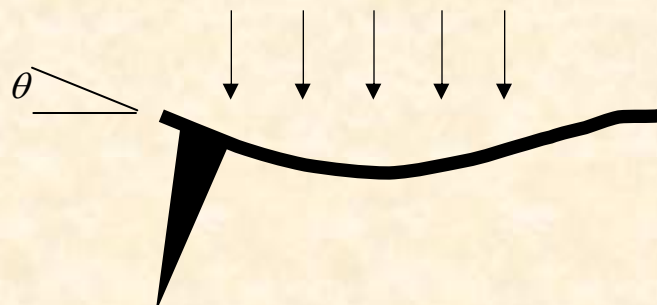
NL - Non-local interactions

PD - Plastic Deformation

SI - Strong Indentation

CWI - Weak indentation

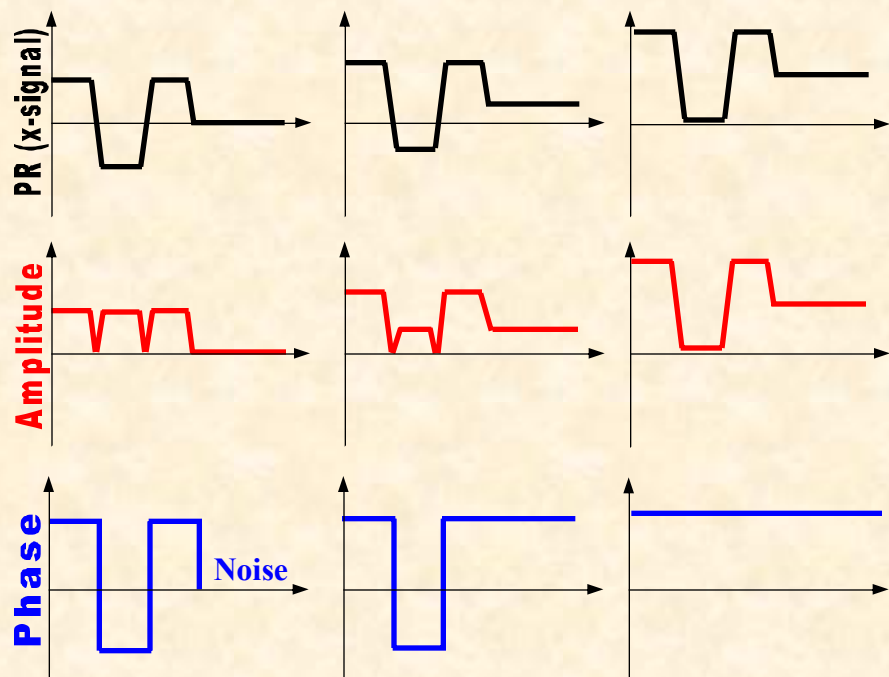
Electrostatic Contribution to PFM



Why quantifying PFM contrast is difficult:

- Tip is in contact - both electrostatic and electromechanical interactions contribute
- Total response contains both local and non-local contributions

Qualitative Aspects of Electrostatic Signal



PFM signal over positive domain

$$PR_+ = d_{33} + F_{nl}(V_{tip} - V_{av})$$

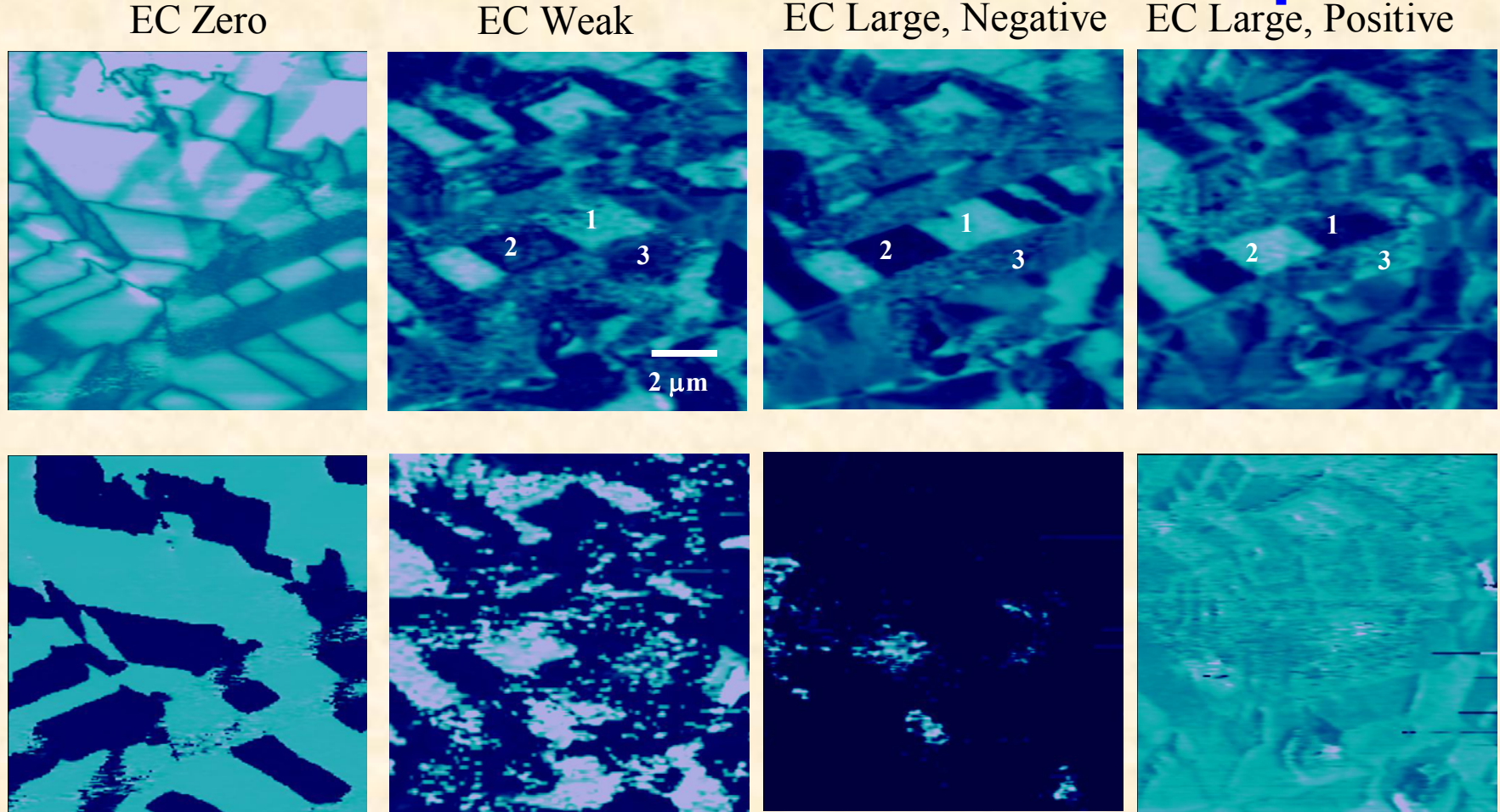
PFM signal over negative domain

$$PR_- = -d_{33} + F_{nl}(V_{tip} - V_{av})$$

Stiffness criterion:

$$PR = d_{eff} + \frac{Lw\epsilon_0\Delta V}{48kH^2}$$

Electrostatic Contribution to PFM - Experiment



How to avoid cantilever effect: $PR = d_{eff} + \frac{Lw\varepsilon_0\Delta V}{48kH^2}$

- ⇒ 1. Take stiff cantilever!
2. Take narrow/short cantilever
3. Image at nulling bias

For $d_{eff} = 50 \text{ pm/V}$, $\Delta V = 5V$, $L = 225 \mu\text{m}$, $w = 30 \mu\text{m}$, $H = 15 \mu\text{m}$, the condition is $k > 0.55 \text{ N/m}$

OAK RIDGE NATIONAL LABORATORY

U. S. DEPARTMENT OF ENERGY

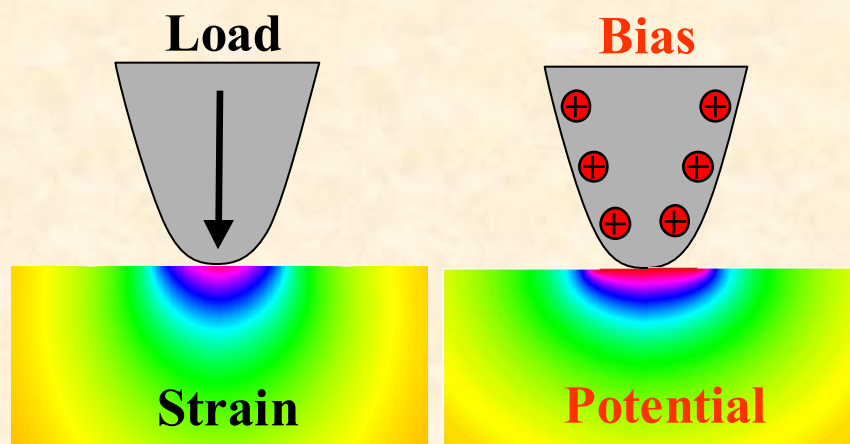
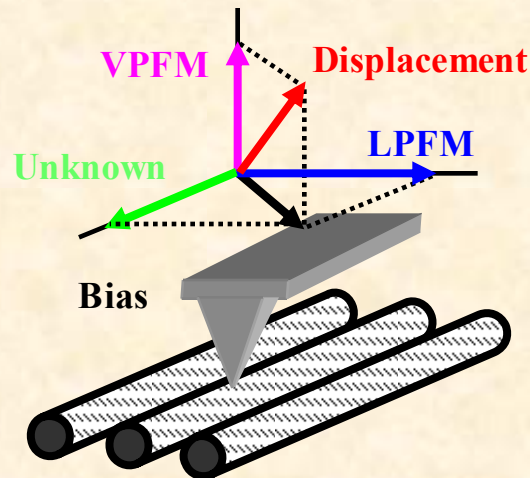


Voltage-dependent contact mechanics

OAK RIDGE NATIONAL LABORATORY
U. S. DEPARTMENT OF ENERGY



Image formation in PFM



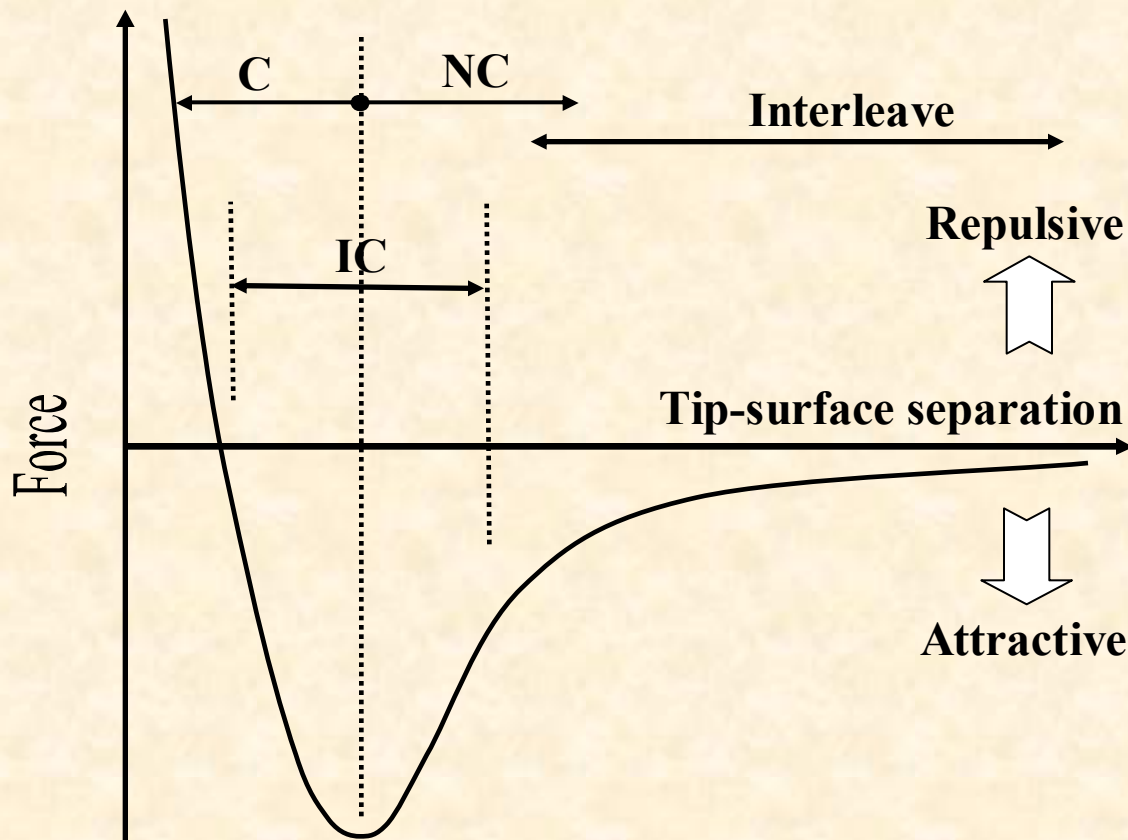
In piezoelectric materials, electrical and mechanical phenomena are coupled

Several competing contributions:

1. Vertical surface response
2. Longitudinal response
3. Torsional response
4. Local electrostatic force
5. Distributed electrostatic force

1. **Tip-surface contact mechanics**
 - origins of PFM signal
2. **Cantilever dynamics**
 - Detection mechanism
3. **Field structure in material**
 - Resolution
 - hysteresis measurements
 - switching phenomena

Force-Distance Curve



Force distance curve does not include bias effects!

Electromechanical Coupling in SPM

Contact Electromechanical Techniques

Piezoresponse Force Microscopy

$$\left(\frac{\partial z}{\partial V} \right)_F$$

Ultrasonic-Electrostatic Microscopy

$$\frac{\partial^2 F}{\partial z \partial V}$$

$$F = F(z, V_{tip})$$

Atomic Force Acoustic Microscopy

$$\frac{\partial F}{\partial z}$$

Ultrasonic Force Microscopy

$$\frac{\partial^2 F}{\partial z^2}$$

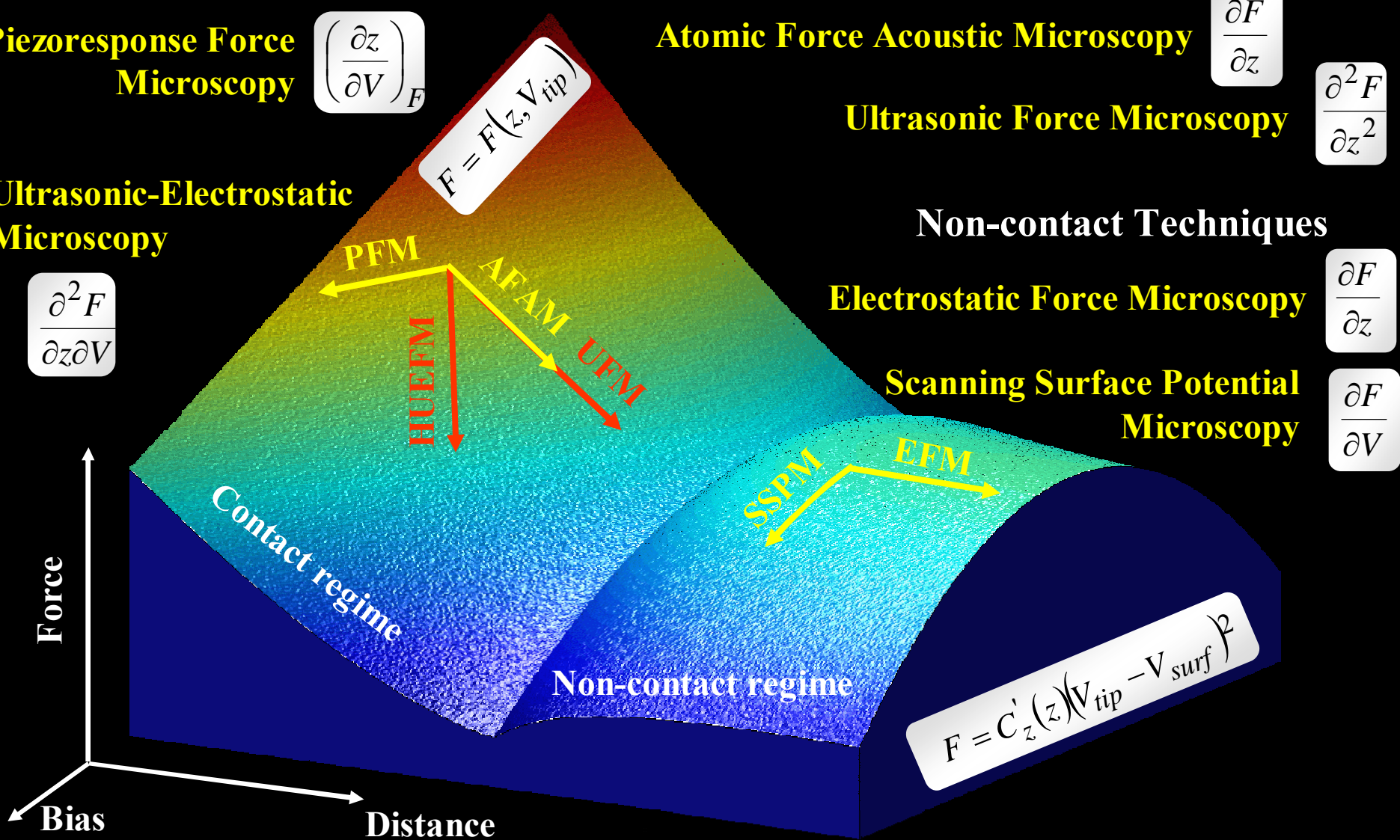
Non-contact Techniques

Electrostatic Force Microscopy

$$\frac{\partial F}{\partial z}$$

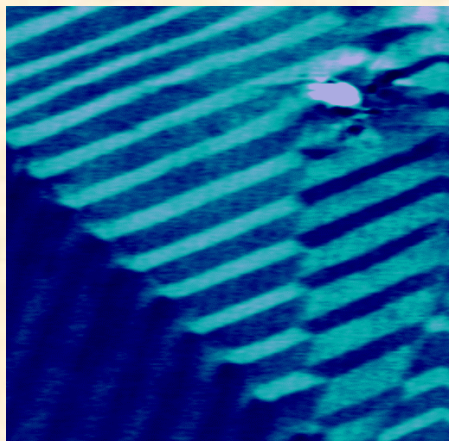
Scanning Surface Potential Microscopy

$$\frac{\partial F}{\partial V}$$

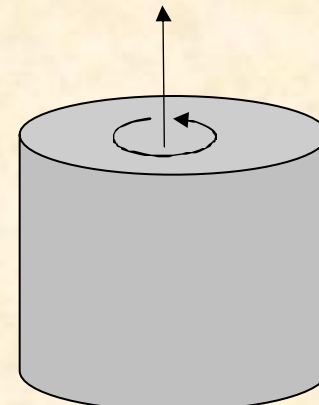
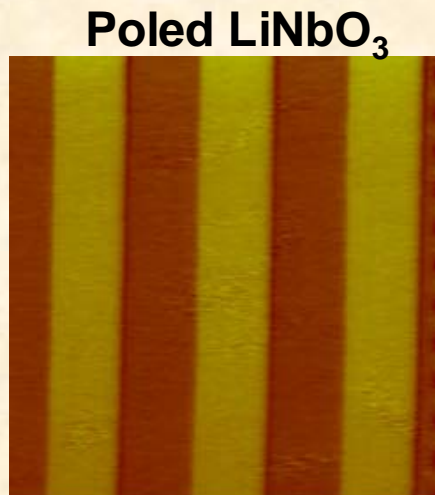


Piezoresponse Force Microscopy of Materials with Out-of-Plane Polarization

Examples: c^+ - c^- domains in BaTiO_3 , periodically poled LiNbO_3 , poled polymers



BaTiO_3

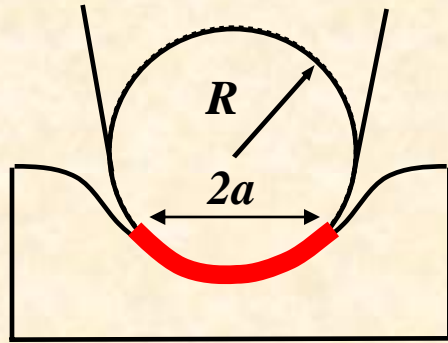


For piezoelectric and elastic properties, tetragonal and hexagonal symmetries are equivalent to transversally isotropic

- The highest symmetry possible for ferroelectric material
- No lateral response component
- A rigorous electromechanical solution exists!
- Starting point to more complex systems

Nanoelectromechanics of PFM

Stiffness Relations



1872: Hertz – spherical indentation of isotropic material

1945: Sneddon – arbitrary indentor shape

1992: Hanson: transversally isotropic material

2002: Karapetian and Kachanov: piezoelectric material

$$\text{Indentation depth: } w_0 = \frac{a^2}{R}$$

Load:

$$P = \frac{4a^3 C_1^*}{3\pi R} + \frac{2a\psi_0 C_3^*}{\pi}$$

Charge:

$$Q = -\frac{4a^3 C_3^*}{3\pi R} + \frac{2a\psi_0 C_4^*}{\pi}$$

a – indentation radius, R – tip radius



Indentation elastic stiffness



Indentation piezoelectric coefficient



Indentation dielectric constant

This is the first **rigorous solution** of spherical indentation problem for piezoelectric material **in analytical functions**.

S.V. Kalinin, E. Karapetian, and M. Kachanov, Phys. Rev. **B**, 2004

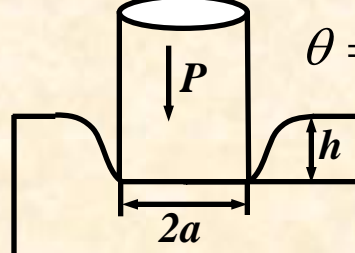
E. Karapetian, M. Kachanov, and S.V. Kalinin, Phil. Mag. 2005

OAK RIDGE NATIONAL LABORATORY

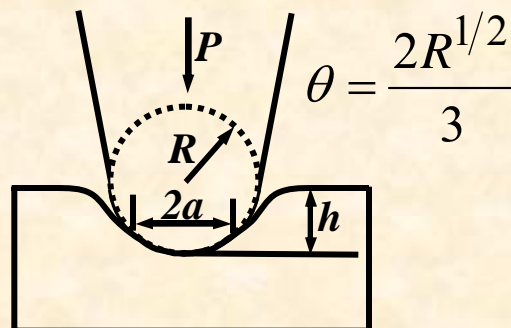
U. S. DEPARTMENT OF ENERGY



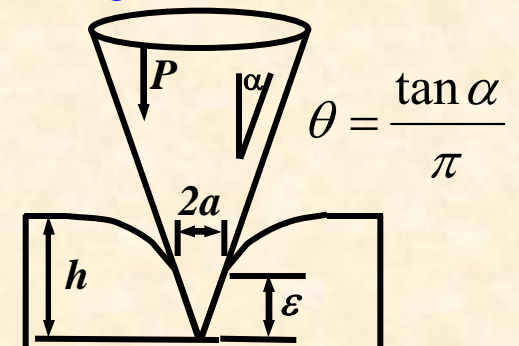
Nanoelectromechanics for Arbitrary Indentor



Flat: $n = 0$



Spherical: $n = 1/2$



Conical: $n = 1$

Load:
$$P = \frac{2}{\pi} \theta \left(h^{n+1} C_1^* + (n+1) h^n \psi_0 C_3^* \right)$$

Charge:
$$Q = \frac{2}{\pi} \theta \left(-h^{n+1} C_3^* + (n+1) h^n \psi_0 C_4^* \right)$$

For uniform field:

$$h = d_{33} V$$

$$Q = d_{33} F$$

Implications:

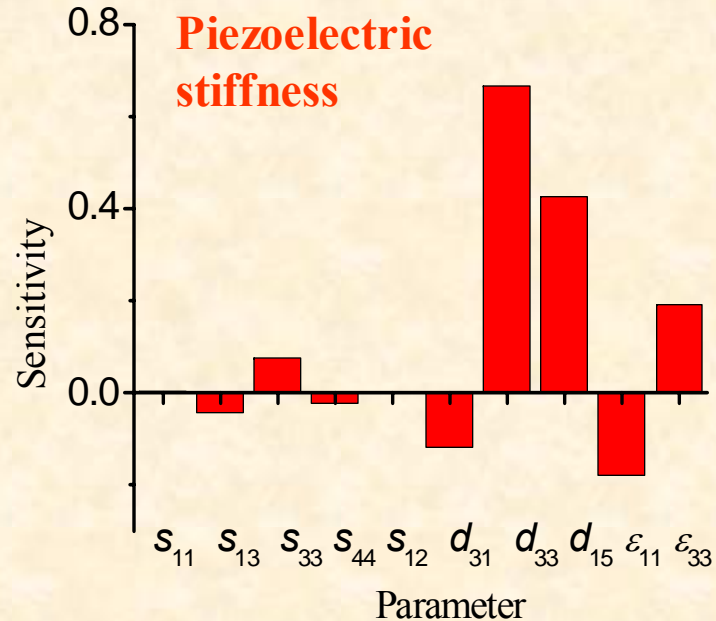
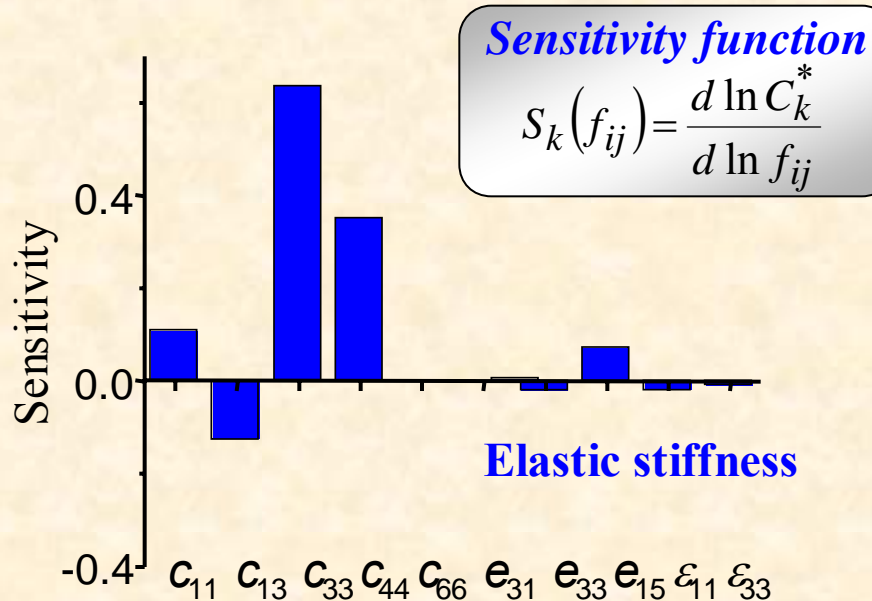
1. In the SPM or indentation experiment, we can determine only indentation moduli, but not the individual elements of elastic, piezoelectric or dielectric tensors
2. In contact problem, indentor shape function and materials properties are decoupled, hence the indentor can be calibrated
3. Experimentally, we can measure C_3/C_1 by PFM and C_1 by e.g. Atomic Force Acoustic Microscopy. In SPM, due to smallness of capacitance, C_4 can not be measured directly

OAK RIDGE NATIONAL LABORATORY

U. S. DEPARTMENT OF ENERGY



Materials Properties and Effective Response

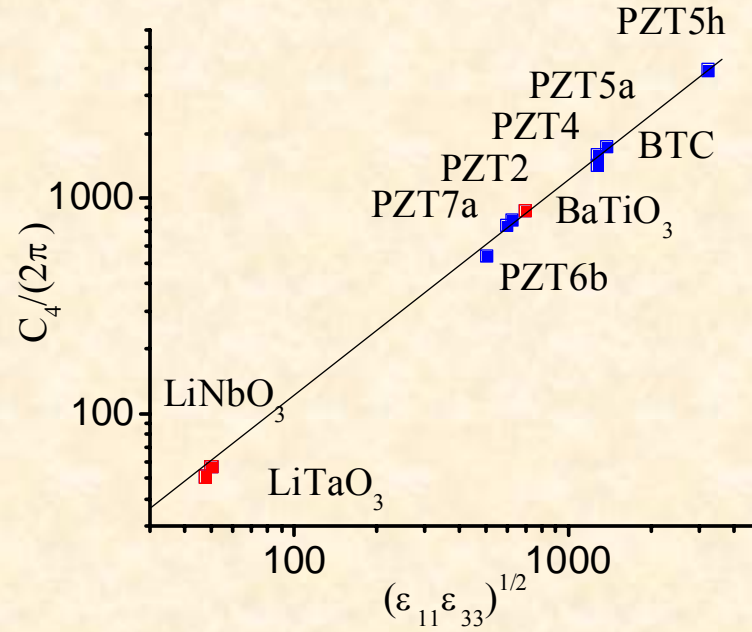
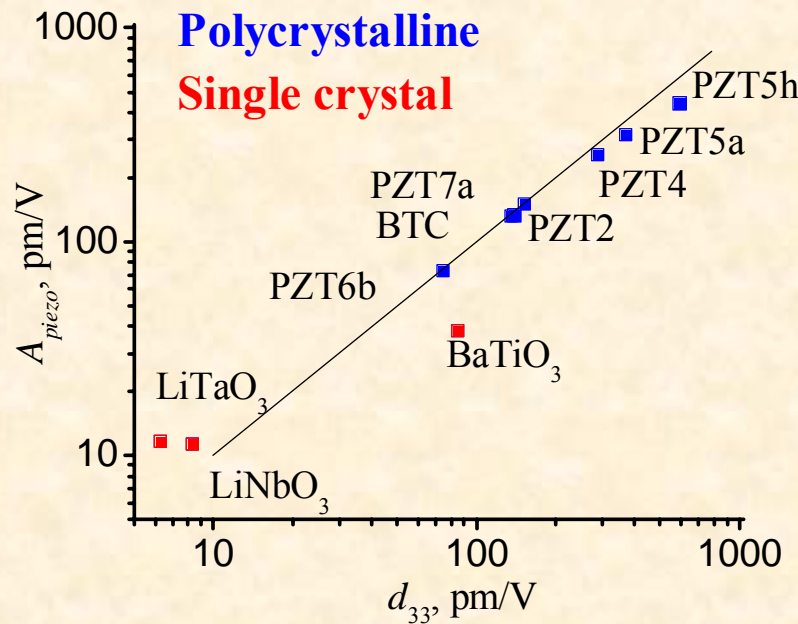


Indentation stiffnesses are complex functions of materials properties:

$$C_i^* = C_i^*(c_{ij}, d_{ij}, \epsilon_{ij})$$

- Elastic indentation module is determined primarily by c_{ij}
- PFM signal is determined by d_{ij} and ϵ_{ij}
- Dielectric properties are determined by ϵ_{ij}

Materials Properties and Effective Response



- Piezoresponse amplitude is a complex function of materials constants
- There is a reasonable correlation between PFM signal and d_{33}
- Indentor charge can be obtained from simple theory

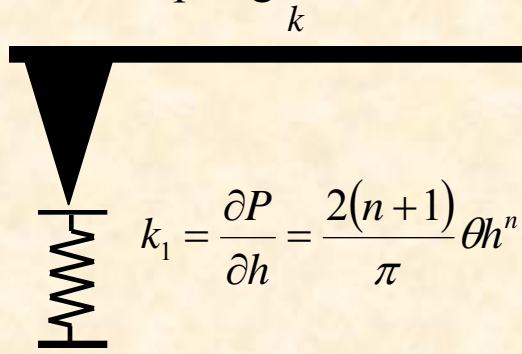
Implications for Electromechanical and Mechanical SPM

$$P = \frac{2}{\pi} \theta \left(h^{n+1} C_1^* + (n+1) h^n V_{tip} C_3^* \right)$$

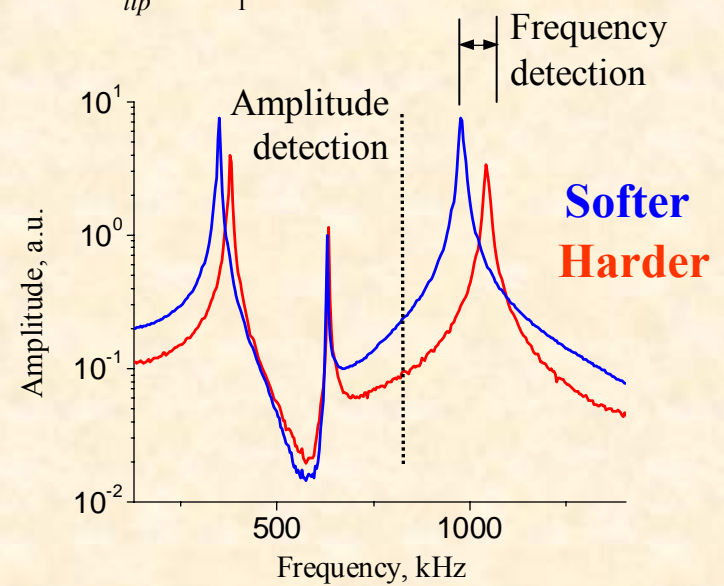
In Piezoresponse Force Microscopy, measured is Independent of tip geometry

$$d_{eff} = \frac{\partial h}{\partial V_{tip}} = \frac{C_3^*}{C_1^*}$$

In Atomic Force Acoustic Microscopy, signal is related to tip-surface spring constant.



$$k_1 = \frac{\partial P}{\partial h} = \frac{2(n+1)}{\pi} \theta h^n C_1^*$$



Positive: PFM signal is independent on tip geometry and topography

Negative: we can not use resonant enhancement in PFM

Approximate Theory for PFM

Rigorous solution is limited:

- Ignores fields outside the contact area (classical limit)
- Limited to transversally-isotropic material
 - no lateral PFM
 - no materials other than (100) surfaces of tetragonal perovskites
- Can not be used to describe PFM signal in
 - thin films
 - nanoparticles
 - domain wall profiles
 - cylindrical domains (PFM spectroscopy)

We need approximate solutions!

Green's Function Model

From rigorous solution, we know that far from contact, fields rapidly approach that for point charge/point force

Rigorous solution: For fully anisotropic materials, the Green's function for point charge/point force for coupled electromechanical problem has recently been derived using linear plane wave method. (V. Borovikov, 2005)

- Arbitrary materials symmetry
 - Can describe vertical and lateral PFM
- Unphysical singularity at origin
 - can not describe switching and spectroscopy
- Ignores effects of tip shape, contact vs. non-contact contributions, etc.

Decoupled Green's Function Model

Decoupled approximation (Schneider, Gopalan, Morozovska-Eliseev-Kalinin)

- Calculate electric field for rigid dielectric, $d_{ijk} = e_{ijk} = 0$
- Calculate strain field using piezoelectric constitutive equations, $X_{ij} = E_k e_{kij}$
- Calculate displacement field using Green's function for non-piezoelectric elastic solid

$$u_i(\mathbf{x}) = \int_0^\infty d\xi_3 \int_{-\infty}^\infty d\xi_2 \int_{-\infty}^\infty d\xi_1 \frac{\partial G_{ij}(\mathbf{x}, \boldsymbol{\xi})}{\partial \xi_l} E_k(\boldsymbol{\xi}) e_{klj}$$

Error estimate: From $D_i = d_{ijk} X_{jk} + \varepsilon_{im} E_m$ we get $E_k = \varepsilon_{ki}^{-1} D_i - \varepsilon_{ki}^{-1} d_{ijl} X_{jl}$

Substituting into $U_{ij} = s_{ijkl} X_{kl} + E_m d_{mij}$

we obtain $U_{ij} = (1 - s_{ijkl}^{-1} \varepsilon_{mp}^{-1} d_{plk} d_{mij}) s_{ijkl} X_{kl} + \varepsilon_{mp}^{-1} d_{mij} D_p$

BaTiO₃: $k_{15}^2 \approx 0.32$ $k_{31}^2 \approx 0.10$ $k_{33}^2 \approx 0.31$

$$k_{ij}^2 = (d_{ij})^2 / (s_{jj} \varepsilon_{ii})$$

PZT: $k_{15}^2 \approx 0.14$ $k_{31}^2 \approx 0.02$ $k_{33}^2 \approx 0.13$

Quartz: $k_{11}^2 \approx 0.01$

For most materials, error is of order of 10-30% or less!

OAK RIDGE NATIONAL LABORATORY
U. S. DEPARTMENT OF ENERGY



Decoupled Green's Function Model

$$u_i(\mathbf{x}) = \int_0^{\infty} d\xi_3 \int_{-\infty}^{\infty} d\xi_2 \int_{-\infty}^{\infty} d\xi_1 \frac{\partial G_{ij}(\mathbf{x}, \xi)}{\partial \xi_l} E_k(\xi) e_{kl}$$

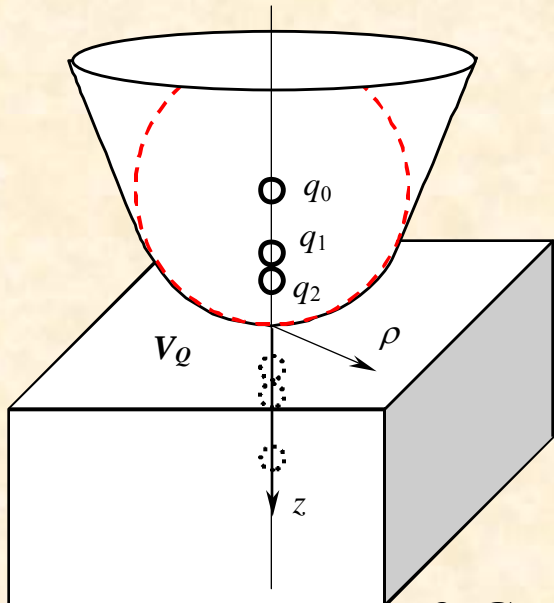
- Calculate electric field for rigid dielectric, $d_{ijk} = e_{ijk} = 0$
- Calculate strain field using piezoelectric constitutive equations, $X_{ij} = E_k e_{kij}$
- Calculate displacement field using Green's function for non-piezoelectric elastic solid

Benefits of decoupled approximation:

- Can take into account any field structure (solve electrostatic problem)
- Arbitrary materials symmetry (as given by dielectric, piezoelectric, and elastic tensors)
- Can naturally be used to describe microstructural elements such as variations in elastic properties, domain walls, etc.
- Can be further simplified by assuming special materials symmetries for elastic and mechanical properties

Electric Field Structure

1. Represent tip using image charge series or multipole expansion



2. Solve Laplace's equation

$$\begin{cases} \epsilon_0 \epsilon_{ij} \frac{\partial^2}{\partial x_i \partial x_j} V(\mathbf{r}) = 0, & z \geq 0 \\ \epsilon_0 \Delta V_0(\mathbf{r}) = -Q \cdot \delta(z+d) \delta(x) \delta(y), & z < 0 \end{cases}$$

with boundary conditions

$$\epsilon_{3j} \frac{\partial}{\partial x_j} V(z=0) = \frac{\partial}{\partial z} V_0(z=0),$$

$$V(z=0) = V_0(z=0)$$

3. General answer

$$V(\mathbf{r}) = \frac{Q}{2\pi\epsilon_0} \int_{-\infty}^{\infty} dk_x \int_{-\infty}^{\infty} dk_y \frac{\exp(-ik_x x - ik_y y)}{2\pi} \cdot \frac{\exp(-d\sqrt{k_x^2 + k_y^2} - z\lambda(k_x, k_y))}{\left(\sqrt{k_x^2 + k_y^2} + (i\epsilon_{31} k_x + i\epsilon_{32} k_y + \epsilon_{33}\lambda)\right)}$$

4. Transversally-isotropic

$$V_Q(\rho, z) = \frac{Q}{2\pi\epsilon_0(\kappa+1)} \frac{1}{\sqrt{\rho^2 + (z/\gamma + d)^2}}$$

Dielectric constant $\kappa = \sqrt{\epsilon_{33}\epsilon_{11}}$

Dielectric anisotropy $\gamma = \sqrt{\epsilon_{33}/\epsilon_{11}}$

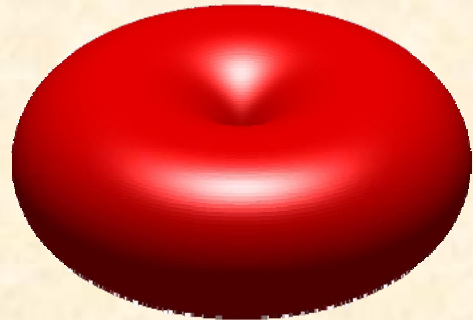
OAK RIDGE NATIONAL LABORATORY
U. S. DEPARTMENT OF ENERGY



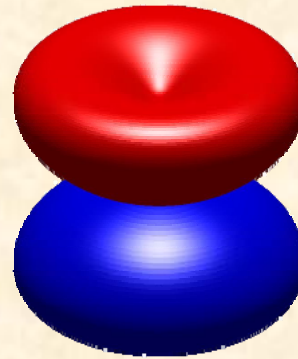
Elastic Green's function

Dielectric surface

BaTiO_3



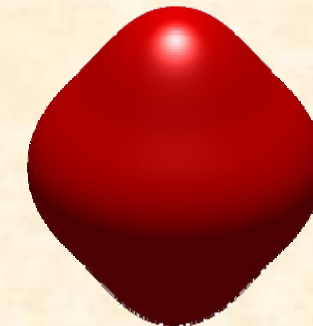
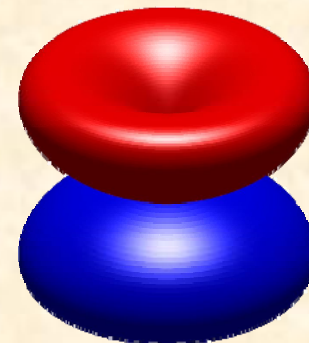
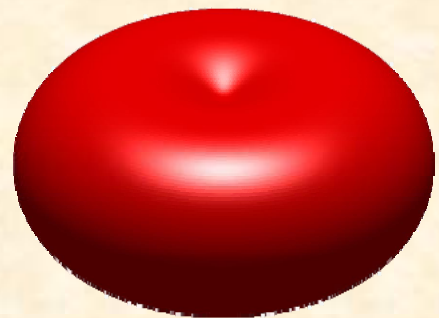
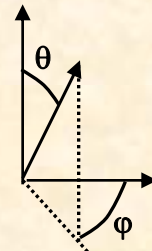
Piezoelectric surface



Elastic surface

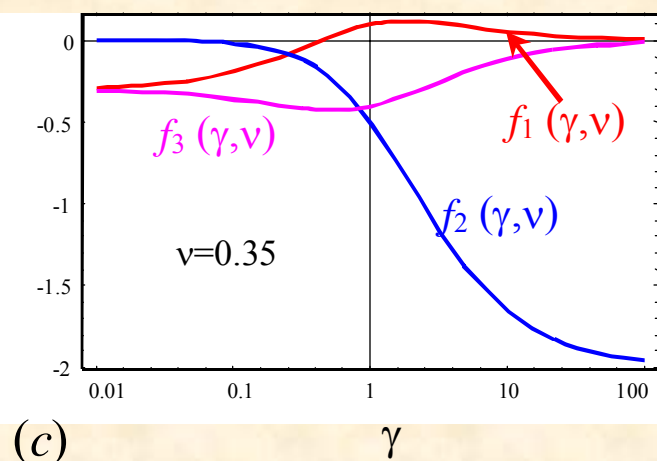
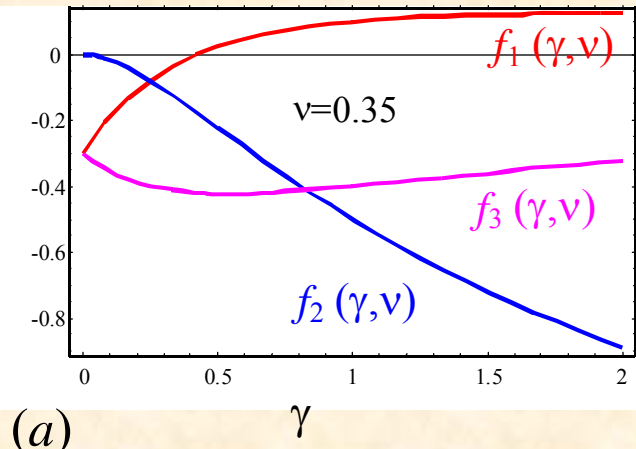


LiNbO_3



The symmetry of most ferroelectrics is close to cubic:
approximate elastic properties as isotropic!

Solution for Transversally Isotropic Material



Surface displacement:

$$u_3(\rho) = V_Q(\rho) \frac{1+\nu}{Y} (e_{31}f_1(\gamma) + e_{15}f_2(\gamma) + e_{33}f_3(\gamma))$$

where

$$f_1(\gamma) = \frac{\gamma}{(1+\gamma)^2} - \frac{(1-2\nu)}{(1+\gamma)}$$

$$f_2(\gamma) = -\frac{2\gamma^2}{(1+\gamma)^2}$$

$$f_3(\gamma) = -\left(\frac{\gamma}{(1+\gamma)^2} + \frac{(1-2\nu)}{1+\gamma} \right)$$

Response Theorem 1: For a transversally isotropic piezoelectric solid in an isotropic elastic approximation and an arbitrary point charge distribution in the tip (not necessarily constrained to a single line), the vertical surface displacement is proportional to the surface potential induced by the tip in the point of contact

Solution for General Anisotropy

For anisotropic material: $u_i(\mathbf{x}) = W_{ijkl}(\mathbf{x})e_{klj}$

where
$$W_{ijkl}(\mathbf{x}) = \int_0^{\infty} d\xi_3 \int_{-\infty}^{\infty} d\xi_3 \int_{-\infty}^{\infty} d\xi_1 \frac{1}{2} \left(\frac{\partial G_{ij}(\mathbf{x}, \xi)}{\partial \xi_l} + \frac{\partial G_{il}(\mathbf{x}, \xi)}{\partial \xi_j} \right) E_k(\xi)$$

**For dielectrically and elastically isotropic material,
we can get close-form answer:**

$$U_{111} = -\left(\frac{7 + 6(1 - 2v)}{32} \right)$$

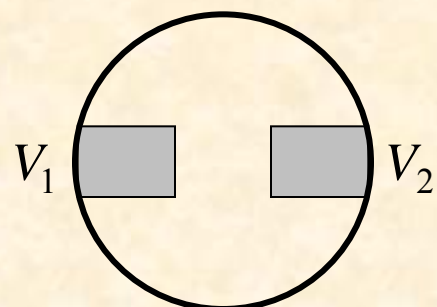
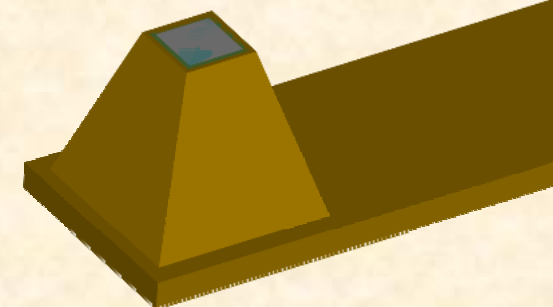
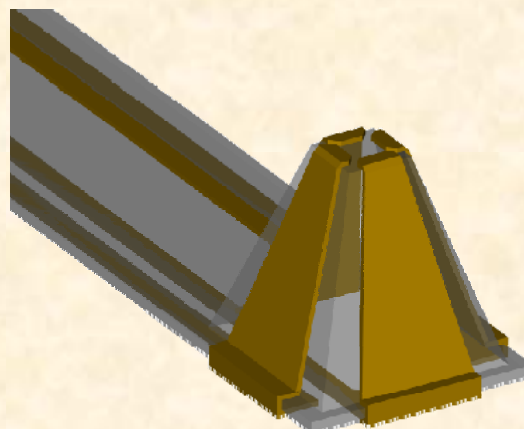
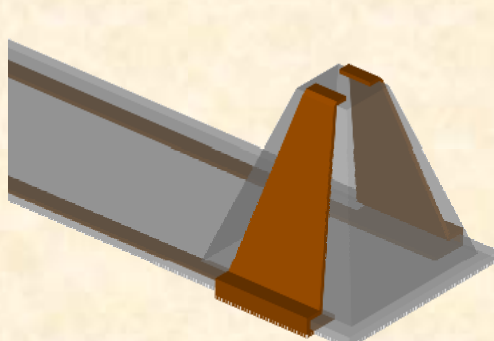
$$u_i(0) = V_Q(0) \frac{1+v}{Y} U_{iak} e_{ka}$$

$$U_{131} = \left(\frac{1 - 2(1 - 2v)}{8} \right)$$

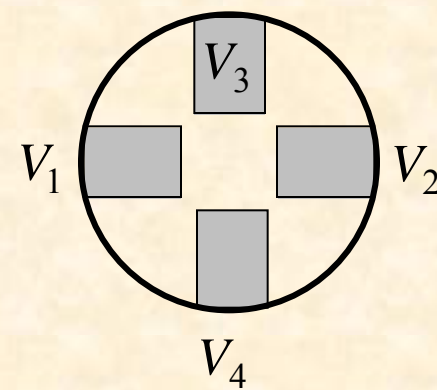
$$U_{333} = -\left(\frac{1 + 2(1 - 2v)}{4} \right)$$

Response Theorem 2: For an anisotropic piezoelectric solid in the limit of dielectric and elastic isotropy, the vertical and lateral PFM signals are proportional to the potential on the surface induced by the tip if the tip charges and the point of contact are located on the same line along the surface normal.

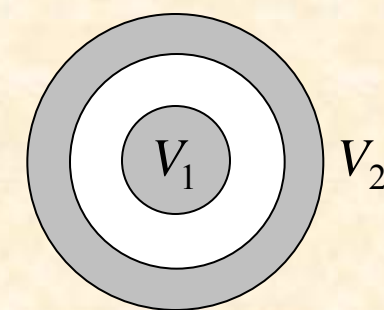
Solutions for non-standard probes



Strip-line



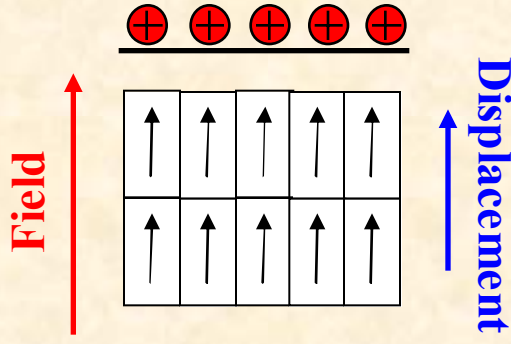
Quadrupole or rotating dipole



Shielded probe

Principles of Orientation Imaging

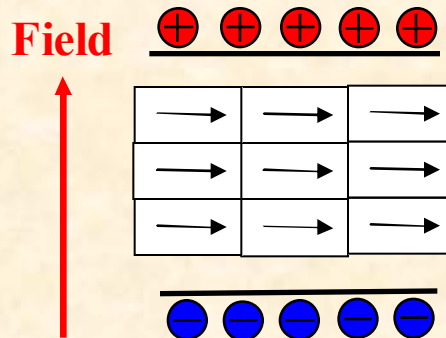
Experiment: measure the mechanical displacement in the applied electric field direction



If the field is
perpendicular to the
c-axis, the
deformation in the
field direction is zero

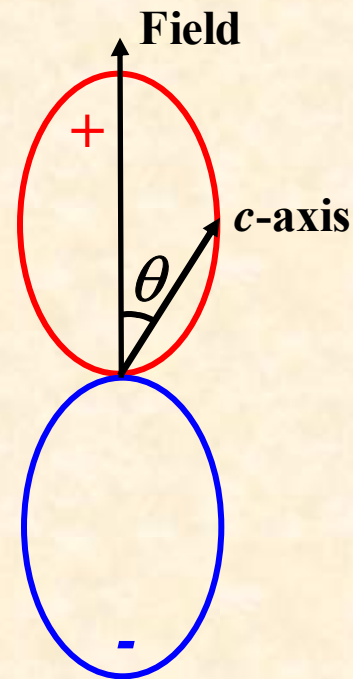
For tetragonal ferroelectric such as BaTiO₃, if the field is **parallel** to the c-axis, there is strong deformation of the crystal in the field direction

$$\delta z = d_{33} E_3 h \quad \text{or} \quad \delta z = 80 \text{V pm}$$



In the general case:

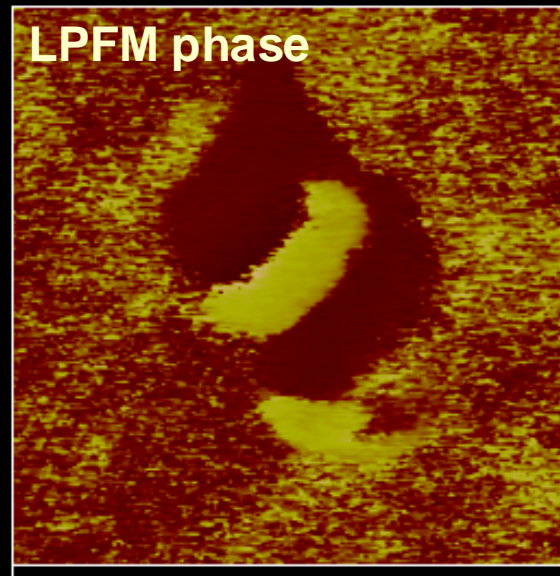
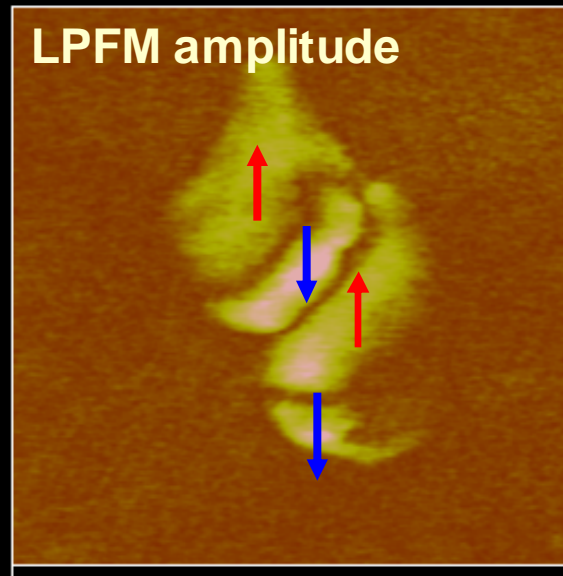
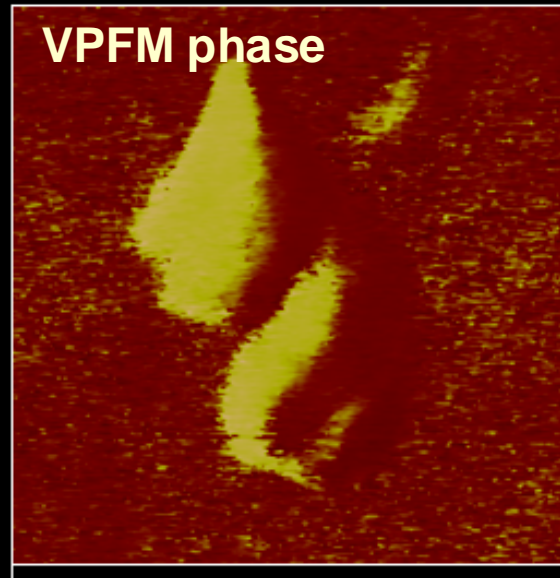
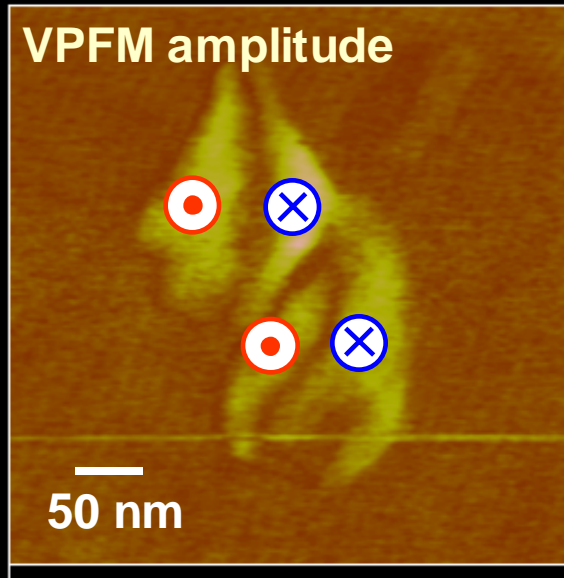
$$\delta z = (d_{15} + d_{31}) \sin^2 \theta \cos \theta + d_{33} \cos^3 \theta$$



From known electromechanical response, we can determine crystal orientation!

- small displacements (10-100 pm)
- spatially localized (< 1 μm)

Toward Single Molecule Imaging

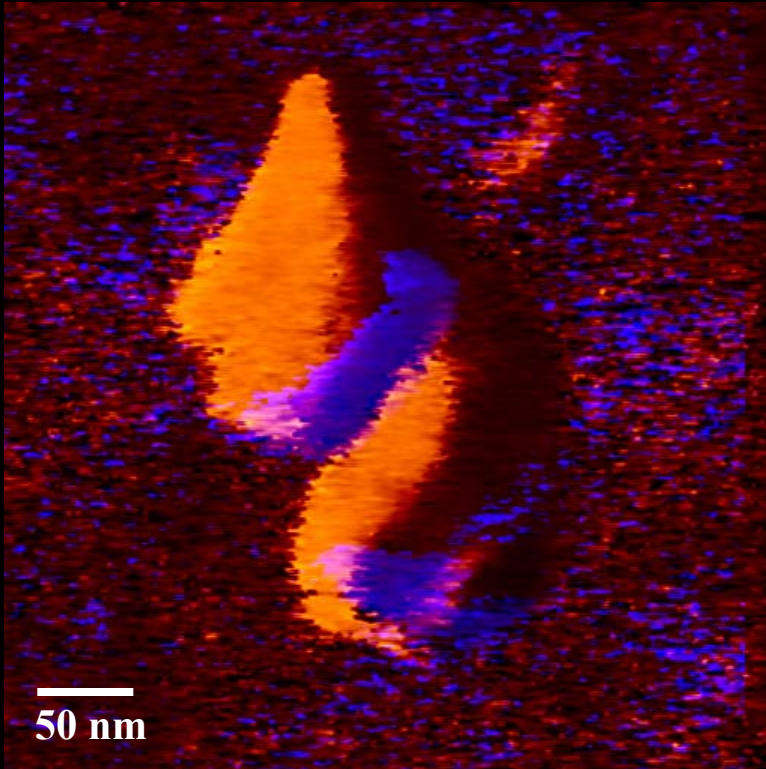


OAK RIDGE NATIONAL LABORATORY
U. S. DEPARTMENT OF ENERGY

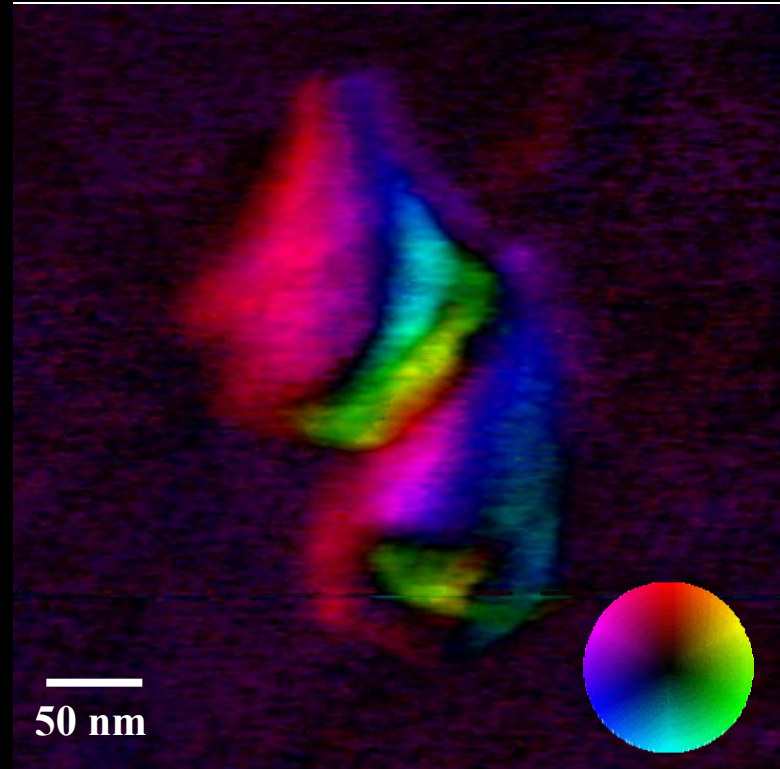


Toward Single Molecule Imaging

Combined Phase Map



2D Electromechanical Map

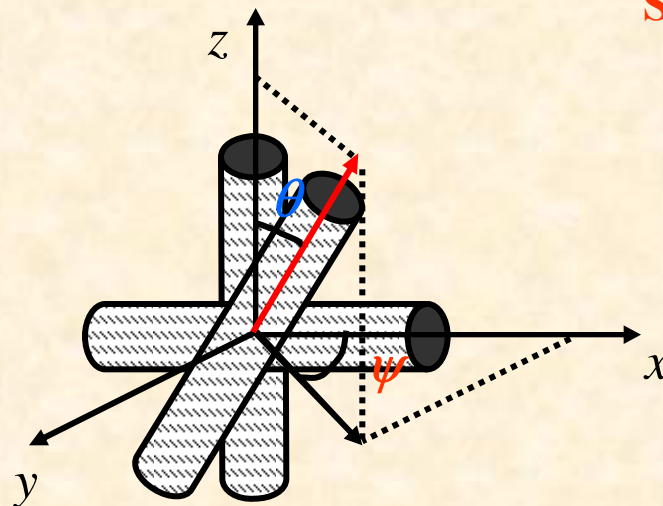


SPM opens a possibility to observe how proteins interact with hydroxyapatite crystals to form these tissues. We are moving to an exciting and completely unexplored area!

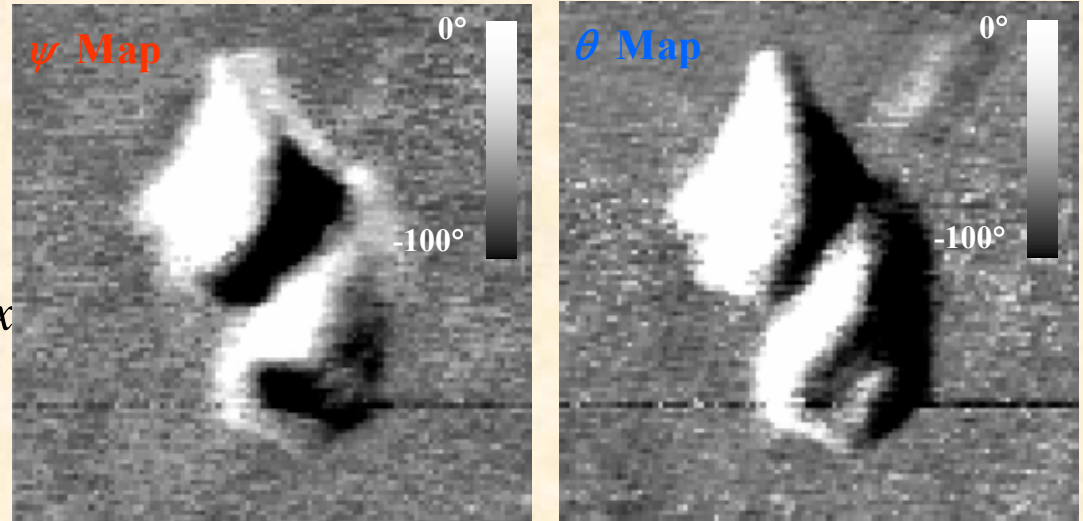
OAK RIDGE NATIONAL LABORATORY
U. S. DEPARTMENT OF ENERGY



Molecular Orientation from PFM Data



Semiquantitative Orientation Map for Collagen Fibril



Tetragonal material (4mm):

$$\begin{pmatrix} 0 & 0 & 0 & 0 & d\theta_5 & d\theta_5 \\ d\theta_1 & d\theta_3 & d\theta_1 & d\theta_5 & 0 & 0 \\ d\theta_1 & d\theta_1 & d\theta_3 & d\theta_5 & 0 & 0 \end{pmatrix}$$

↑
Vertical PFM
Lateral PFM (x)
Lateral PFM (y)

$$d_{ij} = A_{ik}(\phi, \theta, \psi) d_{kl}^o N_{lj}(\phi, \theta, \psi)$$

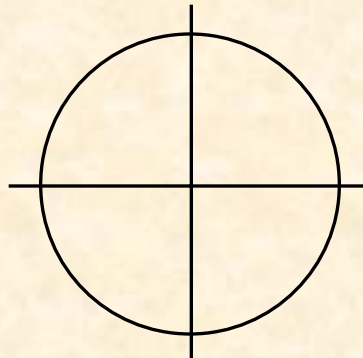
d_{ij} Piezotensor – lab coordinate system

d_{kl}^o Piezotensor – crystal coordinate system

$N_{ij}(\phi, \theta, \psi)$ $A_{ij}(\phi, \theta, \psi)$ Rotation matrices

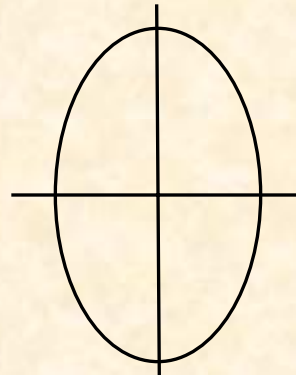
Can we do it any other way?

Scalar



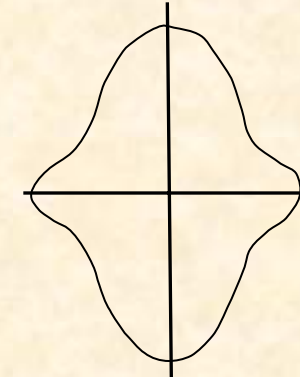
*Temperature,
Potential, etc.*

2nd order tensor



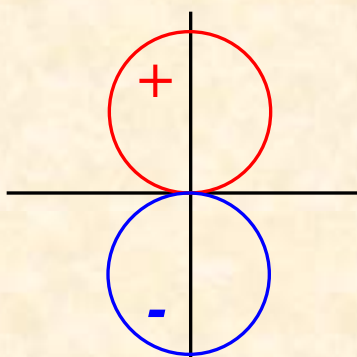
*Dielectric constant
Thermal conductivity*

4th order tensor



*Elasticity, Kerr effect
Electrostriction*

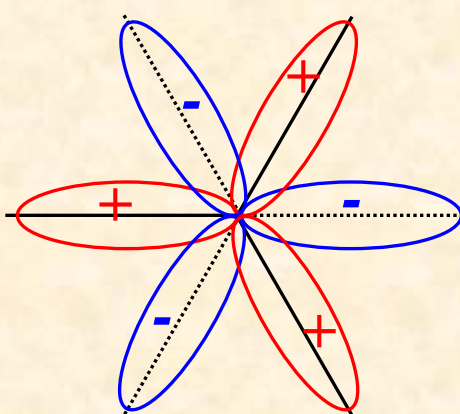
Vector



*Polarization
Magnetization
Pyroelectricity*

OAK RIDGE NATIONAL LABORATORY
U. S. DEPARTMENT OF ENERGY

3^d order tensor



*Piezoelectricity
Electrooptics, SHG*

Orientation Imaging requires:

1. Rank 3 tensor property
2. High spatial resolution
3. Insensitivity to tip geometry or easy calibration

**Piezoresponse Force
Microscopy is perfect!**

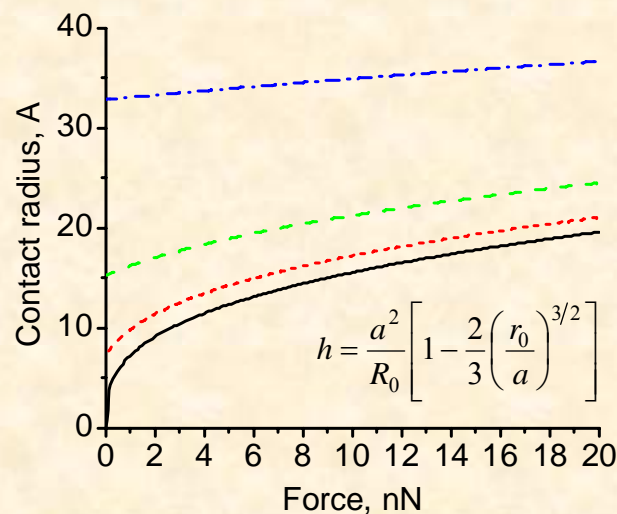
Ideally, we want to probe electromechanical behavior with ~1 pm/V sensitivity at ~0.1- 1 V excitation biases on molecular (biosystems) and unit cell (ferroelectrics) level.

What Limits the Resolution?

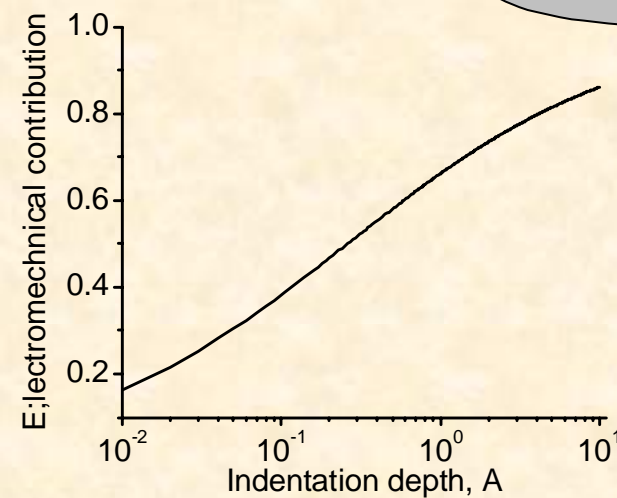
Ideally, we want to probe electromechanical behavior with $\sim 1 \text{ pm/V}$ sensitivity at $\sim 0.1 - 1 \text{ V}$ excitation biases on molecular (biosystems) and unit cell (ferroelectrics) level.

PFM limitations: contact mode technique

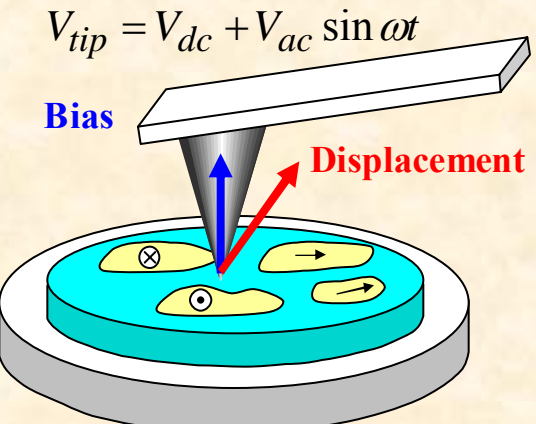
- electrostatic tip-surface interactions
- formation of liquid necks at the tip-surface junction
- large contact force – large contact area (low resolution)
- difficult to use resonant enhancement
- probing dynamic processes



$$a^3 = \frac{R_0}{E^*} \left\{ P + 3\sigma\pi R_0 + \sqrt{6\sigma\pi R_0 P + (3\sigma\pi R_0)^2} \right\}$$



$$PR = \alpha_a(h) d_3 \frac{k_1}{k_1 + k} + \frac{C'_{sphere}}{k_1 + k} (V_{dc} - V_s)$$



Resolution Theory in PFM

3.4.1. Linear imaging theory

3.4.2. Transfer function, resolution and information limit

3.4.3. Phenomenological resolution theory in PFM

- lock-in effect
- resolution function
- image reconstruction

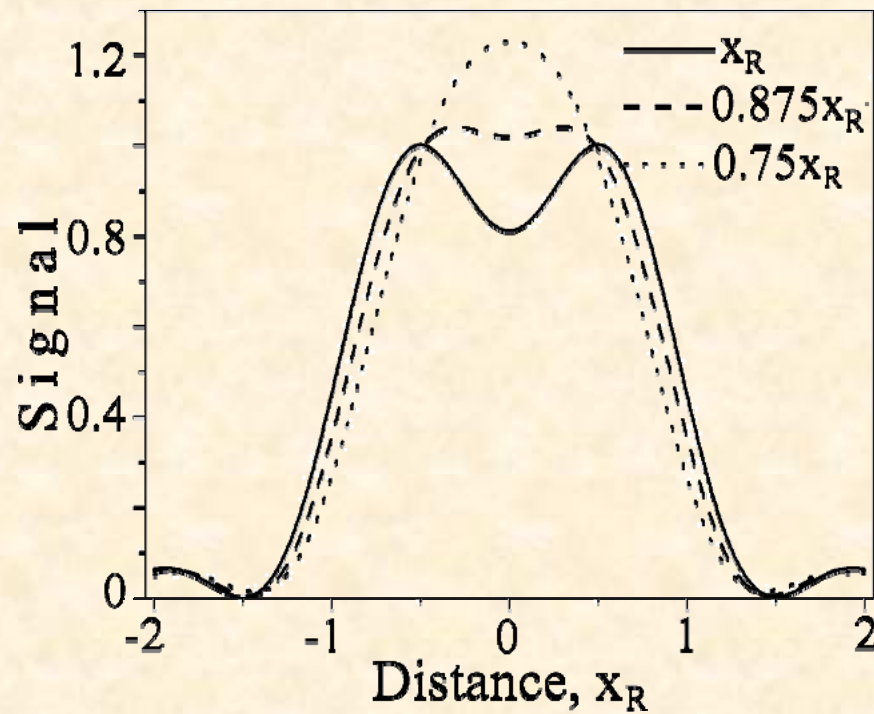
3.4.4. Analytical resolution theory in PFM

- Imaging domain walls and stripe domains
- Imaging cylindrical domains
- Effect of materials properties on resolution
- tip calibration

3.4.5. Implications for PFM data analysis

- statistical physics of domains
- domain wall width
- Writable domains
- Invisible domains

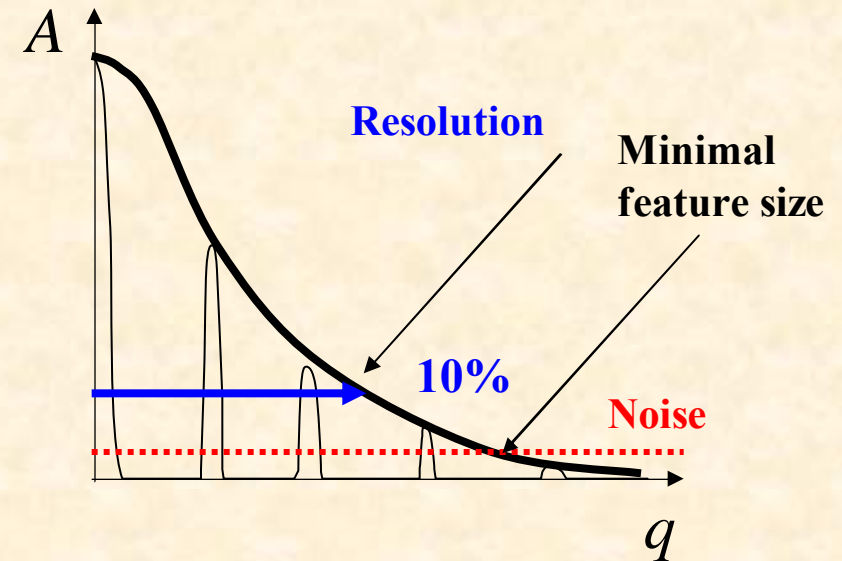
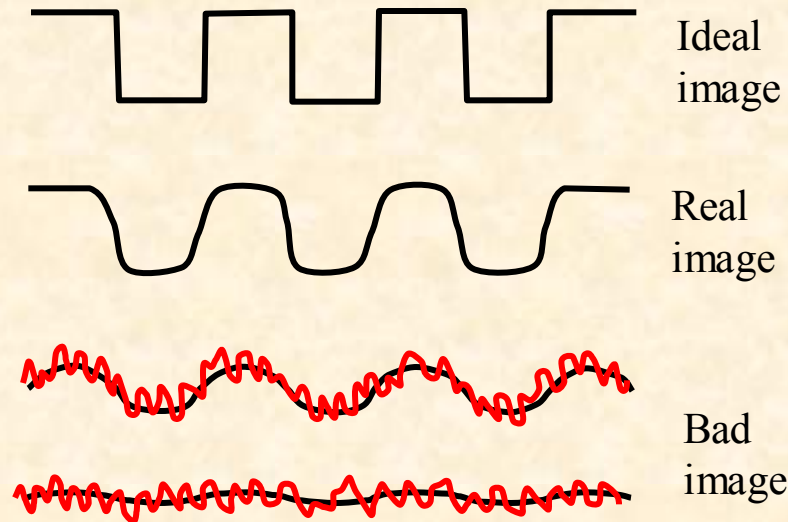
What is Resolution?



Optics: Rayleigh criterion

Transfer Function Theory

Real image always has contributions from probe and material



Linear Imaging Theory

$$\text{Linear Imaging: } I(x) = \int I_0(x-y)F(y)dy + N(x)$$

$$\text{Ideal Image: } I_0(x-y) \quad \text{Transfer function: } F(y)$$

$$\text{Real Image: } I(x) \quad \text{Noise: } N(x)$$

$$\text{Fourier Transform: } I(q) = I_0(q)F(q) + N(q)$$

$$\text{Image Reconstruction: } I_0(q) = I(q)/F(q)$$

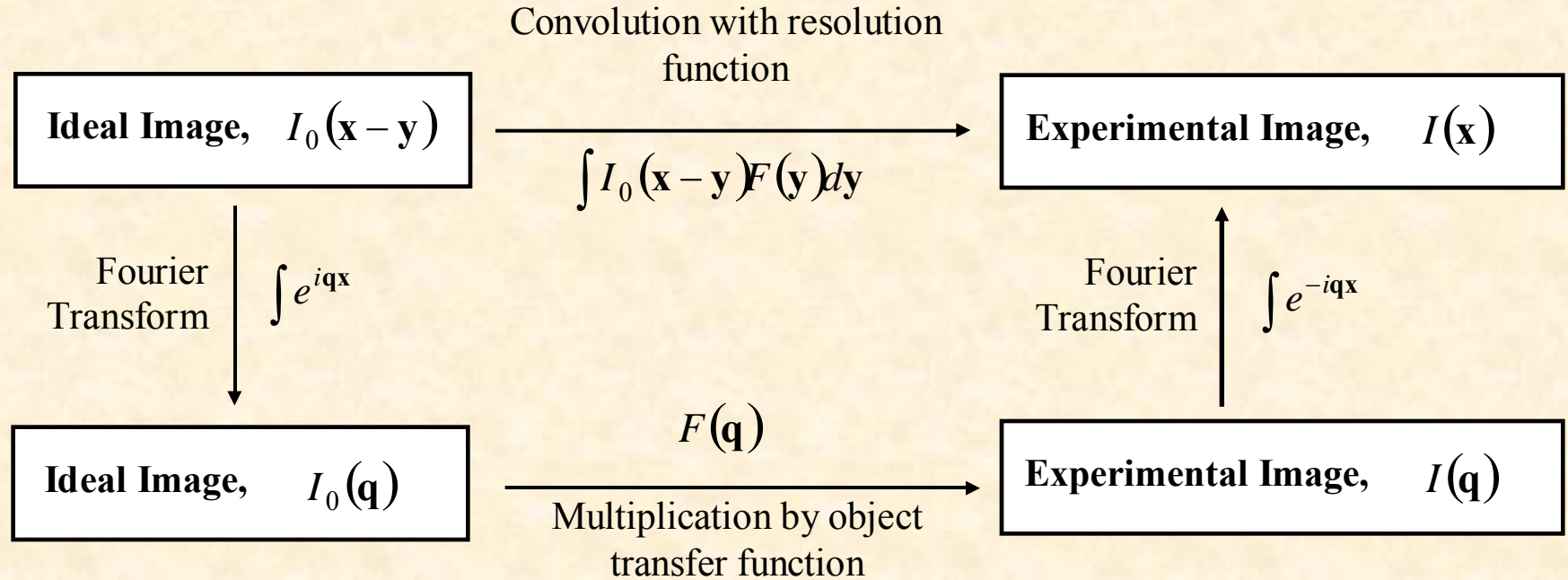
- Ideal image has all Fourier components
- Transfer function decays for high k

We can define lateral resolution as:

- q for which $\text{TF} = 0.1 \text{ TF}(q=0)$
- smallest feature we can detect:

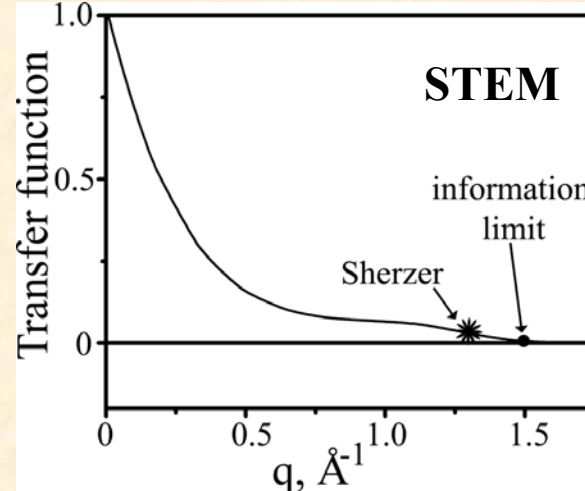
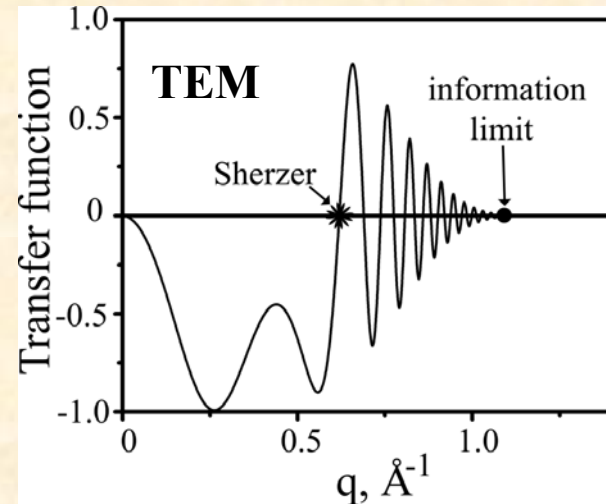
$$I_0(q)F(q) = N(q)$$

Transfer Function Theory

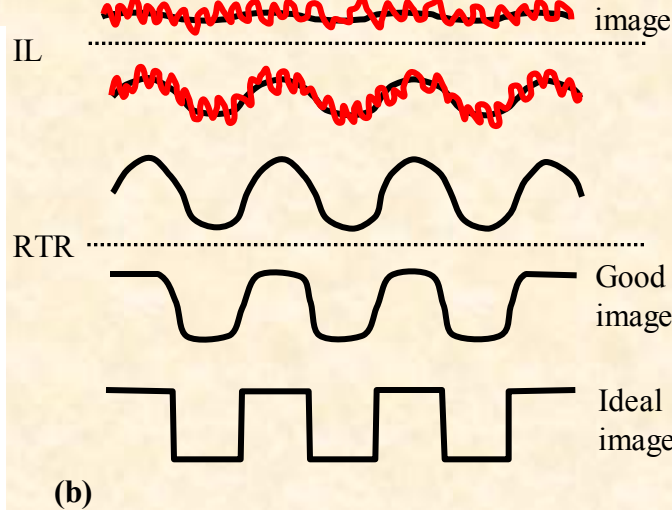
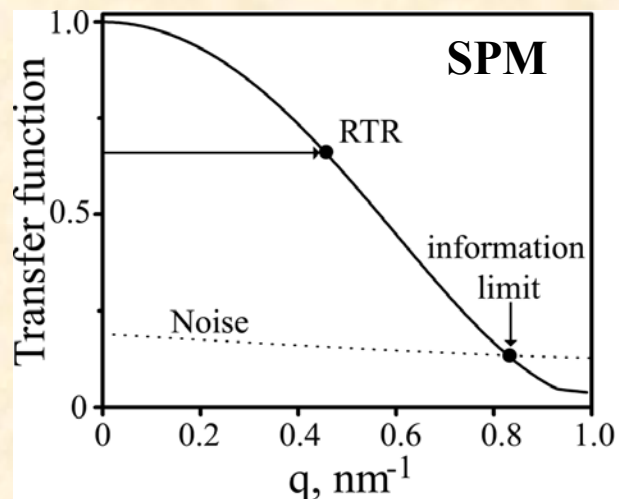


- Establish the resolution and information limits in PFM and its dependence on tip geometry and materials properties
- Develop the pathways for calibration of tip geometry
- Interpret the imaging and spectroscopy data in terms of intrinsic parameters
- Reconstruct the ideal image from experimental data,

Resolution in Transfer Function Theory



In electron microscopy, zeroes in transfer function define Sherzer resolution
Information limit corresponds to frequencies above which there is no information transfer



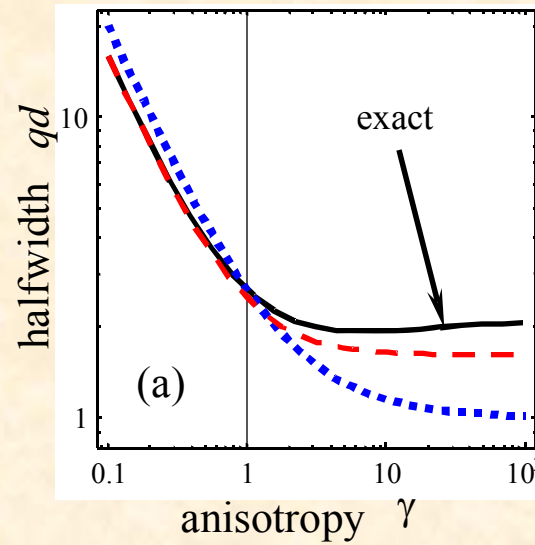
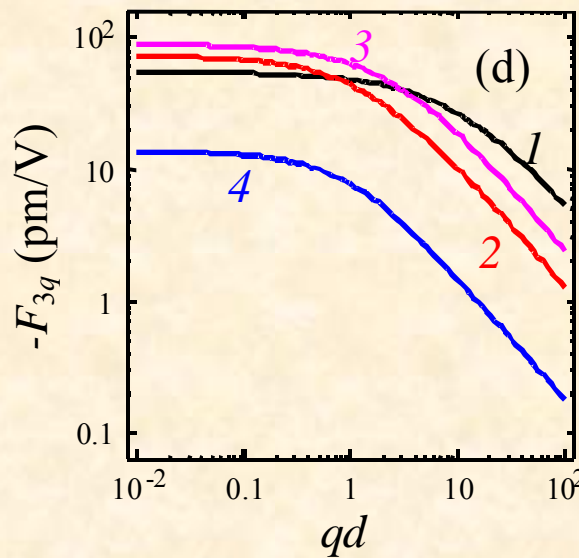
Resolution in PFM

In decoupled approximation, PFM image formation mechanism is linear if material is uniform in z-direction, $d_{mnk}(y - \mathbf{x}'', z) = d_{mnk}(y - \mathbf{x}'')$

PFM Image: $u_3(\mathbf{0}, \mathbf{y}) = \int_{-\infty}^{\infty} d_{mnk}(\mathbf{y} - \xi) F(\xi_1, \xi_2) d\xi_1 d\xi_2$

Transfer function: $F(\xi_1, \xi_2) = \int_{z=0}^{\infty} c_{jlmn} E_k(-\xi_1, -\xi_2, z) \frac{\partial}{\partial \xi_l} G_{3j}(\xi_1, \xi_2, z) dz$

We calculate the resolution function in analytical form:



Point charge model

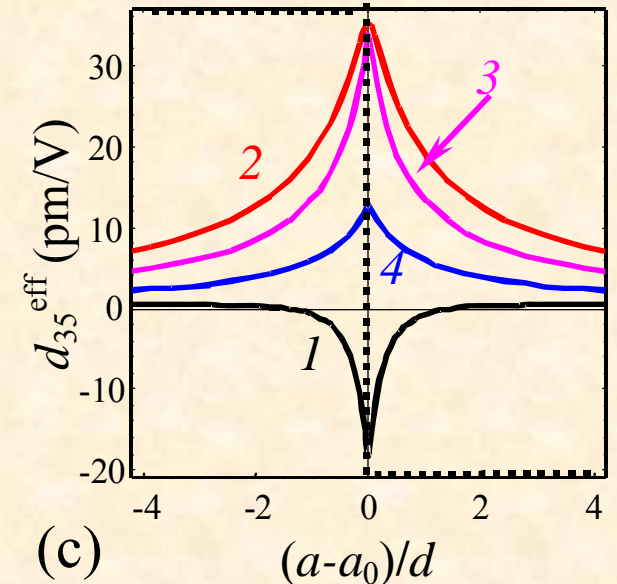
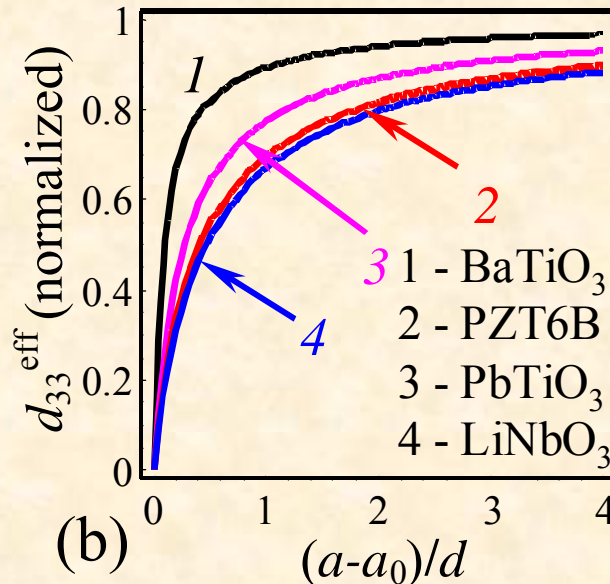
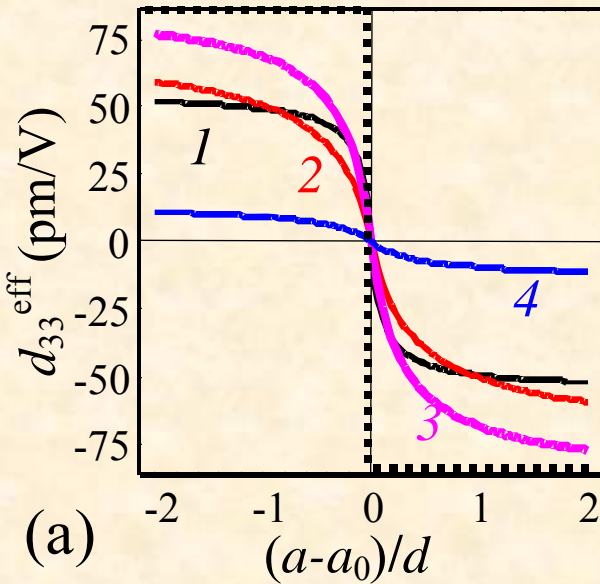
$$r_{\min} \approx \frac{\gamma \epsilon_e R_0}{2\kappa} \frac{1+2\gamma}{(1+\gamma)^2}$$

Sphere-plane model

$$r_{\min} \approx \frac{\gamma \epsilon_e R_0}{\epsilon_e + \kappa} \frac{1+2\gamma}{(1+\gamma)^2}$$

Domain wall profile

Domain wall profile is a natural observable in PFM



Vertical PFM

$$d_{33}^{\text{eff}} \approx d_{03} + \left[\frac{3}{4} \left(d_{33} + \left(\frac{1}{3} + \frac{4}{3}v \right) d_{31} \right) \frac{s}{|s| + 1/4} + \frac{1}{4} d_{15} \frac{s}{|s| + 3/4} \right]$$

Lateral PFM

$$d_{35}^{\text{eff}} \approx d_{01} + d_{33} \frac{3/8}{1+3|s|} + d_{31} \left(-\frac{3/8}{1+3|s|} + \frac{1+v}{1+4|s|} \right) + d_{15} \frac{2/\pi - 3/8}{1+(8/\pi - 3/2)|s|}$$

We can use domain wall profile to calibrate the tip!

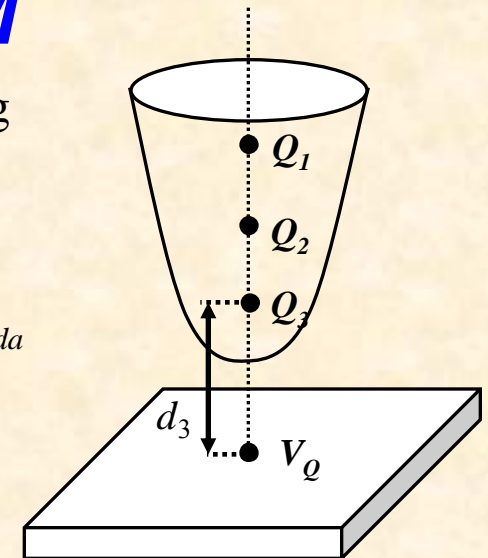
OAK RIDGE NATIONAL LABORATORY
U. S. DEPARTMENT OF ENERGY



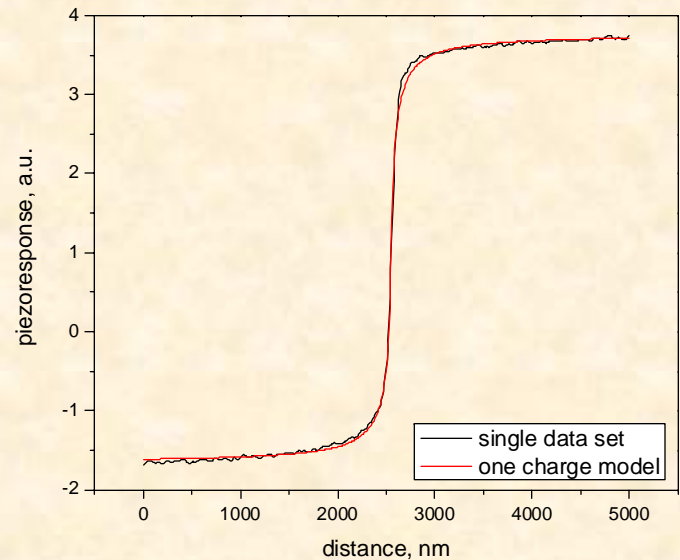
Tip Calibration in PFM

We can determine tip parameters by fitting domain wall profile using model of superposition of point charges

$$F[u_3] = \int \left(PR(a) - \frac{1}{2\pi\epsilon_0(\epsilon_e + \kappa)} \sum_{m=0}^N \frac{Q_m}{d_m} \left(g_{313}\left(\frac{a-a_0}{d_m}, \gamma, \nu\right) d_{31} + g_{351}\left(\frac{a-a_0}{d_m}, \gamma\right) d_{15} + g_{333}\left(\frac{a-a_0}{d_m}, \gamma\right) d_{33} \right)^2 \right) da$$



Material	ϵ_e	Width, nm	Q	d , nm
LiNbO ₃	1	96	1000	92
Epitaxial PZT	1	107	2550	125
PZT in air	1	58	723	86.5
PZT in liquid	80	6	104	11.8

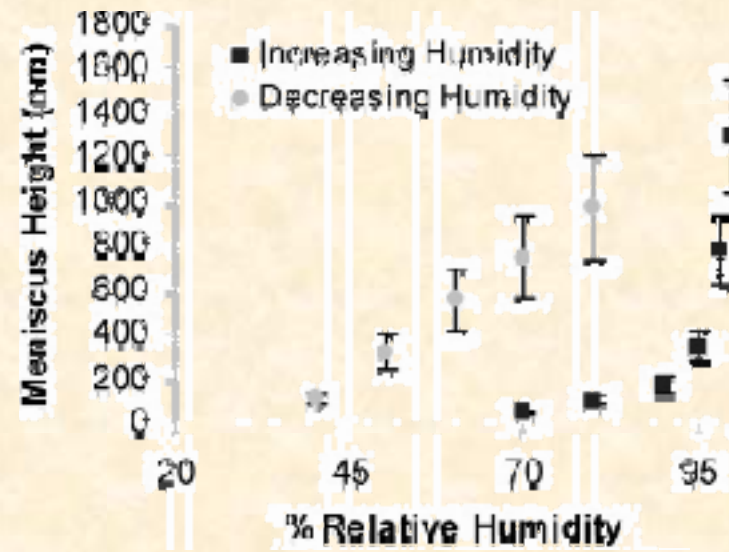
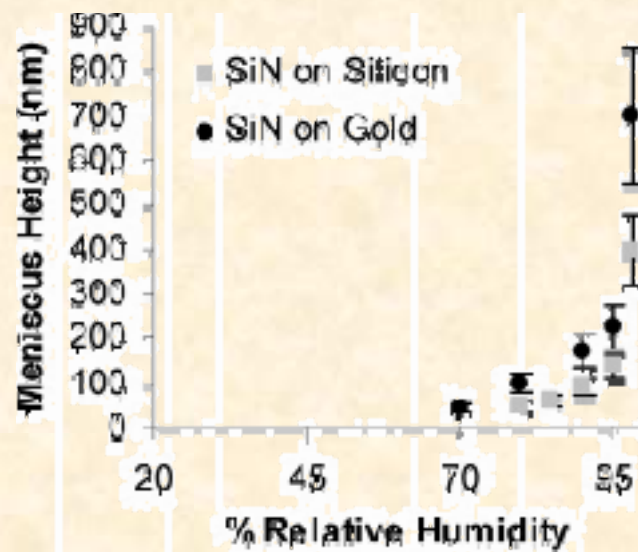
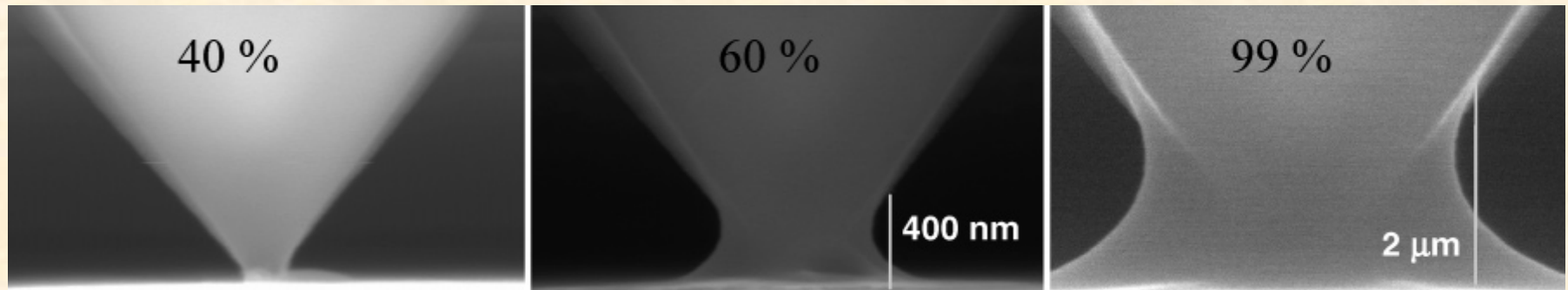


Surprisingly, single charge provides good description

OAK RIDGE NATIONAL LABORATORY
U. S. DEPARTMENT OF ENERGY

UT-BATTTELLE

Why is Tip so Large?

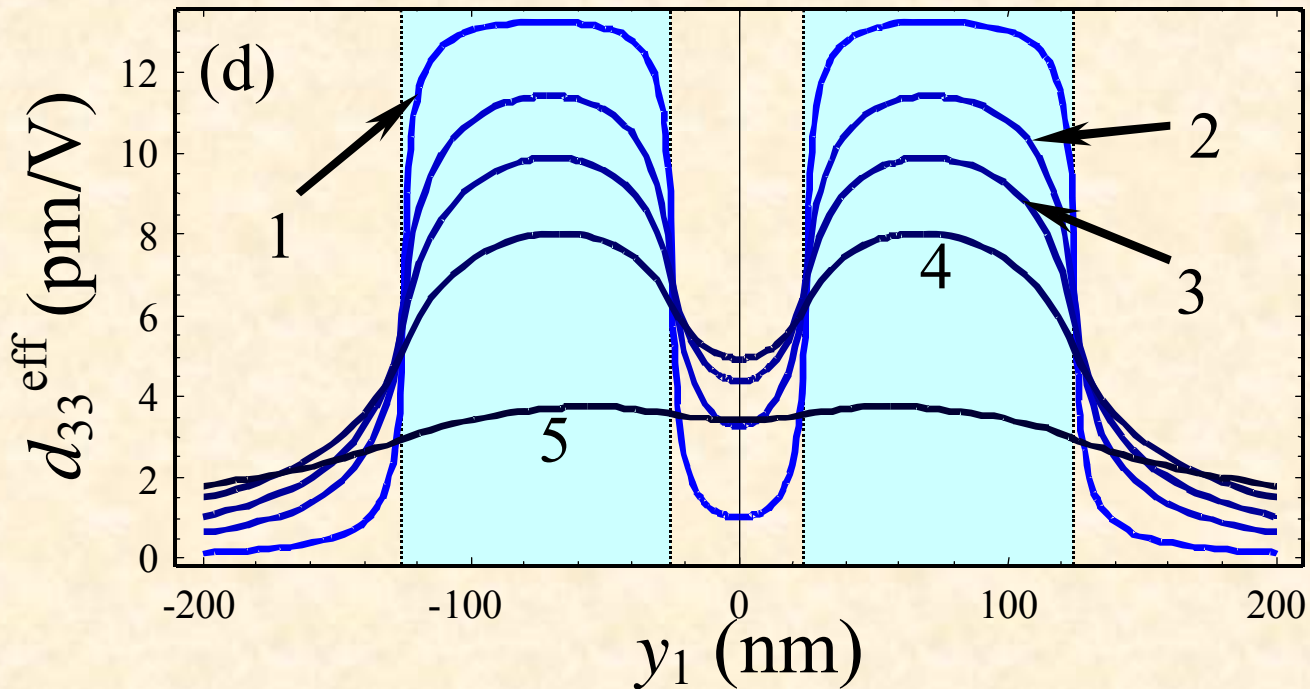


Langmuir 21, 8096-8098 (2005)

OAK RIDGE NATIONAL LABORATORY
U. S. DEPARTMENT OF ENERGY

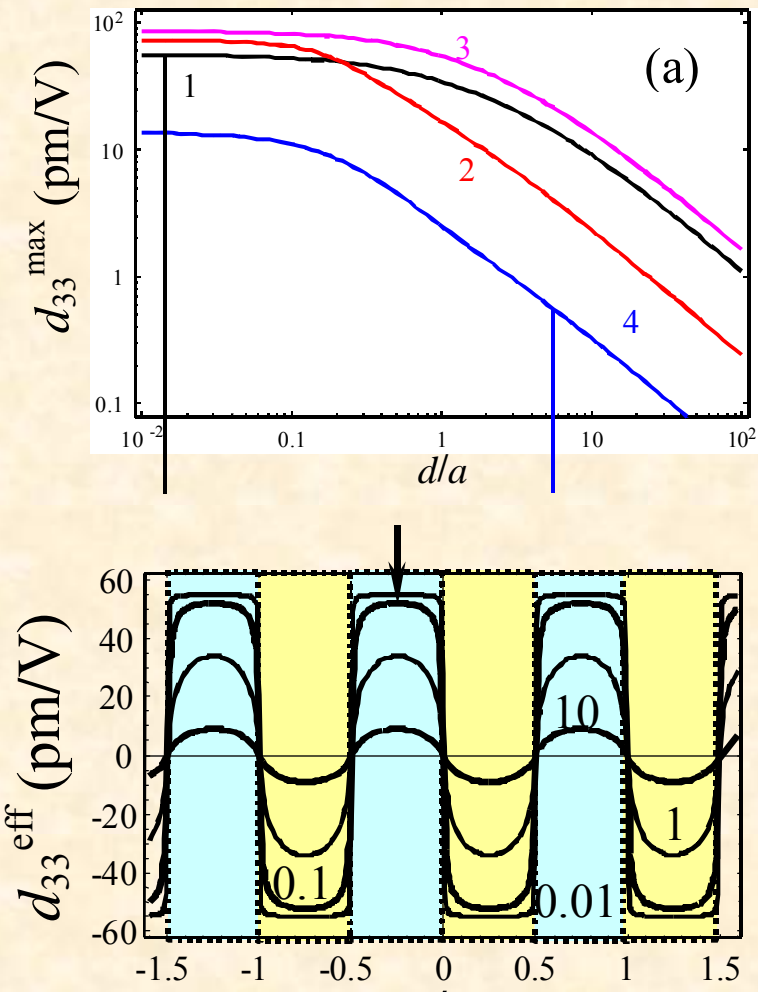
UT-BATTELLE

Effect of finite resolution on imaging



- For low resolutions, domains are difficult to distinguish
- Signal in the center of domain decreases
- However, the domains are always visible

Periodic Domain Structures



Ideal Image

$$d_{klj}(y) = d_{klj} \sum_{n=0}^{\infty} \frac{4}{(2n+1)\pi} \sin\left(\frac{2\pi}{a}(2n+1)y_1\right)$$

Real Image

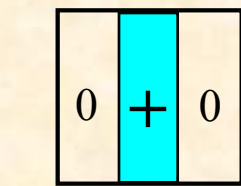
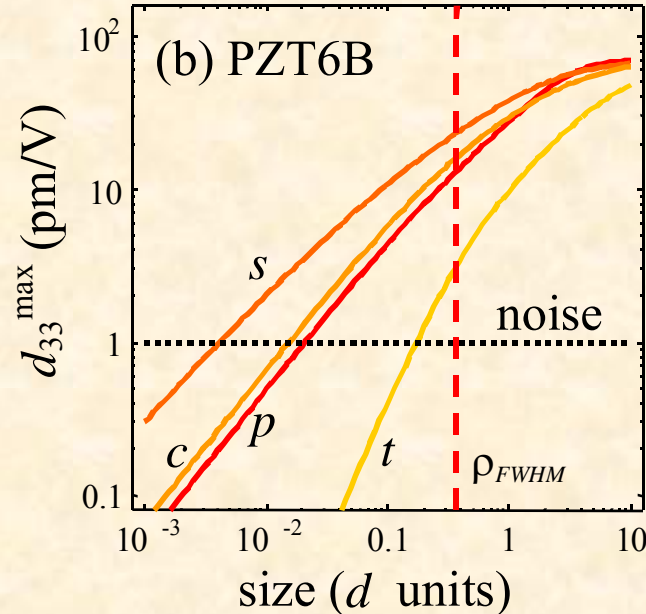
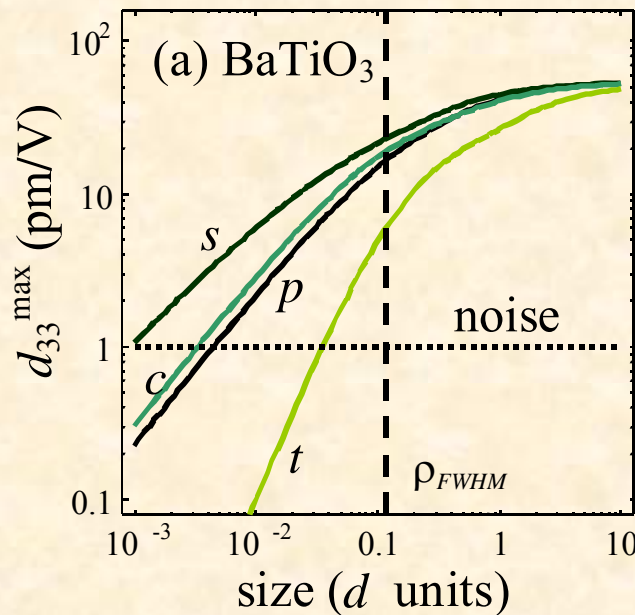
$$u_3(a, y_1) = \sum_{n=0}^{\infty} \frac{4}{(2n+1)\pi} \sin\left(\frac{2\pi}{a}(2n+1)y_1\right) F_q\left(\frac{2\pi}{a}(2n+1)\right)$$

For low resolution, only one component survives:

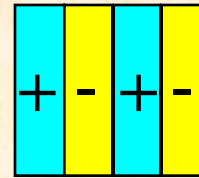
$$u_3(y) = \frac{4}{\pi} \sin\left(\frac{2\pi y_1}{a}\right) F_q\left(\frac{2\pi}{a}\right)$$

Information Limit

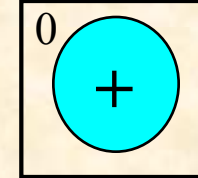
The smallest visible feature size is determined by the noise level of the system



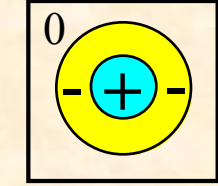
single stripe (s)
size = a/d



periodic stripes (p)
size = a/d



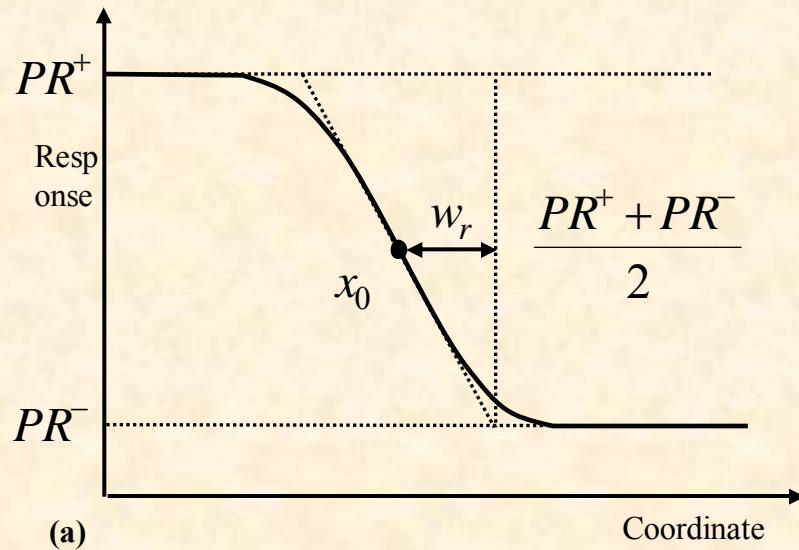
cylinder (c)
size = r/d



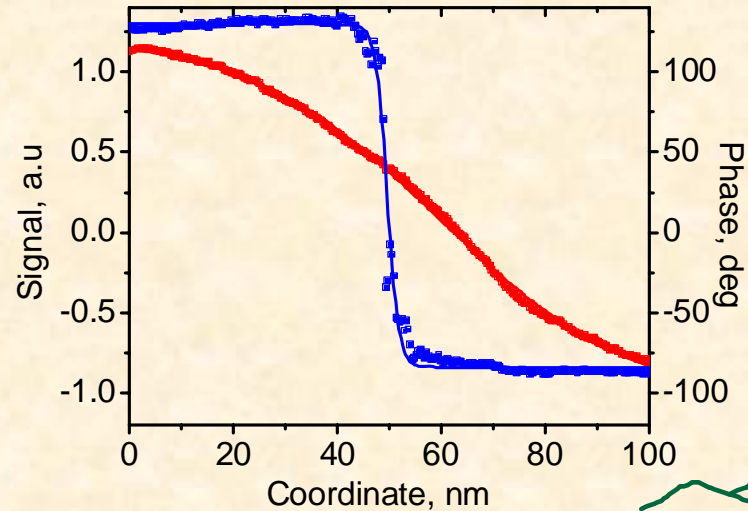
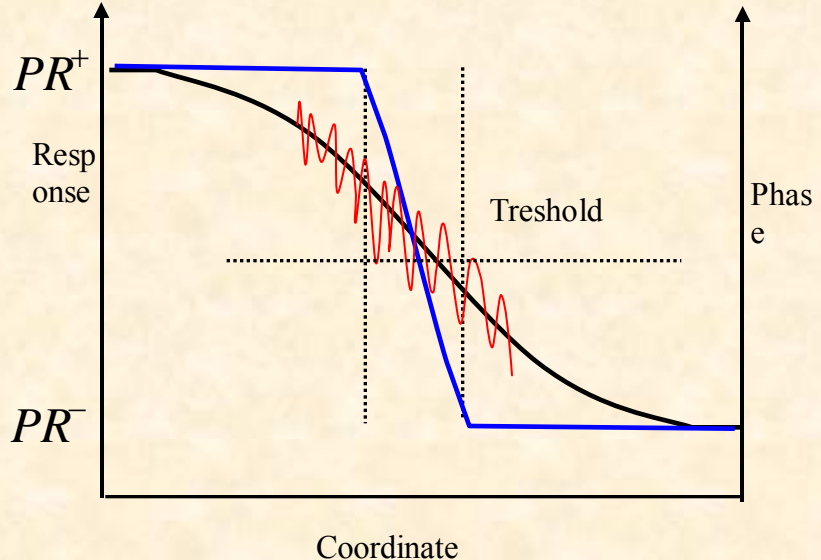
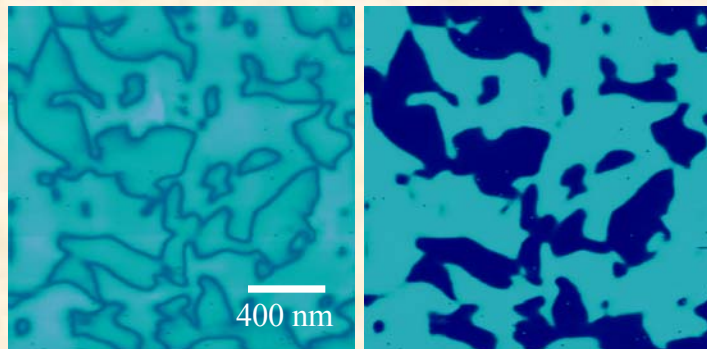
nested cylinders (t)
size = r_o/d

Information Limit

Raleigh resolution in phase image is equal to information limit in mixed signal image



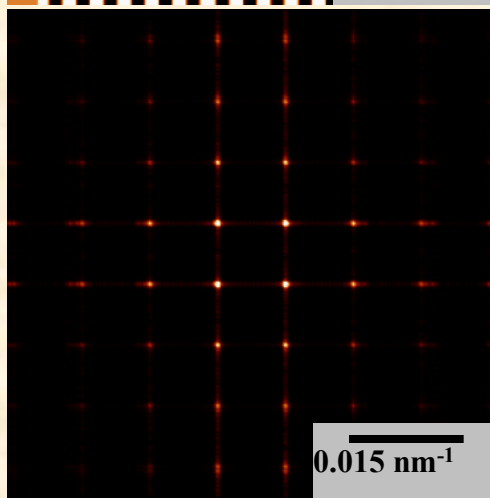
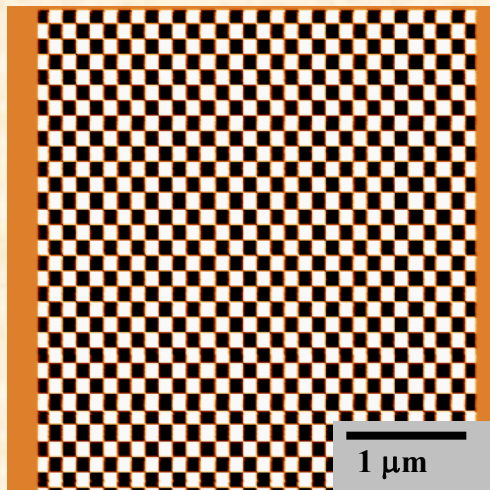
(a)



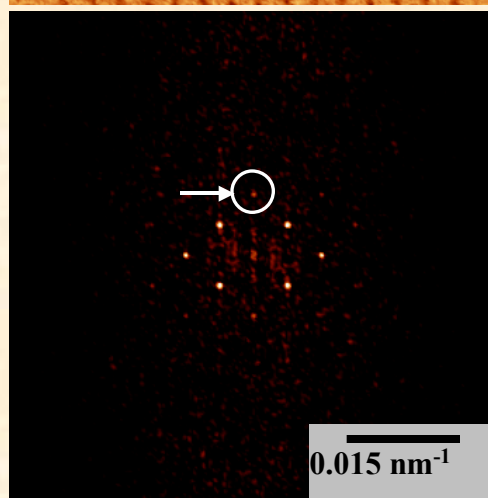
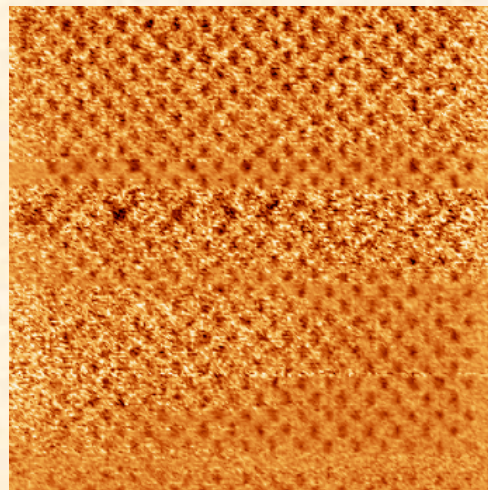
UT-BATTELLE

Lock-In Effect on Imaging

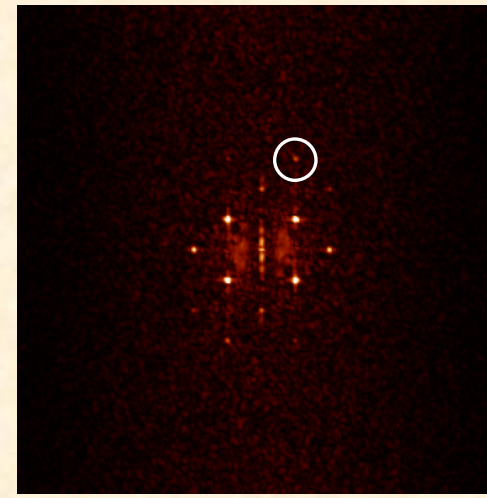
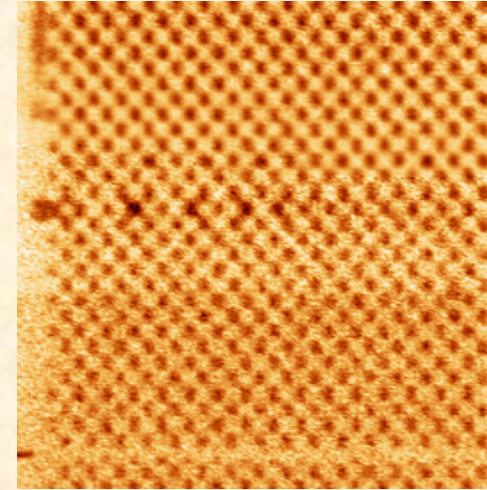
Time in each point ~ 4 ms



Ideal Image

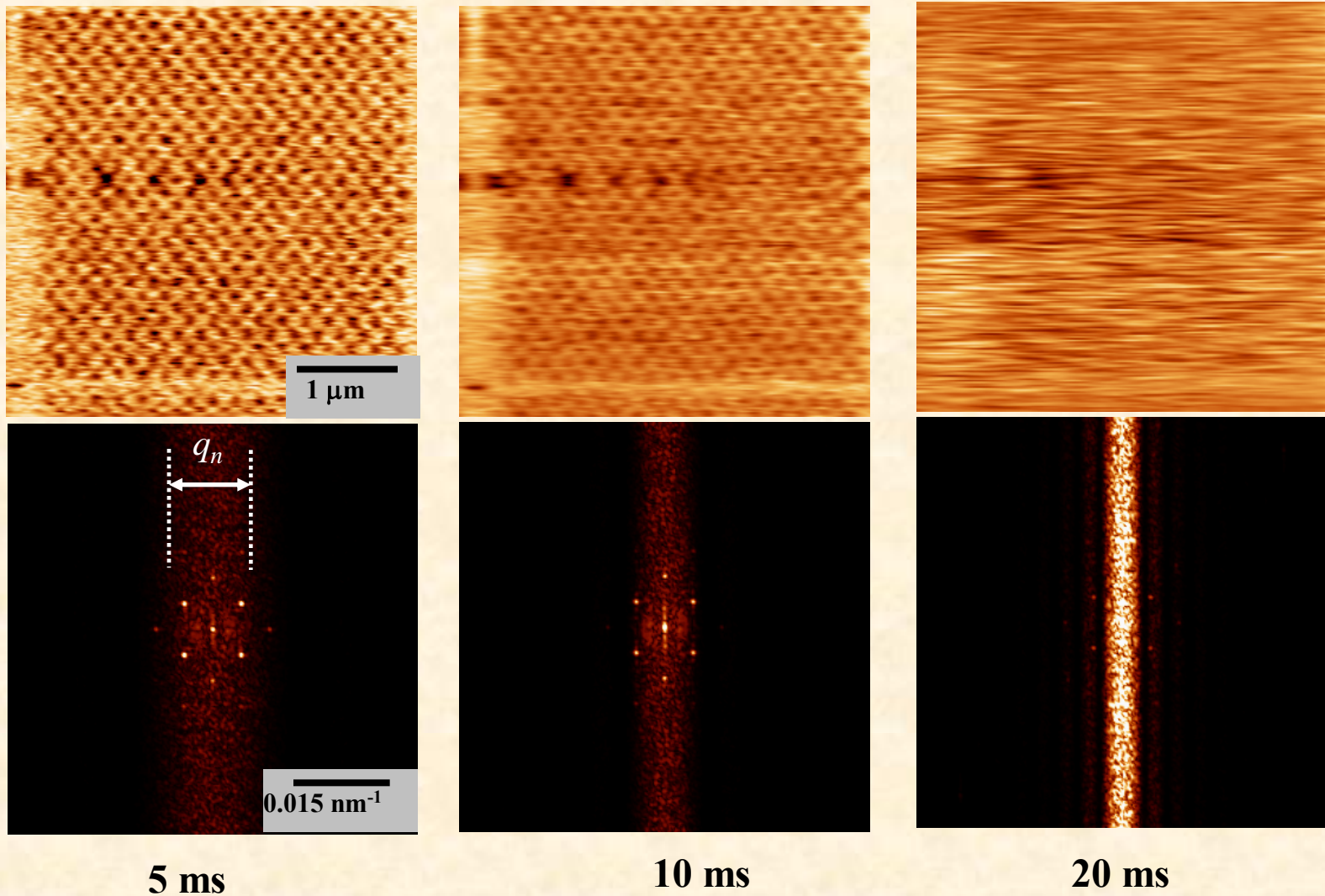


0.5 ms



1 ms

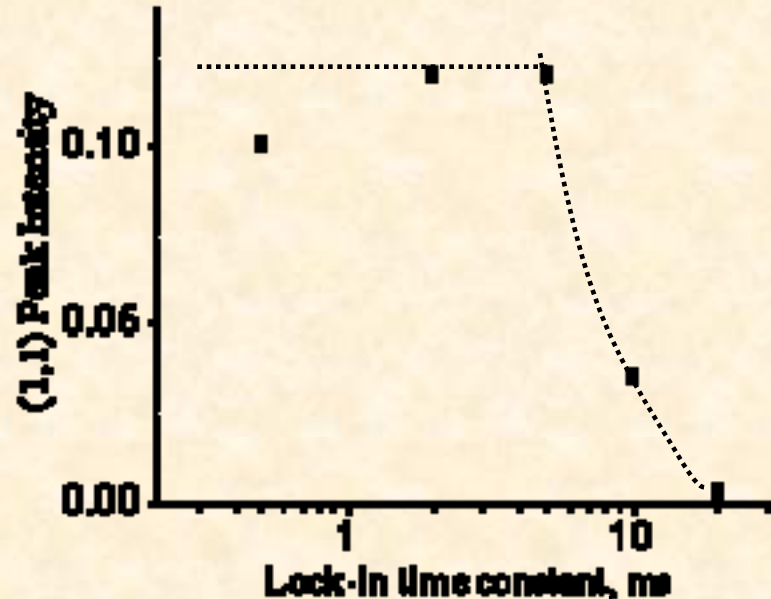
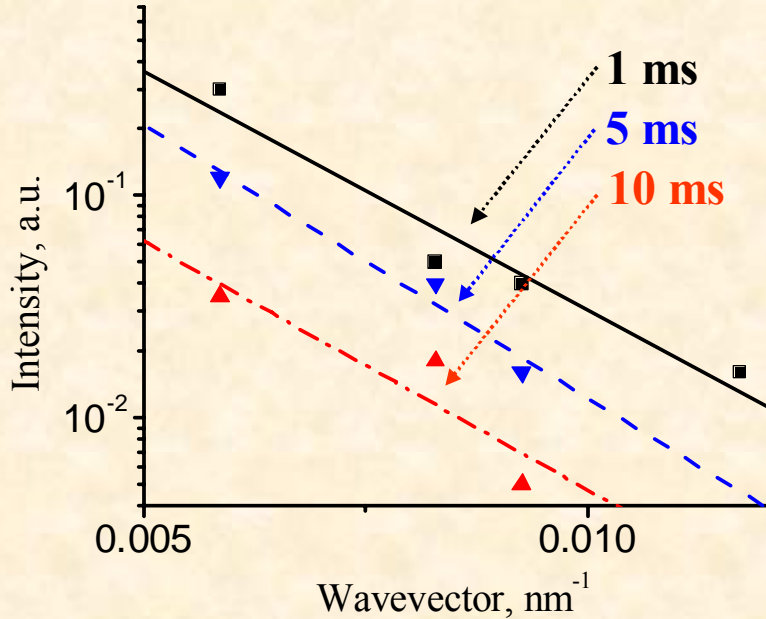
Lock-In Effect on Imaging



OAK RIDGE NATIONAL LABORATORY
U. S. DEPARTMENT OF ENERGY



Lock-In Effect on Imaging



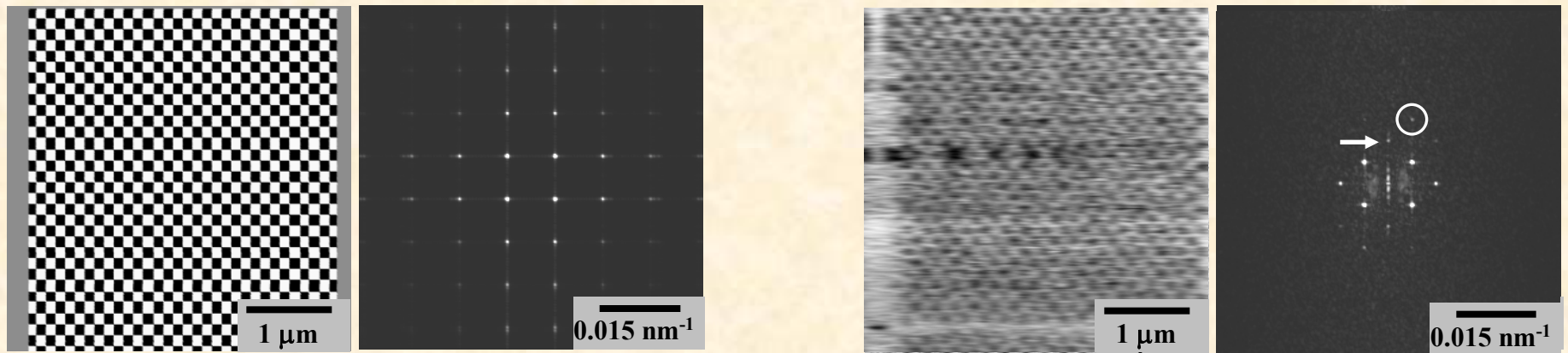
The wavevector dependence of peak intensity: $I(hk) = I_0 \exp(-q/G)$

Resolution function is a product of lock-in and tip parts: $F(\mathbf{q}) = F_{tip}(q)F_{la}(q_x)$

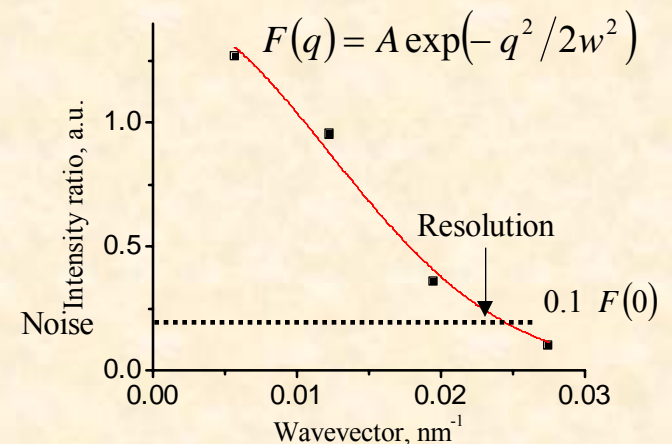
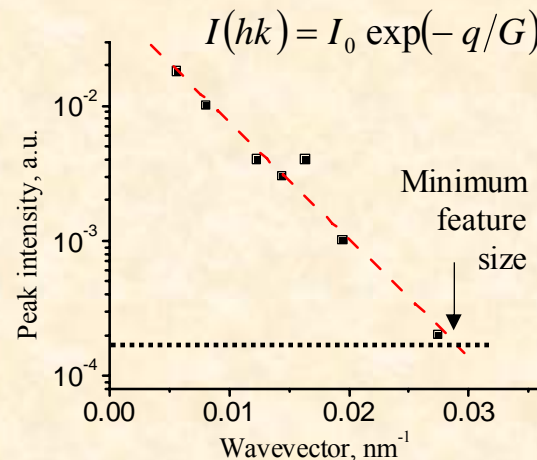
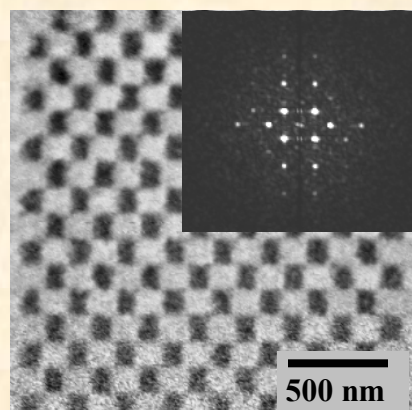
For small time constants $\tau \ll \tau_{pixel}$ we have $F_{la}(q_x) = 1$ but $N(q) \sim \sqrt{\tau_{pixel}/\tau}$

For large time constants noise is small, but image is streaky

Application of Linear Imaging Theory to PFM



Checkerboard standard



Transfer Function and Image Reconstruction

Variable mesh size standard

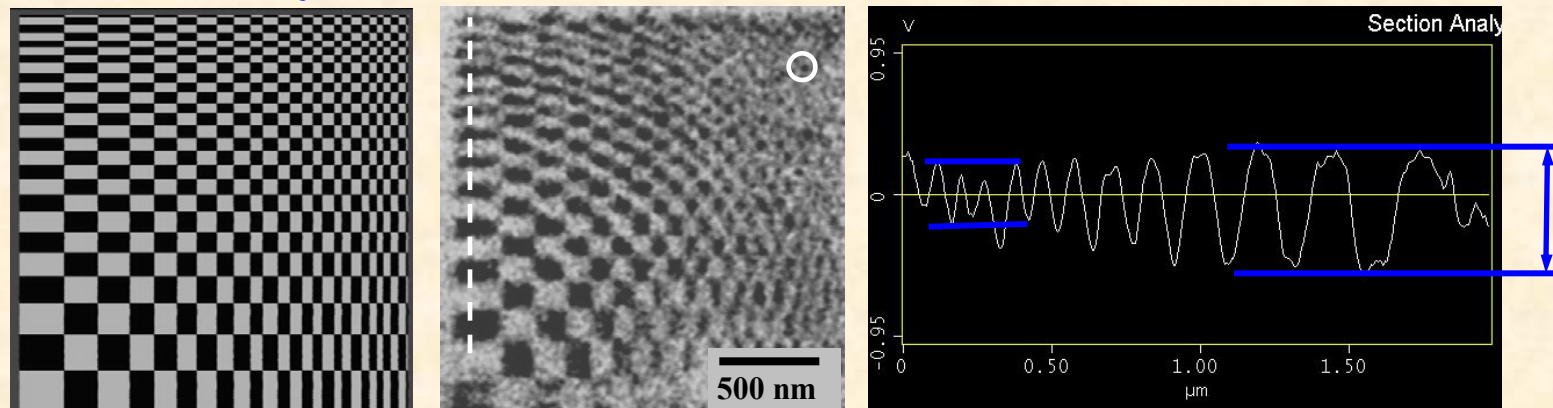
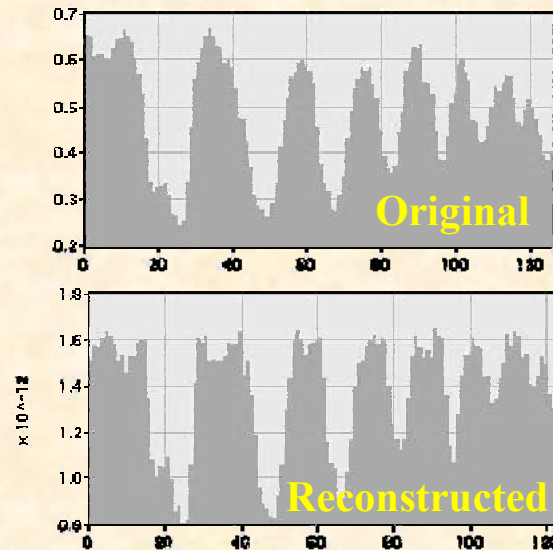
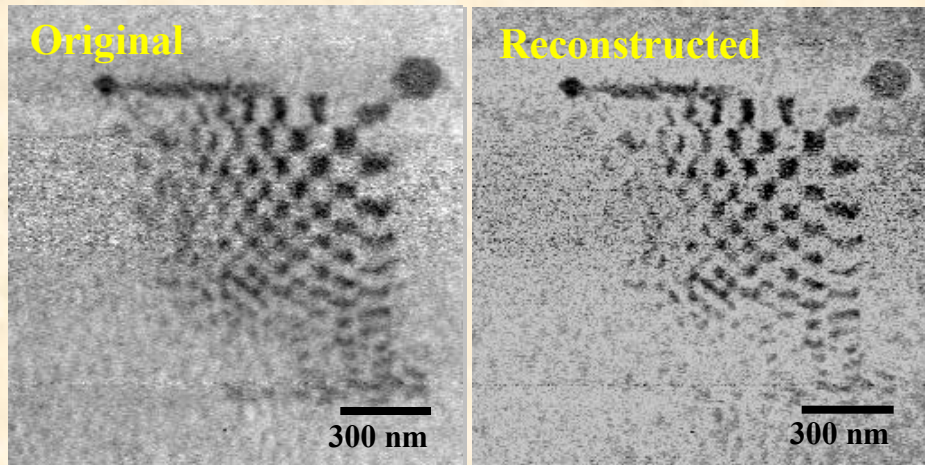
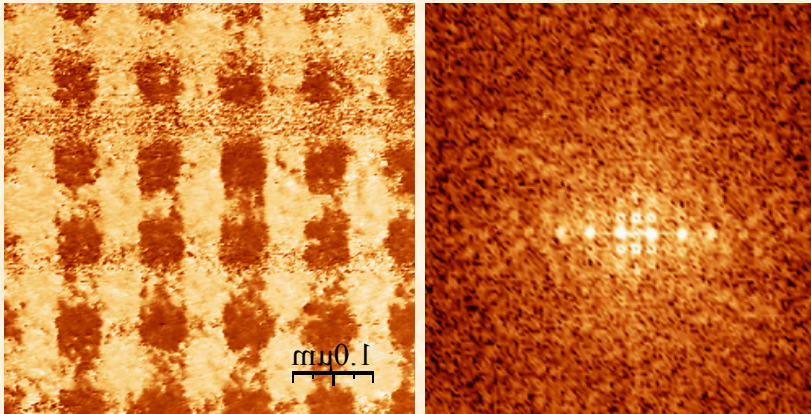


Image reconstruction using transfer function



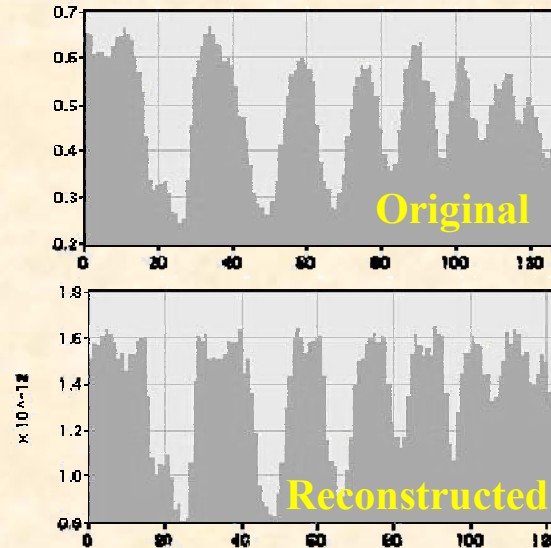
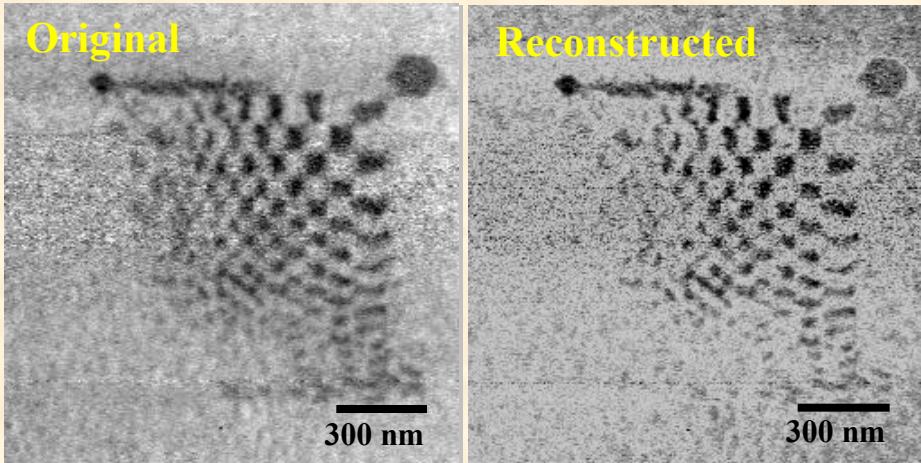
- Variable mesh size standard allow determination of minimal writable/detectable domain size
- Checkerboard standard allows resolution to be determined
- For epitaxial PZT film, minimum domain size is determined by resolution, rather then writing process
- Using known transfer function, PFM image can be reconstructed from experimental data.

Transfer Function and Image Reconstruction



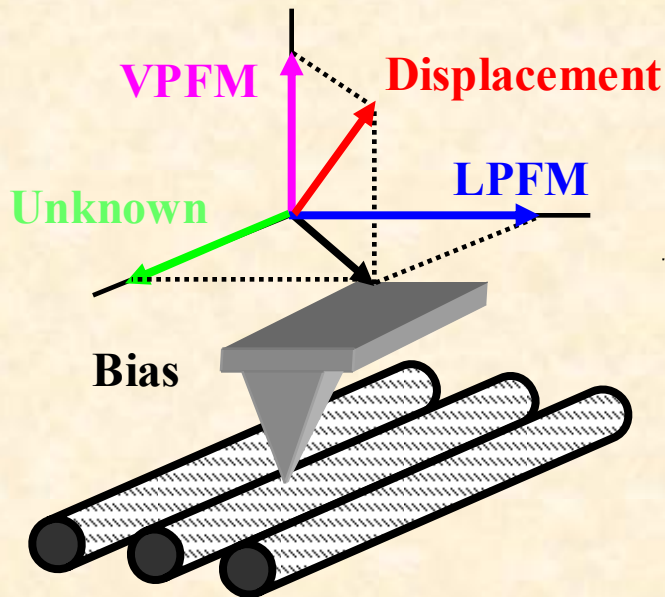
For sol-gel and inhomogeneous films, minimum domain size can be much larger than resolution as controlled by microstructure

Image reconstruction using transfer function



Using known transfer function, PFM image can be reconstructed from experimental data.

Dynamics in PFM



Several competing contributions:

1. Vertical surface response
2. Longitudinal response
3. Torsional response
4. Local electrostatic force
5. Distributed electrostatic force

General calibration:

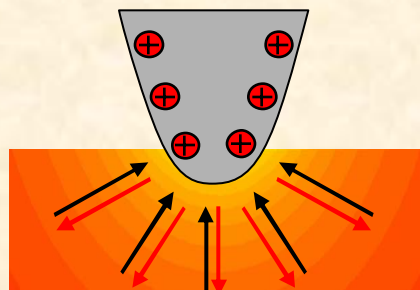
$$\begin{pmatrix} xPR_v \\ xPR_l \\ yPR_v \\ yPR_l \end{pmatrix} = \begin{pmatrix} c & 0 & a \\ 0 & b & 0 \\ 0 & c & a \\ b & 0 & 0 \end{pmatrix} \begin{pmatrix} w_1 \\ w_2 \\ w_3 \end{pmatrix} V_{ac} + \begin{pmatrix} 0 \\ q \\ 0 \\ q \end{pmatrix} V_{ac} (V_{dc} - V_{surf})$$

Different contributions to signal can be distinguished by frequency-dependent measurements; however, this approach is not universal

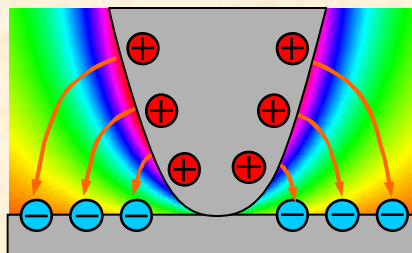
OAK RIDGE NATIONAL LABORATORY
U. S. DEPARTMENT OF ENERGY

 UT-BATTELLE

Contributions to VPFM Contrast

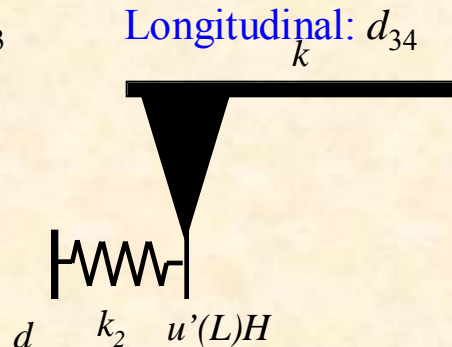
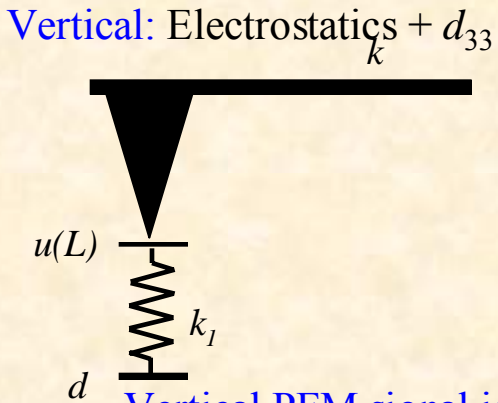


Local Piezoeffect

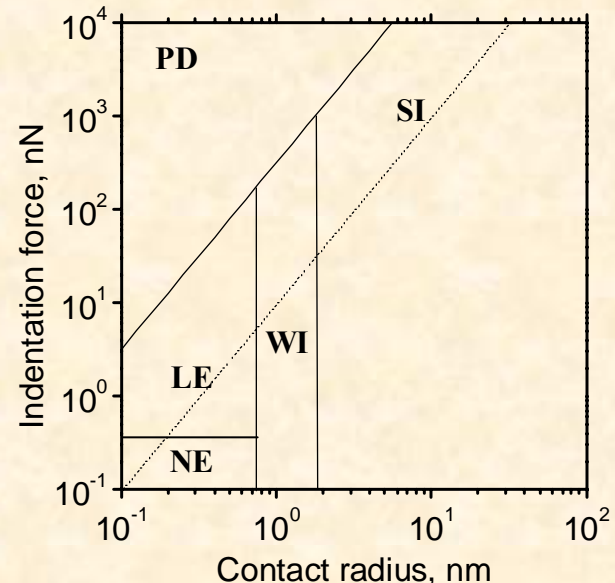


Local Electrostatic Force

- Electromechanical response of the surface and local electrostatic force operate in tip-surface junction.
- In a realistic system, longitudinal tip displacement and distributed electrostatic forces contribute to vertical PFM signal

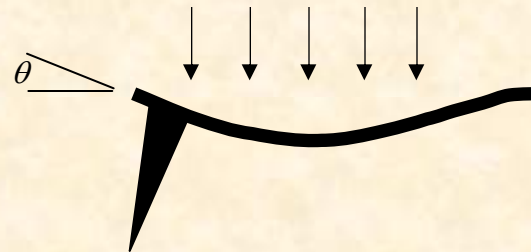


Vertical PFM signal is a sum of 4 contributions dependent on frequency and geometric properties of the cantilever, and contact stiffness.

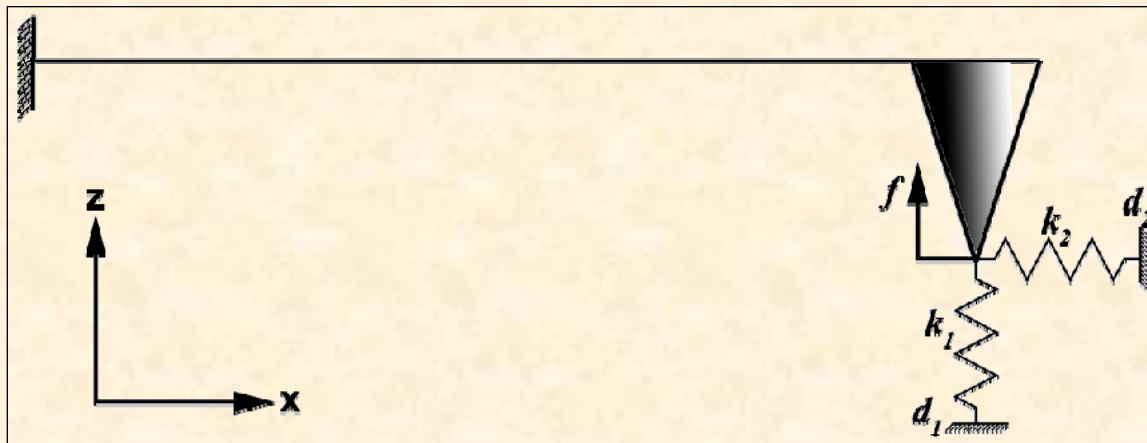


Kalinin and Bonnell, PRB 2001

Non-local electrostatic



General Solution for Beam Equation



Beam equation:

$$\frac{d^4 u}{dx^4} + \frac{\rho S_c}{EI} \frac{d^2 u}{dt^2} = \frac{q(x,t)}{EI}$$

Boundary conditions:

$$EIu_0''(L) = k_2 H (\tilde{d}_2 - u_0'(L)H)$$

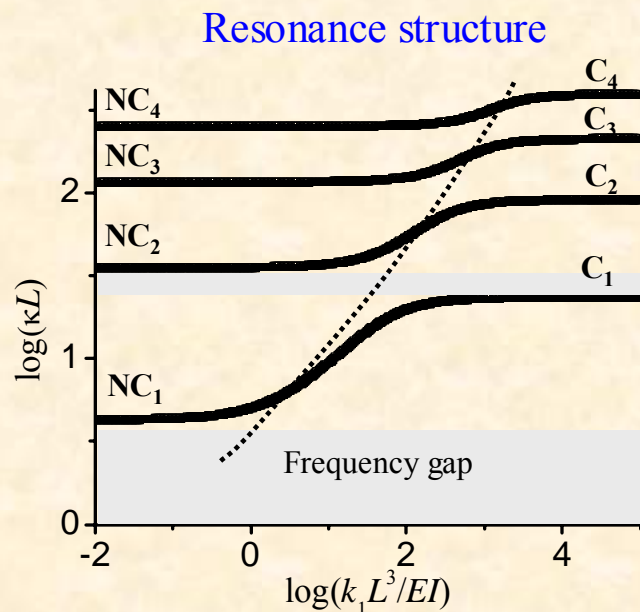
$$EIu_0'''(L) = -f_0 + k_1(u_0(L) - d_1)$$

General solution:

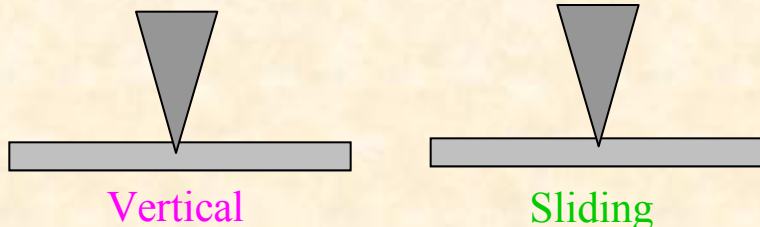
$$\theta_{tot} = \frac{A_v(\beta)d_1 + A_l(\beta)d_2 + A_e(\beta)f_0 + A_q(\beta)q_0}{N(\beta)}$$

- Superposition of vertical, longitudinal, local electrostatic, and non-local electrostatic terms
⇒ can be analyzed separately
- Resonances are determined by the elastic properties of material only
⇒ can not be used to separate responses
⇒ AFAM measurements with electric excitation
- Antiresonances can be used to nullify chosen response component

General Solution for Beam Equation



Cantilever geometry



- Depending on the geometric parameters of the cantilever, response can be vertical and lateral

Frequency behavior

Longitudinal:

$$\frac{A_l(\beta)}{N(\beta)} \sim \frac{1}{\omega^{1/2}}$$

Vertical and local electrostatic

$$\frac{A_v(\beta)}{N(\beta)} \sim \frac{A_e(\beta)}{N(\beta)} \sim \frac{k_1}{\omega}$$

Non-local

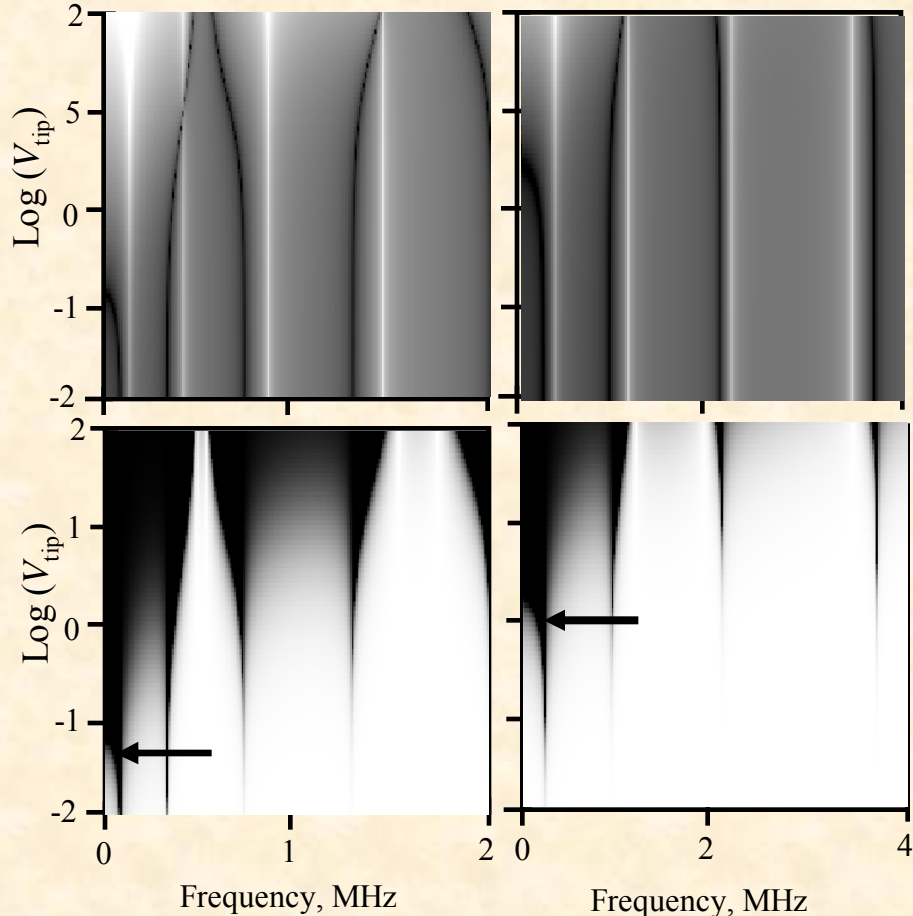
$$\frac{A_q(\beta)}{N(\beta)} \sim \frac{1}{\omega^{3/2}}$$

- All components decrease with frequency
- Non-local decays fastest
- Longitudinal – slowest, but there is onset of sliding friction

- Well studied in the context of AFAM
- Resonances depend only on elastic properties of material
- **But: for non-planar tip spring constant (and resonant frequency) are bias dependent!**
- The optimal detection regime depends on mode number and ratio of cantilever spring constant and spring constant of tip-surface junction

Cantilever Buckling Effect

Soft: $k = 0.1 \text{ N/m}$

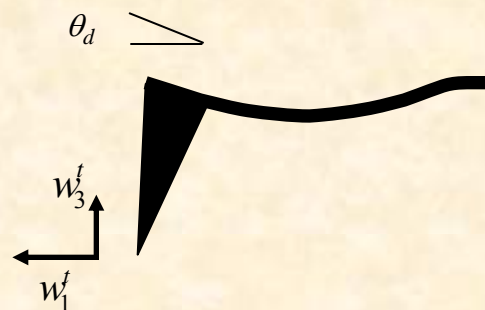


PFM signal: $z_{1\omega} = z_{eff}^0 + d_{33}V_{ac}$

Effective deflection: $z_{eff}^0 = -Lw\varepsilon_0 V_{ac} \Delta V / 48k_{eff} H^2$

Which cantilever is stiff enough:

$$d_{33}V_{ac} \gg z_{eff}^0 \Rightarrow k_{eff} \gg k^* = \frac{Lw\varepsilon_0 \Delta V}{48d_{eff} H^2}$$

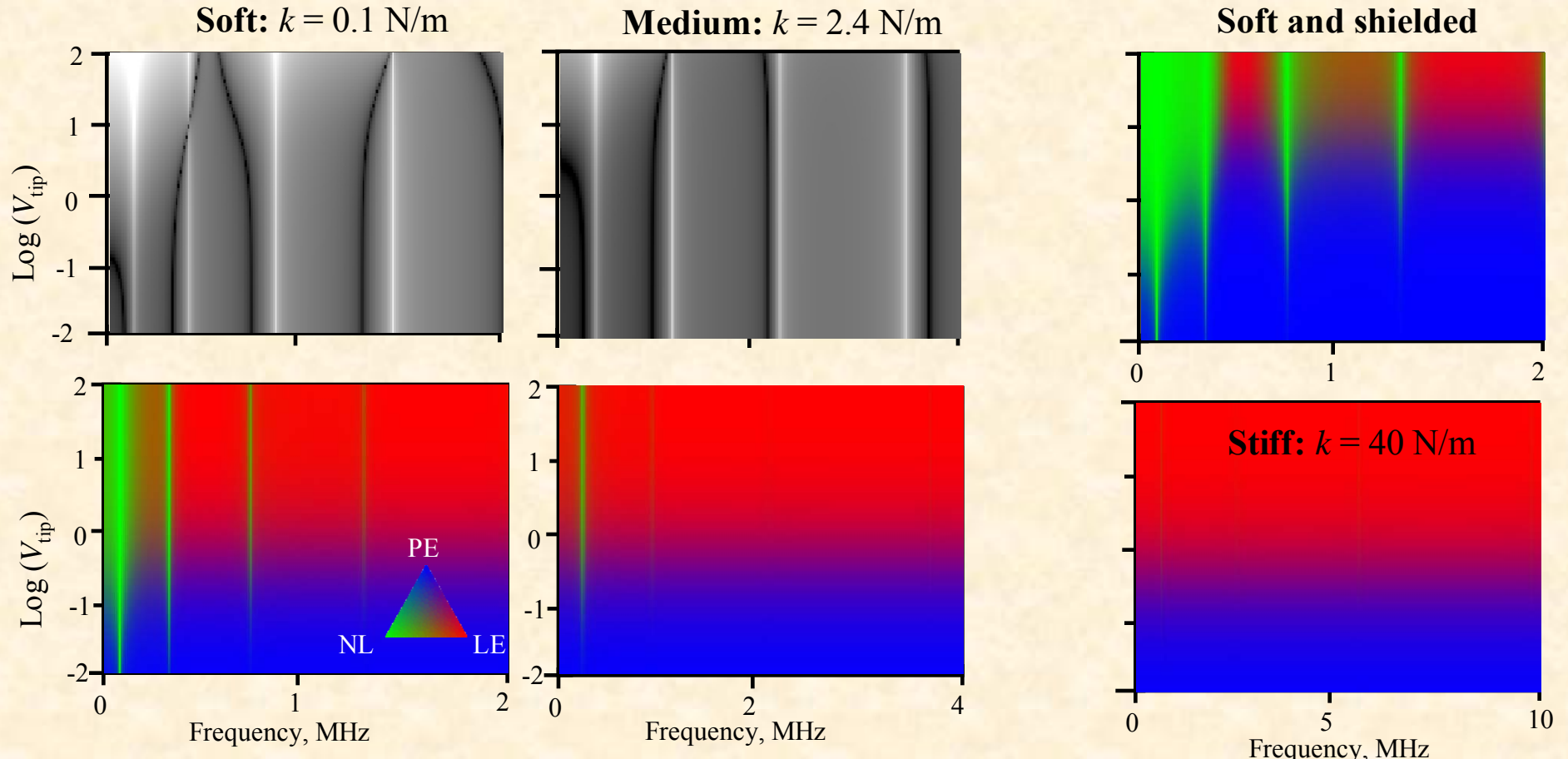


- Use of stiff cantilevers
- Positioning the beam and the nodal point for flexural mode (B. Huey)
- Imaging at high frequencies

OAK RIDGE NATIONAL LABORATORY
U. S. DEPARTMENT OF ENERGY

 UT-BATTELLE

Cantilever Buckling Effect

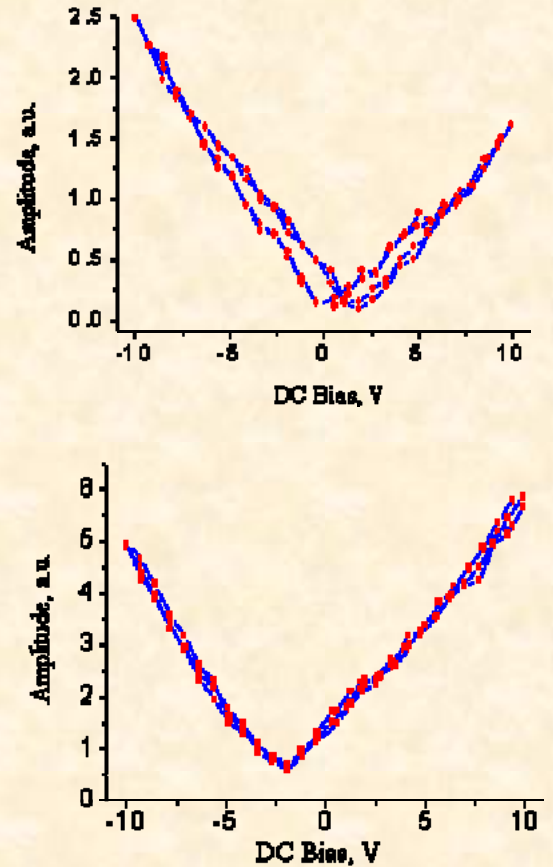
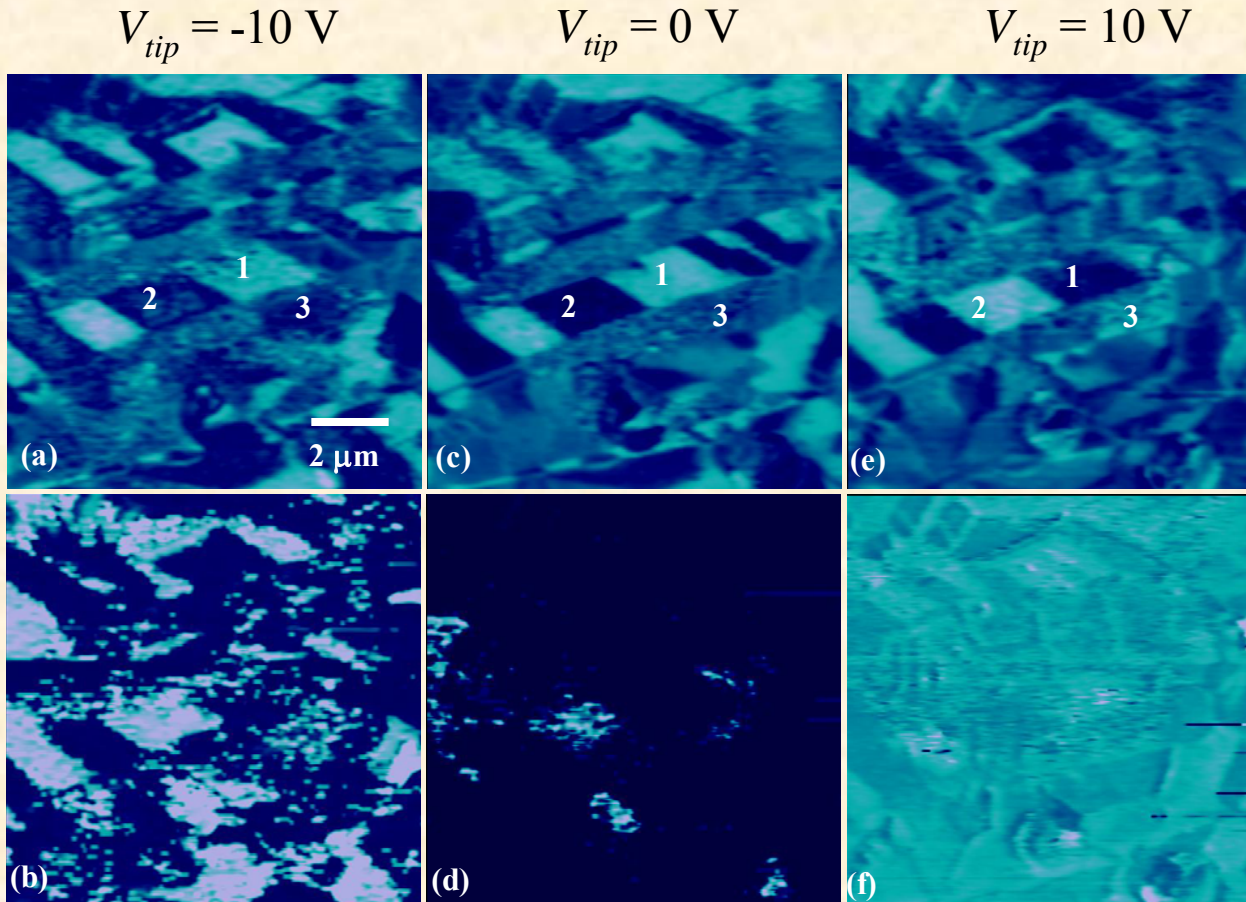


- The relative contributions of the responses do not change near the resonances
- Non-local electrostatics dominate near antiresonances
- Cantilever stiffness and frequency do not affect relative local electrostatic and piezoelectric signal
- Contact stiffness does

OAK RIDGE NATIONAL LABORATORY
U. S. DEPARTMENT OF ENERGY



Electrostatic Effect on Imaging

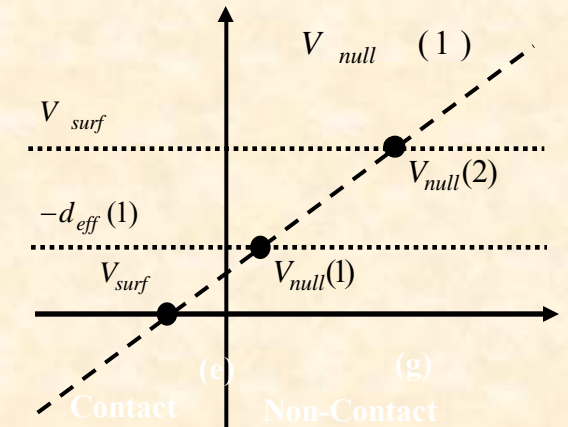
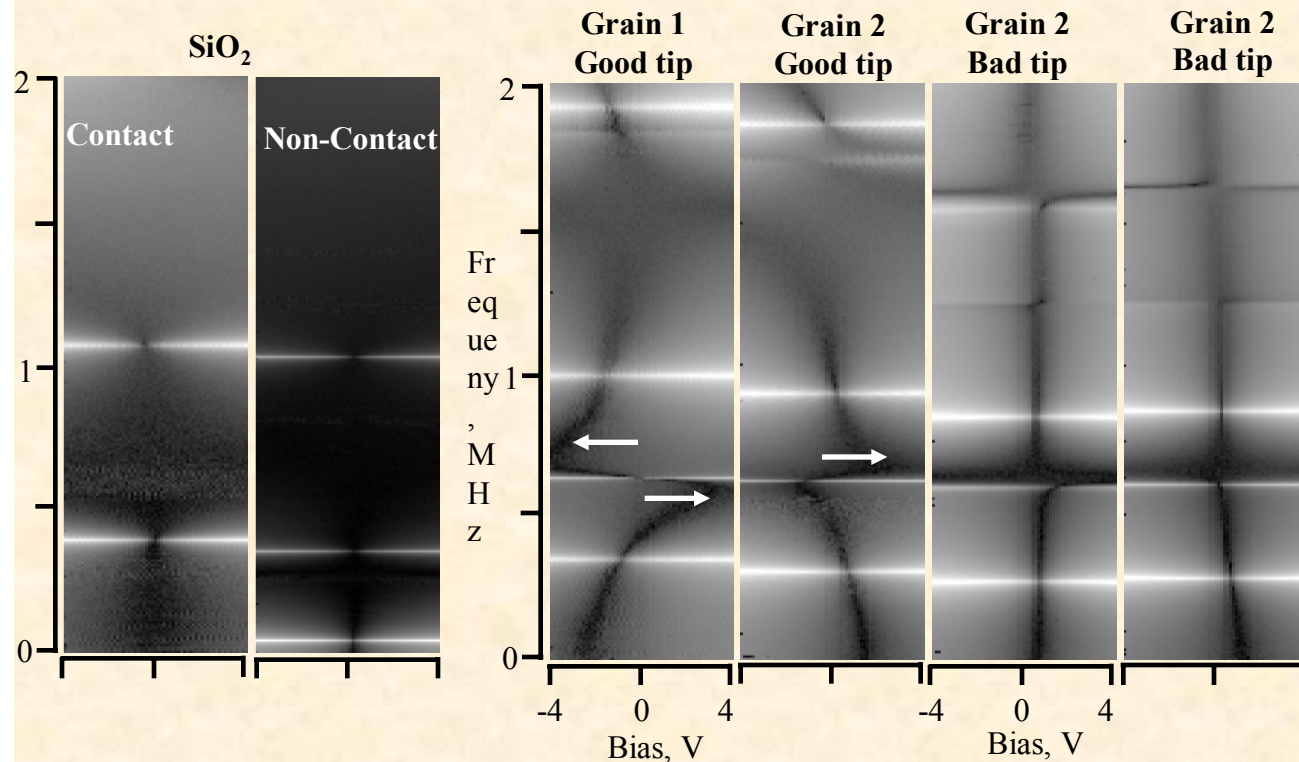


- Electrostatic contribution can strongly affect apparent contrast
- For non-piezoelectrics, yields V-type hysteresis loops
- For switchable ferroelectrics, can be subtracted (since it is conservative)
- For piezoelectrics, difficult to separate

OAK RIDGE NATIONAL LABORATORY
U. S. DEPARTMENT OF ENERGY

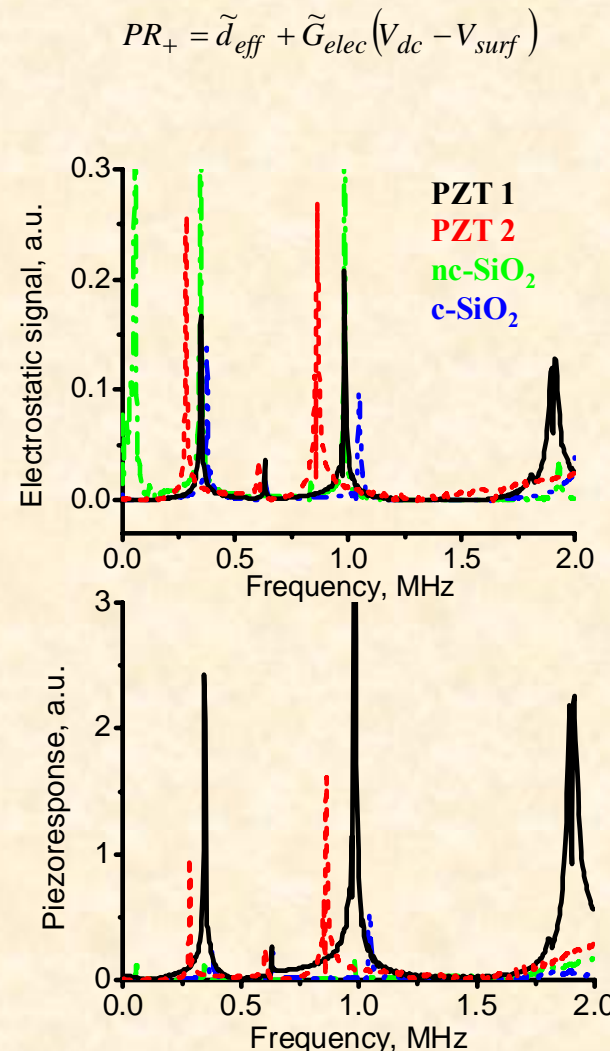
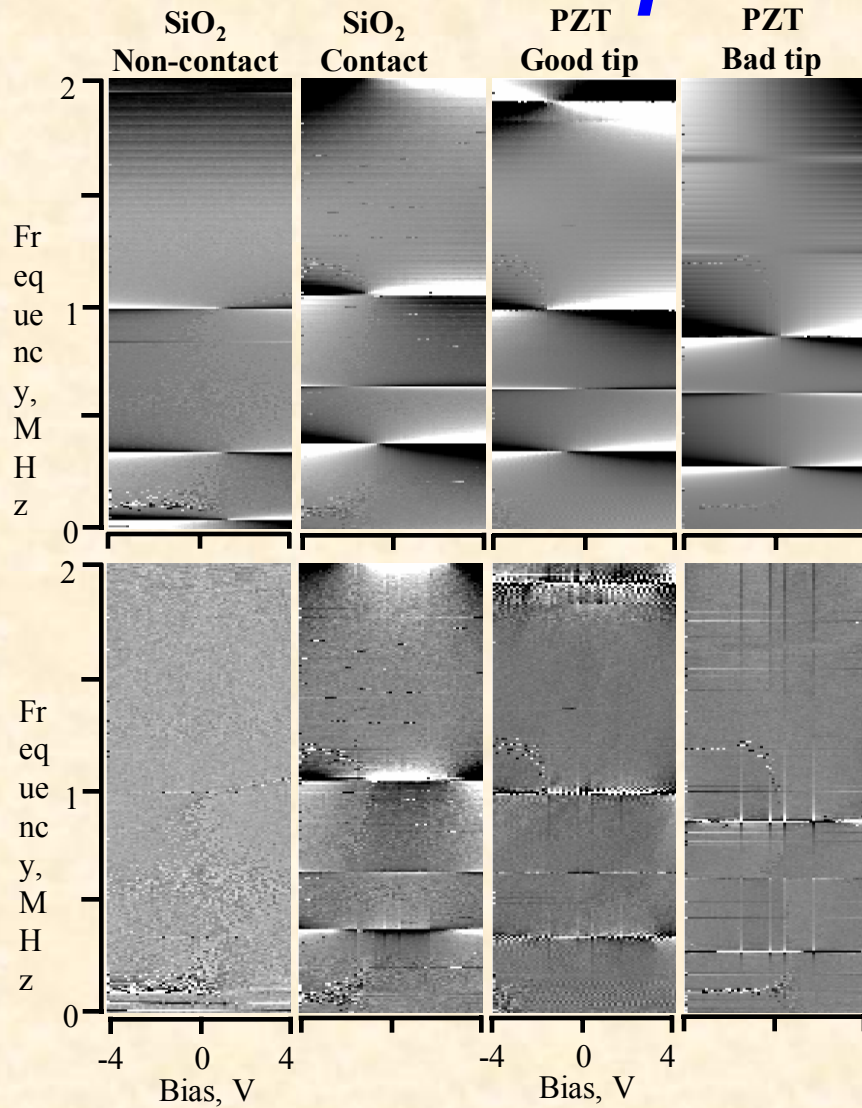


2D Spectroscopy



- Frequency dependence of nulling potential is a measure of relative electrostatic and electromechanical contributions to the signal
- This is also valid for NC-AFM based Kelvin probe

Separation of signals



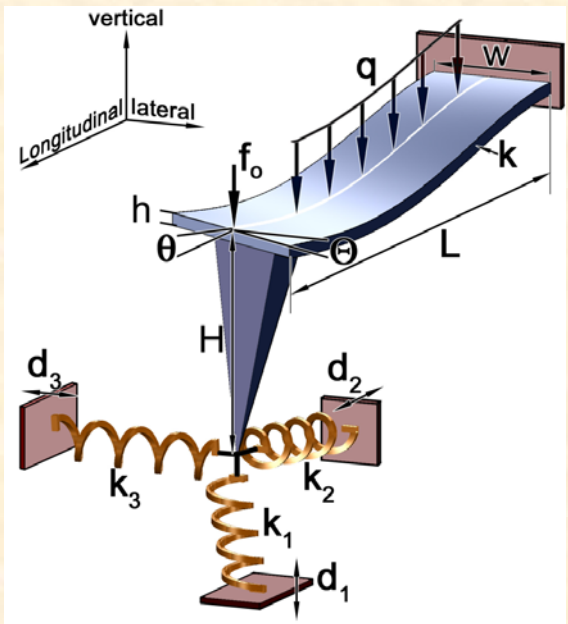
- Electrostatic contribution can be unambiguously determined as a function of frequency
- Electromechanical contribution can be determined only if surface potential is known

OAK RIDGE NATIONAL LABORATORY

U. S. DEPARTMENT OF ENERGY



PFM Equation



PFM Signal in the Low-Frequency Limit:

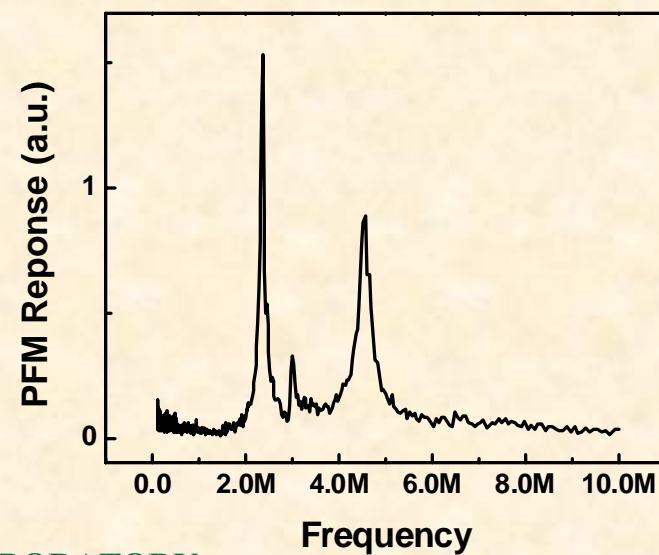
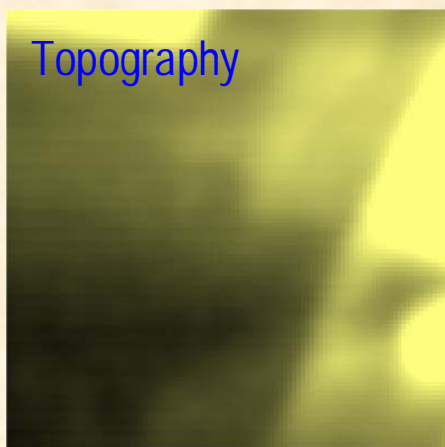
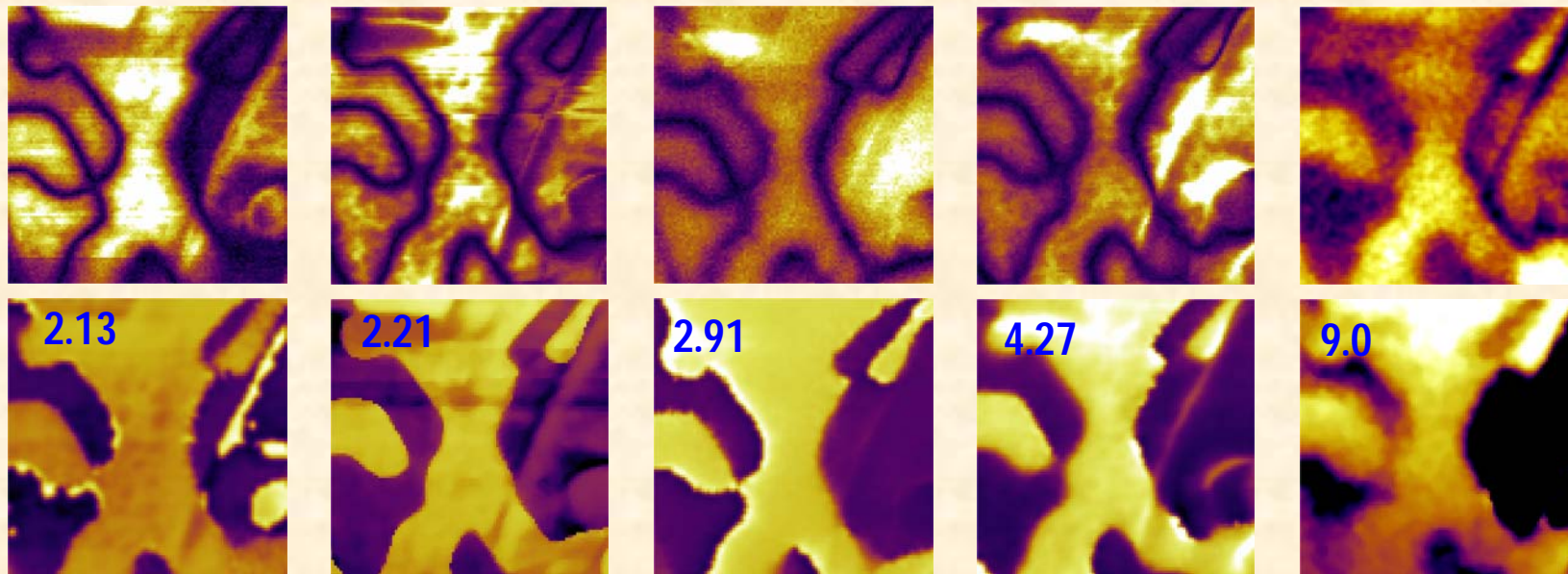
$$PR = \alpha_a(h) \tilde{d}_{33} \frac{k_1}{k_1 + k} + \frac{C_{sphere}^+ + C_{cone}^+}{k_1 + k} (V_{dc} - V_s) + \frac{C_{cant}^+}{24k} (V_{dc} - V_{av})$$

↑ Non-local electrostatic contribution
↑ Local electrostatic contribution
Electromechanical contribution

Electromechanical imaging requires high contact stiffness

- Vertical PFM is optimal at high (~ 1 MHz) frequencies
 - better S/N ratio
 - cantilever stiffening improves contact
 - limited by bandwidth of detector
 - at very high frequencies, no signal transduction
- Lateral PFM is optimal at 10 – 100 kHz
 - problems with friction

Optimal Frequency for PFM



Resonance enhancement in PFM

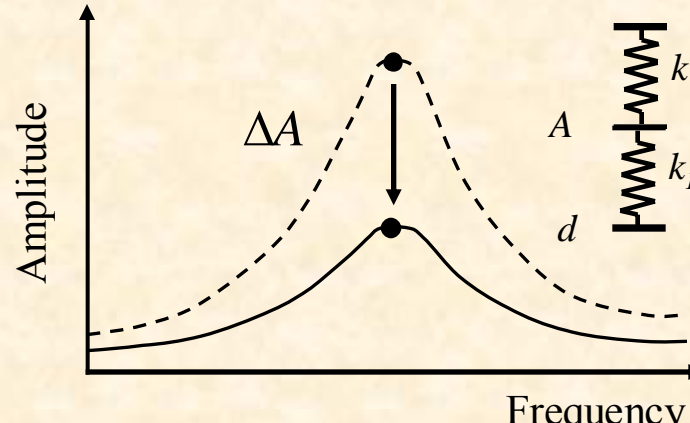
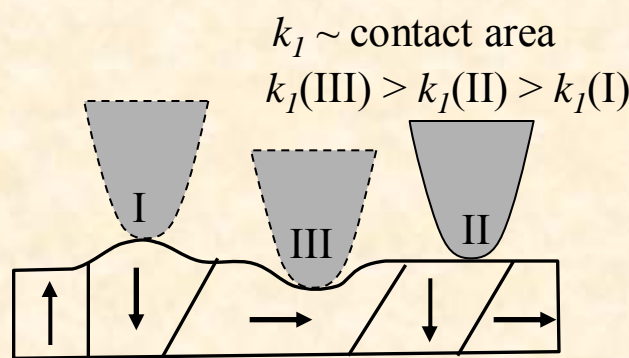
- Away from the resonance: low signal
- At the resonance: strong cross-talk
- Vicinity of the resonance: optimal

If the frequency is too high:

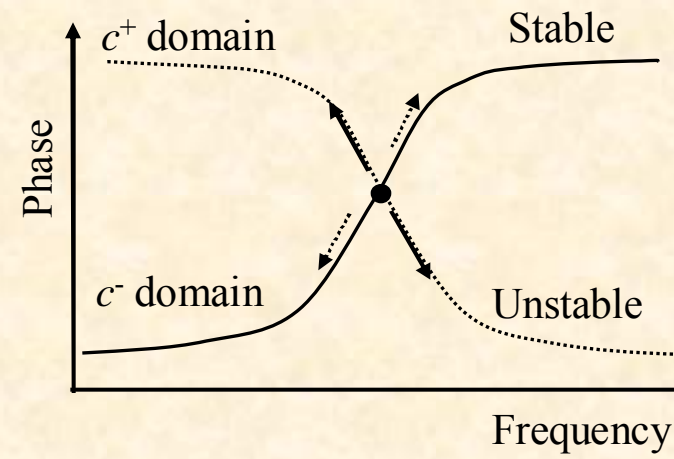
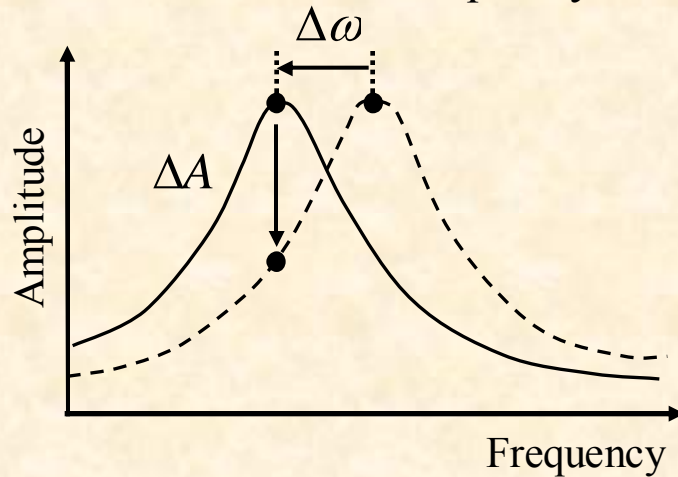
- Cantilever does not respond
- Photodiode bandwidth

Resonant Enhancement in PFM

To image weakly piezoelectric materials or high resolution spectroscopy, we need to detect small (1-10 pm) surface displacements. Can we use resonant enhancement?



- Problem 1:** resonant frequency depends on topography, and not on electromechanical response!
- Problem 2:** Standard PLL frequency-tracking loops are unstable



Solution: fast acquisition of amplitude-frequency curve in the vicinity of resonance

OAK RIDGE NATIONAL LABORATORY

U. S. DEPARTMENT OF ENERGY